Title:

High-dimensional microbiome interactions shape host fitness

Authors:

Alison L. Gould,[1,2] Vivian Zhang,[1,2] Lisa Lamberti,[3,4] Eric W. Jones,[5] Benjamin Obadia,[1] Alex Gavryushkin,[3,4,6] Nikolaos Korasidis,[3] Jean M. Carlson,[5] Niko Beerenwinkel,[3,4] William B. Ludington[1,7*]

1. UC Berkeley, Dept Molecular & Cell Biology, Division of Genetics, Genomics & Development, Division of Immunology & Pathogenesis
2. equal contributors
3. ETH Zurich, Dept Biosystems Science & Engineering
4. Swiss Institute of Bioinformatics, Basel, Switzerland
5. UC Santa Barbara, Complex Systems Group, Dept Physics
6. Dept Computer Science, University of Otago, New Zealand
7. lead contact

* correspondence: ludington@carnegiescience.edu

Abstract:

Gut bacteria can affect key aspects of host fitness, such as development, fecundity, and lifespan, while the host in turn shapes the gut microbiome. Microbiomes co-evolve with their hosts and have been implicated in host speciation. However, it is unclear to what extent individual species versus community interactions within the microbiome are linked to host fitness. Here we combinatorially dissect the natural microbiome of *Drosophila melanogaster* and reveal that interactions between bacteria shape host fitness through life history tradeoffs. We find that the same microbial interactions that shape host fitness also shape microbiome abundances, suggesting a potential evolutionary mechanism by which microbiome communities (rather than just individual species) may be intertwined in co-selection with their hosts. Empirically, we made germ-free flies colonized with each possible combination of the five core species of fly gut bacteria. We measured the resulting bacterial community abundances and fly fitness traits including development, reproduction, and lifespan. The fly gut promoted bacterial diversity, which in turn accelerated development, reproduction, and aging: flies that reproduced more died sooner. From these measurements we calculated the impact of bacterial interactions on fly fitness by adapting the mathematics of genetic epistasis to the microbiome. Host physiology phenotypes were highly dependent on interactions between bacterial species. Higher-order interactions (involving 3, 4, and 5 species) were widely prevalent and impacted both host physiology and the maintenance of gut diversity. The parallel impacts of bacterial interactions on the microbiome and on host fitness suggest that microbiome interactions may be key drivers of evolution.

keywords:

microbiome, fitness landscape, microbial ecology, epistasis, species diversity, higher-order interactions

Significance:

All animals have associated microbial communities called microbiomes that can influence the physiology and fitness of their host. It is unclear to what extent individual microbial species versus ecology of the microbiome influences fitness of the host. Here we mapped all the possible interactions between individual species of bacteria with each other and with the host's physiology. Our approach revealed that the same bacterial interactions that shape microbiome abundances also shape host fitness traits. This relationship provides a feedback that may favor the emergence of co-evolving microbiome-host units.

Introduction:

Microbiomes and their hosts show evidence of co-evolution (1), however the evolutionary mechanisms maintaining these coevolving units of diversity remain mysterious, and the complexity of microbiomes makes this problem experimentally challenging to address. In 1927, Steinfeld (2) reported that germ-free flies live longer than their microbially colonized counterparts, suggesting that bacteria hinder host fitness. This observation —that the microbiome can impact aging— has been replicated in flies and vertebrates (3, 4). However, a decrease in lifespan does not necessarily indicate a negative impact on the host. Organisms in their environment are selected for their fitness, which is a function of lifespan, fecundity, and development time (5). Life history tradeoffs can, for instance, increase fecundity at the expense of lifespan (6-8) providing different strategies for fitness. These observations set up two major questions: what is the role of an individual bacterial species versus interactions between them in determining host lifespan, and how is lifespan related to overall host fitness?

Identifying the host effects of specific bacteria has been difficult, in part due to high gut diversity but also because interactions between bacteria can depend on context, both in terms of neighbor species and the gut environment (9). For example, a bacterium may produce a specific B-vitamin in response to its neighbors (10, 11). This response may impact the host, and host feedbacks can mitigate or exacerbate changes in the microbial community (12). However, specific examples may be misleading, as the true complexity of a gut microbiome has never been exhaustively quantified. Thus, it remains an outstanding challenge to reverse engineer the interaction networks that characterize community microbiome-host effects relative to host interactions with individual bacterial species. Doing so would allow us to address the role of microbial community complexity in shaping the co-evolutionary trajectory with the host. However, quantifying the set of all possible interactions of *n* species is a combinatorial problem involving 2^n distinct bacterial communities. As *n* approaches the diversity of the mammalian gut with hundreds of species, this challenge becomes experimentally unfeasible.

The gut microbiome of the fruit fly *Drosophila melanogaster* is an effective combinatorial model because as few as five species of bacteria consistently inhabit the gut of wild and laboratory flies (13-15), yielding 2^5 possible combinations of species. Here, we isolated the five core fly gut bacteria species in culture, constructed germ-free flies by bleaching the embryos, and reinoculated the newly emerged

85 adult flies via continuous association with defined flora using established protocols (16, 17). We made
86 the 32 possible combinations of the five bacterial species commonly found in the fruit fly gut:
87 *Lactobacillus plantarum* (*Lp*), *L. brevis* (*Lb*), *Acetobacter pasteurianus* (*Ap*), *A. tropicalis* (*At*), and *A.*
88 *orientalis* (*Ao*). We then quantified the microbiome composition and resultant host phenotypes of (i)
89 development time, (ii) reproduction, and (iii) lifespan to determine the relationship between gut
90 microbe interactions and host fitness. We tested to what extent the presence and abundance of
91 individual bacterial species account for the fly physiology phenotypes we measured.
92
93 Finally, we introduce a mathematical framework to deconstruct microbiome-host complexity by making
94 a conceptual analogy between the presence of bacterial species and the occurrence of genetic
95 mutations (18, 19). This approach allowed us to calculate the complete microbiome-host interaction
96 space, and it revealed significant interactions between 2, 3, 4, and 5 species that have large impacts on
97 host physiology, contributing to differential life history strategies that could impact host evolution.

Results

Microbiome diversity confers a life history tradeoff

We hypothesized that microbiome-induced lifespan changes might be due to changes in life history strategy, such as a tradeoff with fecundity or development. We therefore set up an experiment to measure how defined species compositions change each of the host traits of lifespan, fecundity, and development time, which have been found to co-vary in life history tradeoffs (6, 7). We measured these traits concomitantly in the same experiment so that we could sum them together to calculate overall fly fitness (Fig. 1A).

We first isolated each of the five species of bacteria found in our laboratory flies: *Lactobacillus plantarum* (*Lp*), *L. brevis* (*Lb*), *Acetobacter pasteurianus* (*Ap*), *A. troplicalis* (*At*), and *A. orientalis* (*Ao*). In order to test whether groups of bacteria have additive effects, we made each of the 32 possible combinations of the 5 species (including germ-free; Fig. 1A). We then made germ free flies and inoculated them with defined bacteria compositions at 5-7 days post-eclosure to reduce variation in development and gut maturation (20).

We performed five technical replicates of each experiment with 10 males and 10 females together in the same vial. The five replicates were performed over two separate biological replicates for a total of 100 adult flies per each of the 32 treatments. We transferred the flies every three days to fresh food that was inoculated with fresh bacteria in order to reduce the effects of bacterial growth on the food. To measure lifespan, we recorded the number of live flies daily. To measure fecundity, we kept the old vials that flies were transferred from and counted the number of emerged live adults. To measure development time in the population experiments where egg laying took place for three days, we counted the number of days for the first adult to emerge from a pupal case.

We first asked the role of individual bacterial species on fly lifespan. Consistent with previous studies, our germ-free flies survived the longest (Fig. 1B). However, only *Lp, At*, and *Ao* shortened lifespan, while flies aged with *Lb* and *Ap* had equivalent survival to germ free flies. We next asked the effect of microbial diversity on fly lifespan. Germ-free flies survived ~20% longer than flies colonized by all five bacteria (mean lifespan ± standard error of the mean, 53.5 ± 1.5 germ-free vs. 43.5 ± 1.1 for 5-species gnotobiotics). Overall, we found a decrease in survival over many bacterial associations as we increased gut diversity (Fig. 1B inset, S1, S2; $r=-0.54$, $p=0.002$, $n=32$, Spearman correlation), consistent with the gut microbiome having a pathogenic effect on the host.

We next asked whether the reduction in lifespan was offset by a life history tradeoff in fecundity. Decreased lifespan corresponded to an increase in fecundity for female flies (average daily fecundity vs. lifespan: $r=-0.50$, $p=0.003$, $n=32$, Spearman correlation; Fig. 1C) and is not explained by differences in fly activity (Fig. S3). Such life history tradeoffs are well-documented in the literature and are believed to constitute a differential allocation of resources between long-term body maintenance and reproduction (5, 21). By adjusting its life history strategy, an individual organism can adapt to a heterogeneous environment.

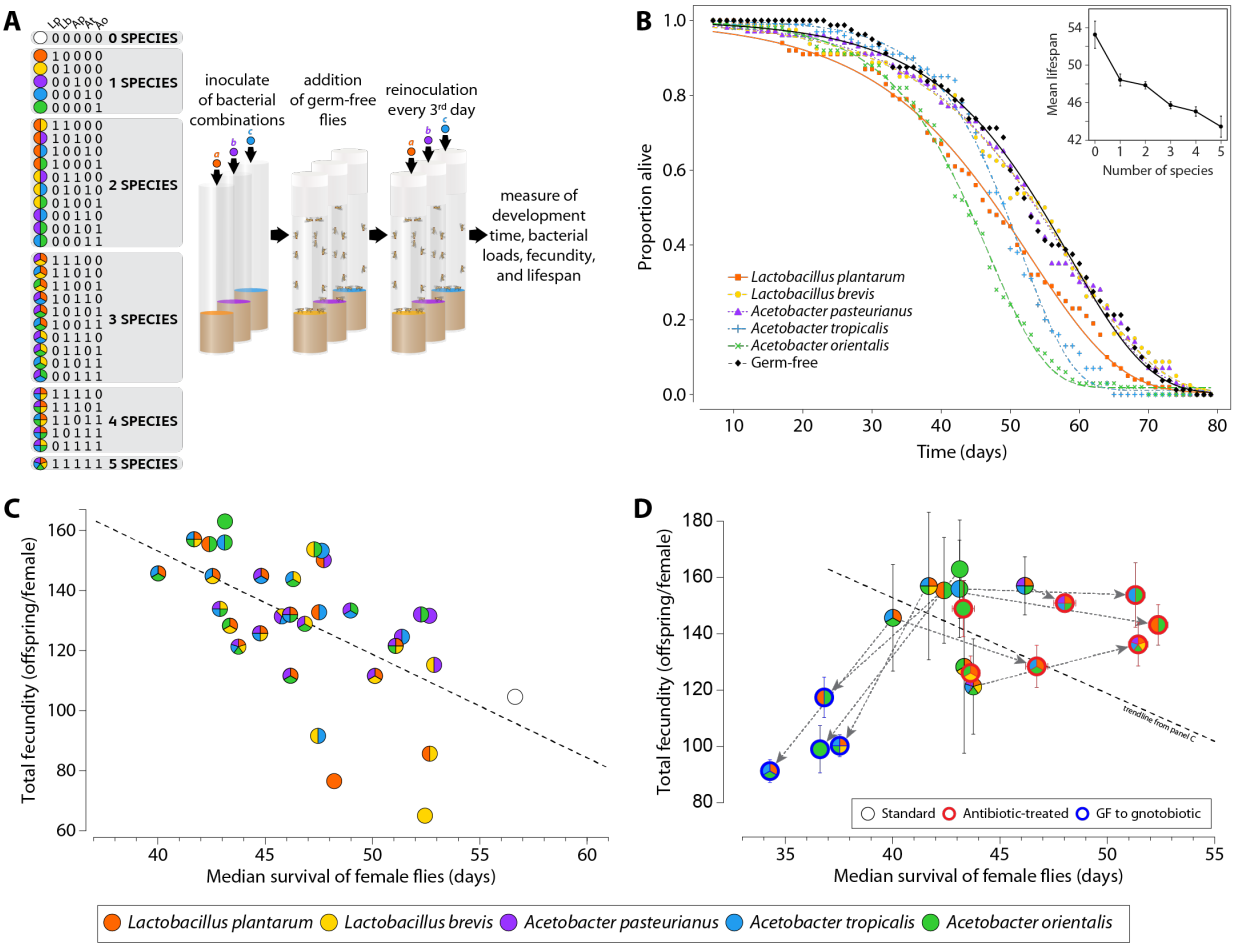

Figure 1. The microbiome induces a life history tradeoff between lifespan and reproduction. (**A**) Experimental design. The multi-color pies indicate which species are present in a given combination along with the corresponding binary code. Each species abbreviation (Lp, Lb, Ap, At, Ao) is indicated above its corresponding locus in the binary string. Both notations, colored pies and binary are used consistently throughout the manuscript. The color code is included redundantly in the figures to aid the reader. (**B**) Single bacterial associations decrease fly lifespan. (**B inset**) Microbiome diversity decreases fly lifespan. (**C**) In agreement with prior reports, higher fecundity is associated with shorter lifespan. This tradeoff is apparent for average daily fecundity as well as total fecundity per female. (**D**) The lifespan fecundity tradeoff can be broken by putting flies on antibiotics after their peak reproduction (red circles = gnotobiotic flies treated with antibiotics; see Methods) after 21 days, which encompasses the natural peak fecundity (Fig. S4). Note the shifts in lifespan between the regular treatment, the antibiotic treatment, and the late-life bacterial inoculation treatment. Lifespan was significantly extended, whereas total fecundity stayed high. Shifting germ-free flies to gnotobiotic treatment after 21 days post-ecolsion decreased lifespan without increasing reproduction (blue circles = germ-free flies made gnotobiotic 21 days post-eclosion). n=100 flies per treatment for the standard and antibiotic-treated experiments n=60 flies per treatment for the germ-free switched to gnotobiotic experiment. Error bars show S.E.M.

Individual flies cannot adaptively modulate their life history strategy to achieve late life fecundity

The life history tradeoff suggests that a fly born into stark conditions in the wild could maximize its fitness by first acquiring a longevity-promoting microbiome and then converting to a fecundity-promoting one when environmental conditions improve. Female flies are primarily reproductive in the

first part of their life, with a gradual decay in fecundity approaching middle age (Fig. S4). To test whether individual flies can switch life history strategy over their life time, we aged germ-free flies for 21 days (roughly middle age) and then associated these flies with fecundity-promoting bacteria. There was no significant increase in total fecundity for these flies and a significant decrease in lifespan compared to germ-free flies (Fig. 1D; p=0.054 for fecundity, n=275 flies pooled across four bacterial combinations, two sample one-sided t-test, p>0.05 for all pairwise combinations after Tukey's multiple comparison correction of two-sample one-sided t-tests; $p=2x10^{-7}$ for lifespan, n=400 flies pooled across four bacterial combinations, two-sample one-sided t-test; p<0.001 for 4 of 4 combinations after Tukey's correction for multiple pairwise comparisons, n=100 flies per combination, two-sample one-sided t-tests; see Fig. 1D for specific bacterial combinations). These results are consistent with the simple hypothesis that a fly's reproductive window cannot be extended by late-life improvement in nutrition.

Antibiotics break the life history tradeoff

As tired parents, we hypothesized that reproduction may shorten lifespan. To examine this hypothesis, we used antibiotics to remove the microbiome of high-fecundity female flies and measured the resulting change in lifespan. We first allowed female flies with high-fecundity microbiomes to reproduce for 21 days (to a level greater than the total lifetime fecundity of germ-free flies; Fig. S4), and we subsequently eliminated the microbiome using an antibiotic cocktail (ampicillin, tetracycline, rifamycin and streptomycin). In general, the midlife elimination of gut flora lengthened the female fly lifespan by roughly 15% compared to flies continuously fed live bacteria (Fig. 1D; $p=9x10^{-7}$, n=560 flies pooled across bacterial combinations; p<0.05 for 4 of 7 combinations after Tukey's correction for multiple pairwise comparisons, n=80 flies per combination, two-sample one-sided t-test; see Fig 1D for specific bacterial combinations). Average daily fecundity decreased slightly (Fig. 1D; p=0.01, n=560 flies pooled across bacterial combinations; p>0.05 for all 7 combinations after Tukey's correction for multiple pairwise comparisons, n=80 flies per combination, two-sample one-sided t-test; see Fig 1D for specific bacterial combinations). This result demonstrates that the life history tradeoff is not necessarily fixed and suggests that fly lifespan is shortened by some aspect of the bacteria rather than by reproduction. However, two specific bacterial combinations yielded no increase in lifespan when removed from their host by antibiotics: *Ao* and *Lp+Lb+Ao*, suggesting a hysteresis in host physiology induced by these two combinations. Interestingly, the intermediate microbiome composition, *Lp+Ao*, did not show this hysteresis, nor did the similar composition *Lp+At+Ao* (Fig 1D) (with antibiotic elimination of the microbiota extending lifespan) suggesting specificity of the microbiome composition in this hysteresis. These experiments demonstrate that interactions between bacteria significantly impact in the host's ability to adjust its physiology. We examine interactions later in the manuscript.

Microbiome compositional heterogeneity increases host physiological plasticity

Phenotypic plasticity, such as the microbiome-induced lifespan fecundity tradeoff, can allow animals to match their physiology to a heterogeneous environment, increasing overall fitness. We quantified the variation in lifespan, fecundity, and development time as a function of the number of bacterial species present. While average fecundity did not vary as a function of increasing species diversity (r=0.07, p=0.7, n=32, Spearman correlation), the variance in fecundity between bacterial combinations with the same number of species decreased as species were added (Fig. 2A, S2-3; r=–0.91, p=0.08, n=4 diversities, Pearson correlation; p=0.001, t-test comparing deviations with 1 or 2 species vs. 3 or 4 species). We similarly analyzed the variation in development times. On our replete food, both germ-free and flies colonized with all 5 bacterial species had a ~10-day development time (Fig. 2B). We hypothesized that fly development would be relatively robust to changes in bacterial composition. However, as we dissected the 5-member bacterial community, we observed faster average development time with increasing bacterial diversity (Fig. 2B; Fig. S2; n=32 bacterial combinations, r=–0.43, p=0.01, Spearman

correlation coefficient). Notably, the fastest development times did not change significantly: flies associated with *Ao* had rapid development regardless of the other species present (Fig. 2B), suggesting that the presence of *Ao* sets development time. We did not observe a significant change in lifespan variation as a function of species diversity (Fig. 2C). The overall decrease in variation for development time and fecundity demonstrates that higher microbiome diversity can homogenize phenotypic plasticity, which would reduce the range of life history strategies available to flies. Thus, fly populations may benefit from having lower microbiome diversity in the wild.

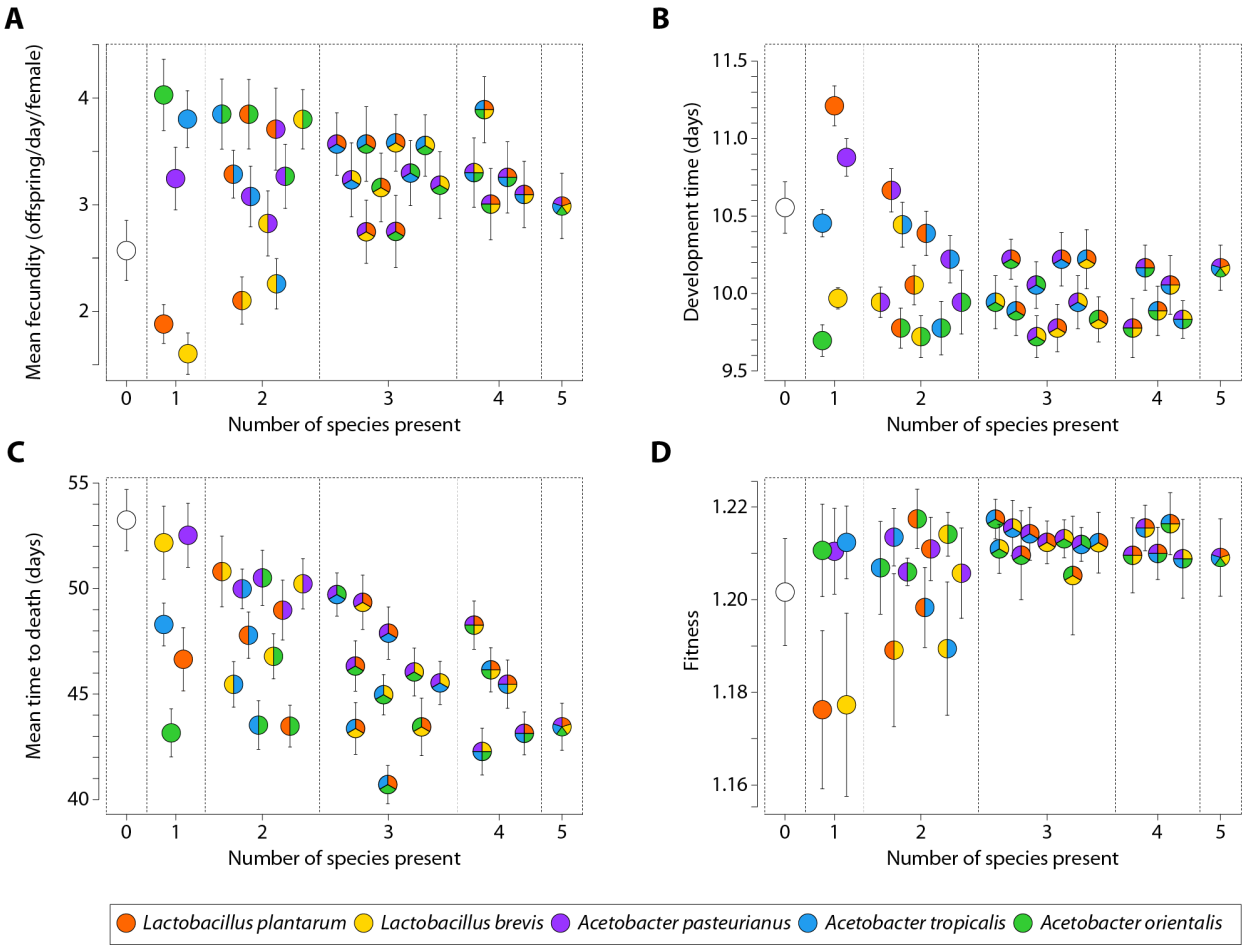

Figure 2. Microbiome diversity impacts host physiology. (**A**) Mean fecundity per female per day was measured concomitantly with development time and adult survival over the flies' lifespans. Median n=65 vials measured per bacterial treatment. Variation in fecundity decreases as gut diversity increases (Fig. S2, S4). (**B**) The number of days to adulthood was measured as the first pupa to emerge from an individual fly vial during the lifespan experiment. The development time increases as gut diversity increases. Median n=24 per bacterial treatment (Fig. S2). (**C**) Lifespan decreases as gut diversity increases. Median n=100 flies per bacterial treatment (Fig. S1, S2). (**D**) Fitness calculations using a Leslie matrix populated with data from **A-C** reveals an increase in fitness and a decrease in fitness variation between different microbiomes as gut diversity increases. Error bars are S.E.M. for **A-C** and S.E.E. for **D**.

Host fitness is relatively constant for different lifespans due to life history tradeoffs

Fitness is a function of fecundity, development, and lifespan, which gives an estimate of the maximum rate of population growth. We wondered whether the observed differences in lifespan were balanced

221 by differential rates of fecundity and development or whether these differences in fly physiology
222 actually made flies with distinct microbiome compositions more and less fit. To address this question,
223 we combined our data for development, fecundity, and lifespan in a Leslie matrix (22), a classical model
224 of discrete population growth, to calculate organismal fitness under each bacterial association. Overall,
225 fitness was relatively consistent across many distinct bacterial associations (Fig. 2D). Thus, the changes
226 in lifespan we observed are consistent with a differential allocation of resources to reproduction.
227

228 **The fly gut microbial community is stably associated with its host**

229 The differences in host physiology we observed resulting from different microbiome compositions could
230 be due not only to which species are present but also to their abundances. We next measured the
231 abundances of individual bacterial species in the flies in order to determine the relationship to different
232 fly physiologies. We first prepared gnotobiotic flies as before by inoculating 5-7 day old mated germ free
233 flies with defined bacterial compositions. Flies were transferred to fresh food inoculated with fresh
234 bacteria every third day for a total duration of 10 days before they were washed in 70% ethanol,
235 crushed, plated, and CFUs enumerated (Fig. 3A). The experiments were performed in two biological
236 replicates for a total of 12 female and 12 male flies that were analyzed for each of the 32 bacterial
237 combinations (Fig 3B). To quantify the extent to which bacterial ingestion and bacterial growth in the fly
238 vials are necessary for bacterial colonization of the gut, we prepared a parallel experiment with the only
239 difference being that after the initial 10 days of inoculation, flies were transferred daily to fresh, germ
240 free food for five subsequent days before CFUs enumeration as before. Small but significant differences
241 were observed between the two experiments (Fig. S5), with the flies transferred daily to germ free food
242 for 5 days surprisingly having higher CFU counts than flies plated directly after day 10 of inoculation
243 (Wilcoxon rank sum test, median CFUs for flies transferred to germ free food: $10^{5.65}$ CFUs vs median for
244 flies directly after day 10 of inoculation: $10^{5.59}$ CFUs, p=0.01, N=1536 individual flies). The results suggest
245 ecological interactions between these species, which we address in a later section. The robust
246 colonization observed despite daily transfer to germ free food indicates the gut microbiome is stable
247 under these conditions, which is in contrast to some previous reports (23, 24). A notable difference in
248 experimental setup between this study and previous ones is that we did not include the fungicide
249 methylparaben in our fly media because we found that it inhibits growth of the endogenous fly gut
250 bacteria (25).
251

252 We note that the limit of detection (~1,000-10,000 CFUs) can mask low-abundance colonization. We
253 performed additional CFU enumeration of individual species in individual flies with a limit of detection of
254 10 CFUs. This experiment showed that flies which appeared uncolonized by one or more bacterial
255 species, were likely colonized at levels below the limit of detection after five days of daily transfer to
256 germ free food (12/12 flies colonized with 5 species had all 5 species; 12/12 flies colonized with *Ap* had
257 *Ap*; 12/12 flies colonized with *Ap* + *Ao* had both species; 11/12 flies colonized with *Ap* + *At* were
258 colonized by both species while one was missing only *Ap*; limit of detection was 10 CFUs). These results
259 are consistent with our previous results (17). This indicates that flies are stably colonized with their gut
260 microbiome under our experimental conditions.
261

262 Overall, we observed robust colonization of the fly gut for each bacterial combination (Fig. 3B, S5).
263 Median total bacterial load ranged from 49,000 colony forming units (CFUs) per fly for *Ap* alone to
264 737,000 CFUs per fly for *Lb*+*At*+*Ao*, with an overall median of 425,000 CFUs per fly (Fig. 3B). Increased
265 species diversity significantly increased the total bacterial load (r=0.63, p=0.0001, n=31 bacterial
266 combinations, Pearson correlation). However, on a species-by-species basis, abundance stayed constant

267 or decreased as species diversity increased (Fig. 3C; *Lp*: r=–0.07, p=0.8; *Lb*: r=–0.37, p=0.2; *Ap*: r=–0.50,
268 p=0.06; *At*: r=–0.59, p=0.02; *Ao*: r=–0.55, p=0.03; Spearman correlations).
269

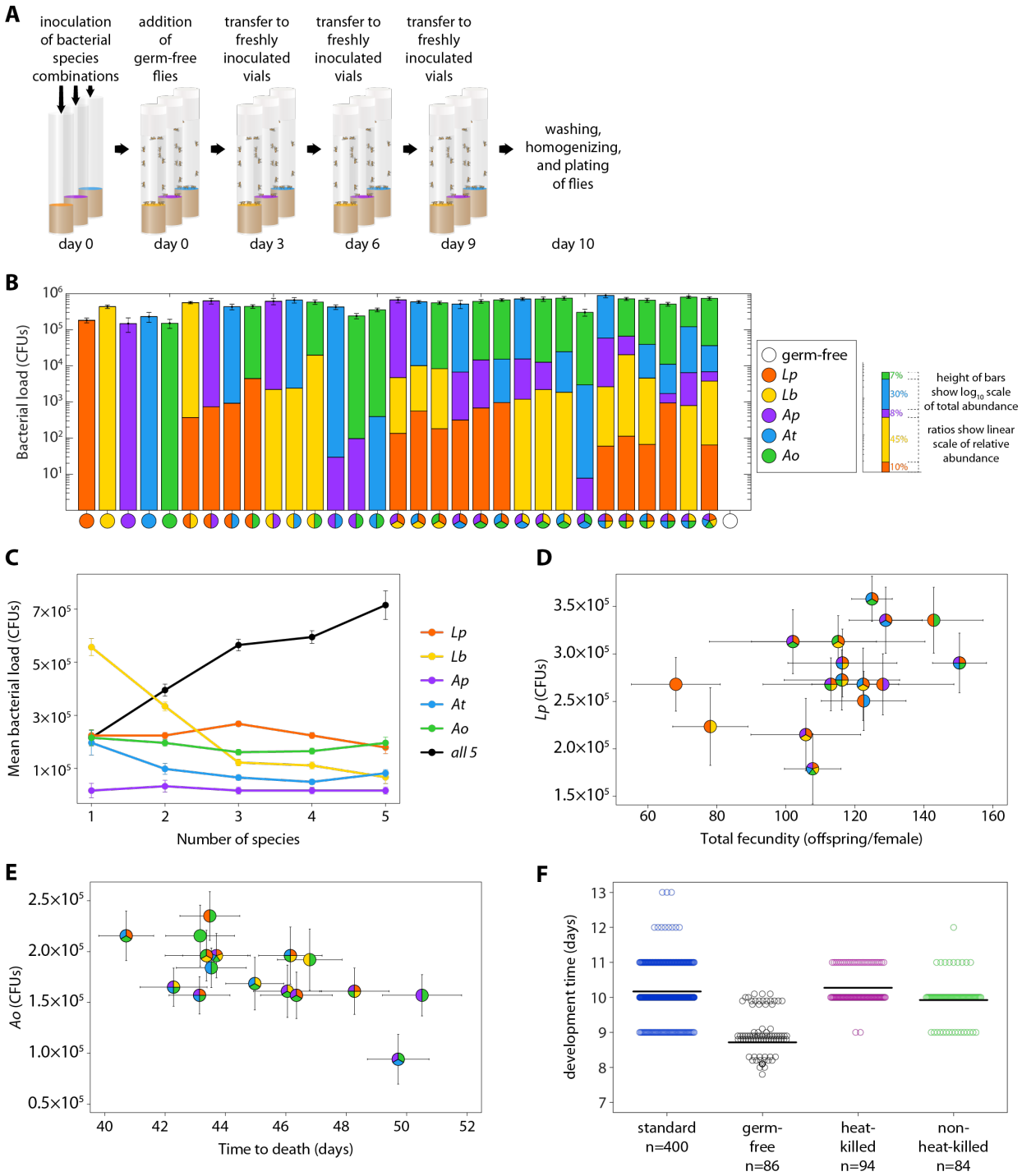

270 **Figure 3. Microbiome abundances correlate with some host physiology traits.** (**A**) Gnotobiotic flies were
271 associated with defined bacterial flora for 10 days before washing, crushing, and CFU enumeration. (**B**) Mean
272 microbiome load ($\log_{10}$ scale) and relative abundances of the different species (linear scale) for all 32 possible
273 combinations of the five species. N=24 replicate flies from 2 independent biological replicates were measured per
274 combination. (**C**) Total bacterial load increases as the number of species increases but *Lb* abundance drops. Mean

abundances were calculated from **B** as a function of the number of species present (see Fig S5 for complete data). (**D**) *Lp* abundance (from **B**) correlates with increased female fly fecundity (from Fig. 1C). (**E**) *Ao* abundance (from **B**) correlates with decreased fly lifespan (from Fig. 1C). (**F**) Development time from embryo to adult is accelerated by live bacteria. Development assay from Fig. 2B was repeated with variation in food preparation and source of embryos. 'Standard': data from Fig. 2B fitness experiment, 'germ-free': embryos from germ-free females placed directly on fresh food inoculated with defined bacteria; 'heat-killed' and 'non-heat-killed': vials from fitness experiment cleared of flies and either seeded directly with germ-free embryos (non-heat-killed) or placed at 60˚C for 1 hour and checked for sterility (heat-killed) before being seeded with germ-free embryos. 'n=###' in figure indicates number of replicate vials assessed. See Fig. S9 for complete bacterial combinations and individual replicates of **F**. All error bars S.E.M.

Presence-absence of individual species more than abundance impacts fly physiology

We next compared the individual species abundances and total bacterial abundances in adult flies with the fly physiology phenotypes (Fig. 2A-C, S2) to ascertain whether there was a relationship. We first calculated the correlation between individual species abundances and each host physiology trait (Fig. S6). The only significant correlations were between *Lp* abundance and female fecundity (Fig. 3D; r=0.52, p=0.04, n=16) and between *Ao* abundance and decreased lifespan (Fig. 3E; r=-0.53, p=0.03, n=16), indicating that these two individual species can explain 27% and 28% of the variation in fecundity and lifespan respectively. In this regard, *Ao* and *Lp* have an outsized effect as individual species. We did not detect other significant relationships between bacterial load and host physiology, leaving the remaining variation (63% of fecundity and 62% of lifespan unexplained by individual species abundances. However, as we showed in Fig. 1D, the interaction between *Ao* and *Lp* can dramatically alter the fly's ability to adjust its physiology when treated with antibiotics, with a 21% change in lifespan (Fig. 1D). Thus, individual bacterial species loads are not necessarily expected to determine impacts on the host.

If the load of individual bacterial species drives host physiology traits, we would expect that higher variation in bacterial load would correspond to higher variation in host traits, yielding a positive correlation. When we calculated the relationship between bacterial load variation and host trait variation, we found little evidence that the host bacterial load drives host physiology traits (Fig. S5-6). Taken together these results suggest that the long term presence of bacterial species (Fig. 1B-D, 2A-C) is more indicative of their effect on host physiology than their abundances (Fig. S6-7).

Development time is correlated to *Acetobacter orientalis* abundance in the food

The link between juvenile development time and adult bacterial composition could be influenced both by bacterial populations in the food and by parental effects. To differentiate between these hypotheses, we performed two experiments. First, we quantified bacterial load in the fly food for 16 bacterial combinations (Fig. S8) after 10 days of larval development. Significantly fewer bacteria occurred per mg in fly food than in the gut of adult flies ($p=1.3 \times 10^{-8}$, n=16 combinations with 20 flies per combination, paired sample t-test), indicating that adult flies accumulate bacteria to levels greater than those of their food. Additionally, there was a significant correlation between total bacterial abundance in fly food and that in fly guts (r=0.69, p=0.003, n=16, Spearman correlation) as previously reported (23). However, in contradiction to our prediction that bacterial load drives development time, there was no correlation between total food bacterial abundance and development time (r=0.018, p=0.95, n=16 total CFUs, Spearman correlation). Instead, an individual species load, *Ao*, sped up development time significantly (r=-0.95, p=0.003, n=7 bacterial combinations with *Ao*, Spearman correlation; Fig. 2B, S7), but there was no correlation with fly physiology for the four other species. Thus, changes in *Ao* abundance in the fly food due to interactions with other bacterial species appear to impact fly developmental timing. As we noted previously, *Ao* shortens lifespan in adults, consistent with the life-history tradeoff noted in Fig. 1C.

324 ***Acetobacter orientalis* association during larval development decreases lifespan in adults**
325 To test whether development with *Ao* causes shortened lifespan versus the alternative hypothesis that
326 *Ao* shortens lifespan though its presence in adults, we reared larvae with *Ao* and then removed bacteria
327 for the entire adult phase by treating the newly eclosed adults with an antibiotic cocktail (ampicillin,
328 tetracycline, rifamycin, streptomycin). We then measured the lifespan of these flies, finding that these
329 flies had shorter lifespan than germ free flies reared in parallel and treated with the same short dose of
330 antibiotics (mean *Ao* survival 35 days vs mean germ-free survival 38 days, t-test, p=0.04, n=100 flies
331 each treatment). The results were equivalent to the fitness experiment where flies were inoculated with
332 *Ao* 5-7 days after eclosion (Fig. 1B,2C), indicating that the effects of *Ao* on lifespan can be established
333 even before adulthood and maintained through hysteresis. However, as we previously showed, this
334 hysteresis is broken by the presence of *Lp* in adulthood (Fig. 1D). Thus, despite the individual impacts of
335 *Ao*, microbiome interactions are crucial to understanding fly physiology.
336
337 **Live bacteria speed up fly developmental**
338 We next tested whether there was a maternal effect on development time by removing the maternal
339 bacterial association. We harvested eggs from germ-free flies, associated them with all 32 bacterial
340 combinations, and measured development times. This experiment uncovered no significant differences
341 in development time compared with the fitness experiment (Fig 1A), indicating that maternal effects do
342 not set development time (Fig. S9). We next tested whether active bacterial metabolism is necessary for
343 development time. We set up a replicate fitness experiment (as in Fig 1A) to measure development.
344 After the first transfer to fresh vials, we took the old vials, allowed all larvae to form pupae, and then
345 removed the pupae. We divided the replicate vials into two groups, a heat killed group and a non-heat-
346 killed group. The heat-killed vials were placed in a humidified (to prevent drying) 60˚C chamber for 1
347 hour (and tested for sterility). All the vials were then inoculated with ~30 germ-free embryos each. Flies
348 inoculated with heat-killed duplicates of the gnotobiotic experiment developed significantly more slowly
349 (p<0.005, n=16, paired sample t-test), suggesting that active bacterial metabolism (26) speeds up fly
350 development (Fig. S9). From a fitness perspective, these results indicate that female flies gain an
351 advantage for their offspring by associating with bacterial consortia.
352
353 **The mathematics of genetic epistasis allow quantification of microbiome interactions**
354 While many studies have suggested that interactions between bacteria could account for emergent
355 properties of the microbiome, there is not a universally accepted mathematical framework to calculate
356 these interactions, nor has there been a comprehensive experiment to systematically measure them.
357 Our complete combinatorial dissection of the fly gut microbiome addresses this experimental need.
358 Here we apply the mathematics of genetic epistasis to measure the interactions between bacterial
359 species. We make the explicit analogy between genes in a genome and microbial species in a
360 microbiome. We apply the framework here to quantify the complexity of the microbiome as the degree
361 of non-additivity in host traits produced by different bacterial combinations.
362
363 We first estimated the interactions between microbiome species by applying a linear least squares fit to
364 a Taylor expansion, where the interactions between *n* species are coefficients of a polynomial of degree
365 *n* ((27); see Math Supplement). Here *n* is five and there are 32 coefficients specifying (i) the one baseline
366 phenotype, (ii) the five single species contributions, and (iii) the 26 interactions due to combinations of
367 bacterial species (1+5+26=32). This approach to calculate epistatic interactions revealed significant
368 effects for each of the bacterial species individually as well as significant interactions between groups of
369 species (Fig. S10). We applied this technique to the complete dataset for fly lifespan, fecundity, and
370 development (Figs 1,2,S10). We detected many significant pairwise interactions as well as interactions of
371 higher order (3, 4 and 5 species). Many of these interactions have equivalent magnitude to the impacts

372 of individual species. For instance, the average lifespan of germ-free flies is 53 days (Fig. 2C).
373 Individually, *Ao* can shorten lifespan by 10 days (Fig. 2C). Pairwise interactions can change mean lifespan
374 by 8 days (Fig. S11). Likewise, flies colonized by all five species of bacteria survive an average of 43 days.
375 Microbiome interactions account for a 12 day (28%) increase in lifespan over the additive prediction
376 (Fig. S11). Overall, these findings demonstrate that microbiome interactions have major impacts on host
377 physiology.
378
379 To further decompose the interaction landscape and to directly calculate the effects, rather than relying
380 on a regression, we applied a combinatorial approach (Box 1), originally developed by Beerenwinkel,
381 Pachter and Sturmfels (BPS) (18) as a framework to calculate epistatic interactions between genes in *n*
382 dimensions, where *n* is the number of genetic loci considered. The method determines interactions
383 directly, rather than as a regression, using the triangulation of an *n*-dimensional cube (see Box 1).
384
385 We were able to apply the method because our 32 bacterial combinations represent the vertices of a
386 five dimensional cube (see binary in Fig 1a). This framework allowed us to calculate the interactions
387 between all gut bacterial species and their impacts on host physiology (Math Supplement). We first
388 validated the method by comparing the results with the Taylor expansion approach. The two methods
389 produced equivalent results that were highly correlated in the magnitudes of the same interactions (Fig.
390 S10). The BPS method allows us to test many more interactions, such as conditional and marginal
391 epistasis. These tests revealed significant effects of species interactions on host physiology and total
392 bacterial load (Fig. 4A-D), with wide prevalence of non-additive pairwise and high-order interactions.
393

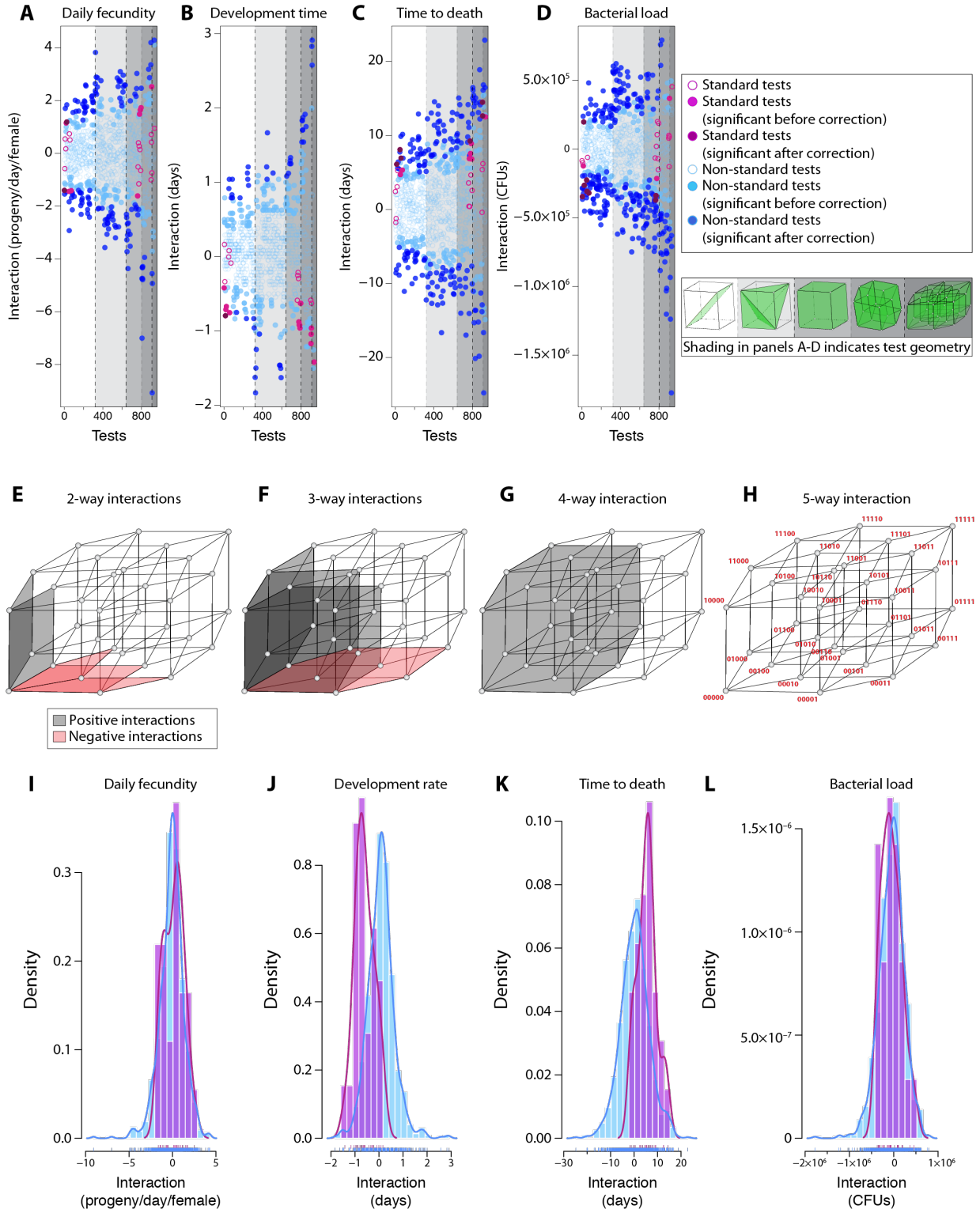

Figure 4. Microbiome interactions change host physiology. (**A-D**) Interactions become stronger as diversity increases. For (**A**) fecundity, (**B**) development, (**C**) lifespan and (**D**) bacterial load, we calculated interactions for standard tests (pink dots) and non-standard tests (blue dots) for phenotype data (Fig. 1,2). See legend for

significance at $p<0.05$. The Benjamini-Hochberg correction was applied for multiple comparison (dark fill color); open circles: non-significant interactions. See Fig. S13 for just standard tests with species identities. (**E-G**) Standard 2-way (**E**), 3-way (**F**), and 4-way (**G**) interactions for daily fecundity explained geometrically. The depicted regions inside the projection of the 5-cube correspond to specific interactions (see **H**). Positive (grey) and negative (red): compare with panel **4C**. (**H**) The vertices the 5-cube correspond to binary coded bacterial combinations as in Box 1. For daily fecundity, the single standard 5-way interaction is not statistically significant and therefore not shaded. (**I-L**) Comparisons between the distributions of standard and non-standard interactions reveal significant shifts, indicating context-dependence of the interactions due to bystander species (see Fig. 5, S12).

Interestingly, development time interactions tended to be negative (Fig. 4B), suggesting that interactions speed up development. Negative epistasis in genetics suggests that two loci are in the same pathway (*i.e.* they are redundant). By analogy, negative microbiome epistasis in development time suggests that redundant mechanisms, such as nutrition (28), might facilitate microbiome effects on the host. In contrast, lifespan interactions tended to be positive (Fig. 4C), suggesting that bacterial interactions synergistically modulate multiple pathways. Fecundity produced both significant positive and negative interactions depending on specific bacterial combinations (Fig. 4A,C), suggesting both synergy and redundancy. We visualize these interactions on the five dimensional interaction landscape to illustrate the nature of the interaction space (Fig 4E-H).

The magnitudes of the interactions, when normalized to the number of bacterial species present, were often as large as the effects of individual species introductions (see Math Supplement, Section 7.1), indicating that the species interactions are equally as important as the individual species themselves.

Box 1: Geometric interpretation of species interactions. In an analogy with genetics, we equate the presence of a bacterial species to the presence of a genetic locus. We use binary strings to denote the species composition. For two species A and B, 00 denotes the absence of both species, 01 and 10 denote the presence of only species A or B, respectively, and 11 denotes the presence of both species (indicated by green shapes). To each such string we associate a phenotype measurement w, for example, fitness. The collection of these phenotype measurements produces a phenotypic landscape (indicated by pink shapes). Like epistatic gene interactions,[9] bacterial species interactions in the fly gut can be described geometrically. A fold in the phenotypic landscape (pink shape) indicates an interaction. Interaction between two species can then be quantitatively described by the 'interaction coordinate' $u_{11} = w_{00} + w_{11} - w_{01} - w_{10}$ measuring non-additivity of the two-species combination. The interaction is positive if the sum of the phenotypes w_{11} and w_{00} is bigger than the sum of the phenotypes w_{01} and w_{10}, e.g. F 1 right panel.

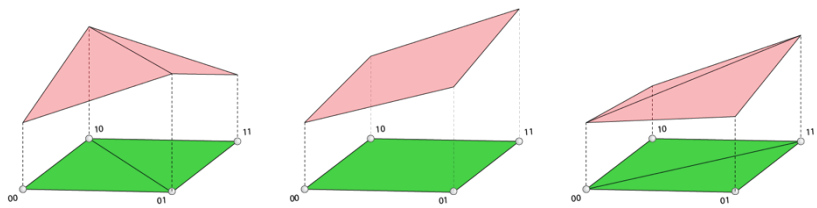

F1. Geometric interpretation of the interaction between two species.
The vertices 00, 10, 01, and 11 of the green rectangle represent the four microbiome compositions for two bacterial species. The heights above the points 00, 10, 01, and 11 represent the corresponding phenotypes. A single flat pink plane connects the four phenotype points if there is no interaction (**center**)—indicating the phenotypes are additive. The figures on the left and right represent cases in which the interaction is negative (**left**) and positive (**right**). In these cases, the red surfaces connecting the four phenotypes are divided into two triangular regions, which indicates an interaction.

This geometric approach for describing interactions generalizes to higher dimensions and yields many quantitative interaction measurements, including standard tests like u_{11} as well as non-standard tests, which compute interactions using fewer than the complete number of vertices on the cube (F2; see BPS[9] and Math Supplement for complete description). Together, these expressions can be used, for instance, to analyze how non-additivity among a subset of species combinations depends on other bystander species (Figs. 5, S12).

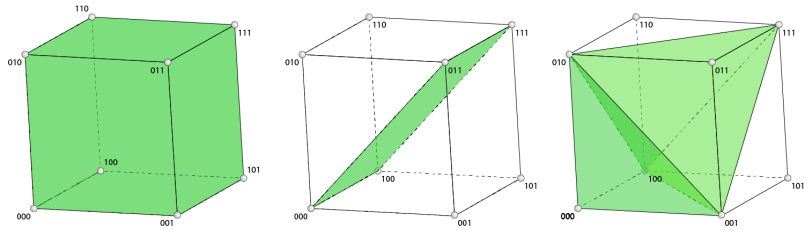

F2. Geometric interpretation of the standard three-species interaction compared with two non-standard interactions.
(**Left**) Standard three-way interaction coordinate, $u_{111} = w_{111} - (w_{110} + w_{101} + w_{011}) + (w_{100} + w_{010} + w_{001}) - w_{000}$, comparing the phenotypes (not drawn) of all eight bacterial combinations, represented as vertices of the cube. (**Center**) By contrast, the vertices of the green rectangular region describe a non-standard test, which yields the interaction coordinate $g = w_{000} - w_{011} - w_{100} + w_{111}$ involving the phenotypes (not drawn) of the four bacterial combinations 000, 100, 011, and 111. (**Right**) The five vertices of the green solid bipyramid delineate a non-standard test, $m = w_{001} + w_{010} + w_{100} - w_{111} - 2w_{000}$, derived from a linear combination of other interactions. This particular bipyramid compares the phenotypes (not drawn) of three single bacterial combinations to the combination with all three species and the germ-free case.

464
465 **Host-microbiome interactions are conditional**
466 Complexity in the microbiome could arise from context-dependent effects, where two species interact
467 differently depending on the presence of a third species. To test for context dependence, we calculated
468 pairwise interactions for each pair of species with each other possible combination of the remaining
469 three species (Fig. 5A, S12A-C). For instance, the pairwise 'interaction coordinate' is the equation

470 $$u_{10001} = w_{00000} + w_{10001} - w_{00001} - w_{10000}$$

471 that calculates the interaction between *Lp* and *Ao* alone, where u_{10001} signifies the interaction between
472 the first and fifth locus (see Box 1), w_{00000} is the phenotype measured for flies with no bacteria, w_{10001}
473 is the phenotype measured for flies with both *Lp* and *Ao*, w_{10000} is the phenotype measured for flies
474 with *Lp* only, and w_{00001} is the phenotype measured for flies with *Ao* only (see Fig 1a for binary code
475 notation; see Box 1 and Math Supplement for explanation of interaction equations). Similarly, the
476 interaction coordinate

477 $$u_{10101} = w_{00100} + w_{10101} - w_{00101} - w_{10100}$$

478 calculates the interaction between *Lp* and *Lb* when *Ap* is present. We refer to u_{10001} as a 'standard test'
479 because it calculates the interaction between all species present. We refer to u_{10101} as a 'non-standard
480 test' because it does not evaluate the effect of the bystander, *Ap*. By comparing the standard and non-
481 standard tests (see Box 1), we found that the vast majority of pairwise interactions depend on context
482 (see Math Supplement), which is an example of conditional epistasis in genetics (18). This context is
483 visualized in Figs. 5 and S12 by the cases where the different colored points, which represent different
484 sets of bystander species, do not coincide for a given test. In some cases a bystander increases the
485 magnitude of an interaction, and in other cases a bystander diminishes or annihilates the interaction.
486 Thus, the interactions measured by the test change depending on the different bystander species. We
487 next extended this analysis to ask if three-way interactions are also context-dependent. Similar to the
488 pairwise case, three-way interactions also depend on the bystander species (Figs. 5B, S12D-F).
489
490 **Low dimensional routes can traverse some high dimensional interactions**
491 In comparing the standard and non-standard tests, we observed some specific cases where a standard
492 test indicated a non-additive interaction, while certain related, non-standard tests for the same species
493 composition indicated an additive interaction (Figs. 5, S12; compare the different tests in Box 1 F2). For
494 instance, consider the standard test for lifespan interactions (black diamond) that indicates a significant
495 three-way standard interaction between *Lp*, *Lb*, and *Ao* (red, yellow, and green pie symbol in Fig. 5B).
496 However, the non-standard test equation (black circle; $i = w_{000} - w_{010} - w_{101} + w_{111}$; Math Supplement)
497 indicates additivity because it's value is not significantly different from zero. This signifies that by
498 considering *Lp* and *Ao* together as a single locus, the *Lp*+*Lb*+*Ao* lifespan is predictable as the sum of the
499 lifespans of *Lb*-colonized flies and (*Lp*+*Ao*)-colonized flies relative to germ-free flies. Therefore, our
500 methods suggest that lower-dimensional routes may exist to additively traverse the high-dimensional
501 microbiome landscape (Figs. 4E-H, 5, S12; Math Supplement's Fig. 1) if we can consider certain subsets
502 of species together as single entities. While we discovered no consistent patterns enabling the inference
503 of these groups *a priori* (Figs. 5, S12), the presence of additive low-dimensional routes suggests a path to
504 predictability. These results emphasize that bacterial species interactions significantly change the
505 impacts of individual species in the microbiome. A major challenge for the future will be to discover the
506 rules and mechanisms by which these low-dimensional interactions scale under increasing diversity.

507

A 2-way bacterial interactions

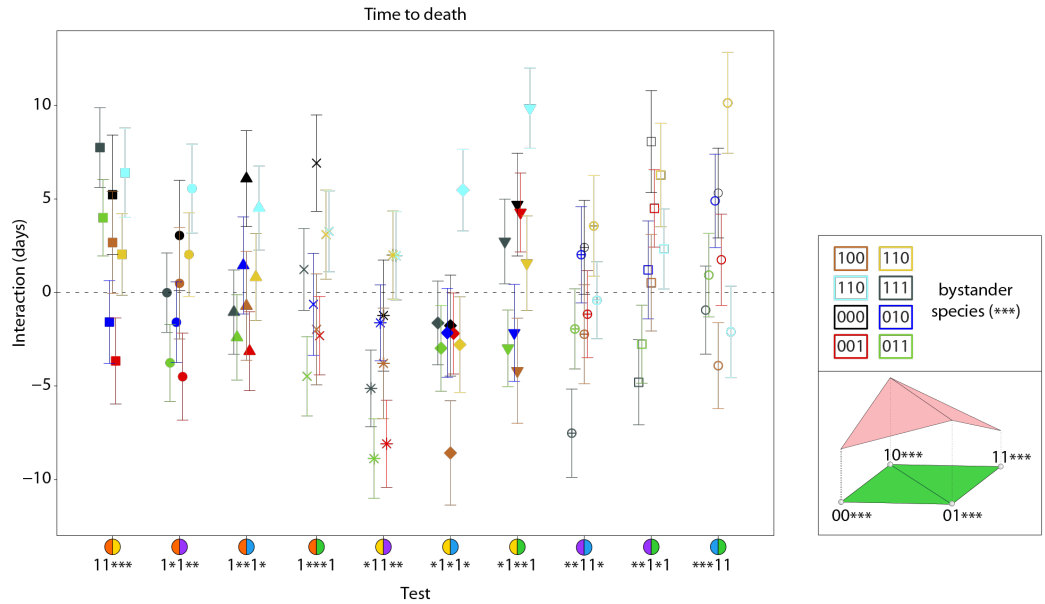

B 3-way bacterial interactions

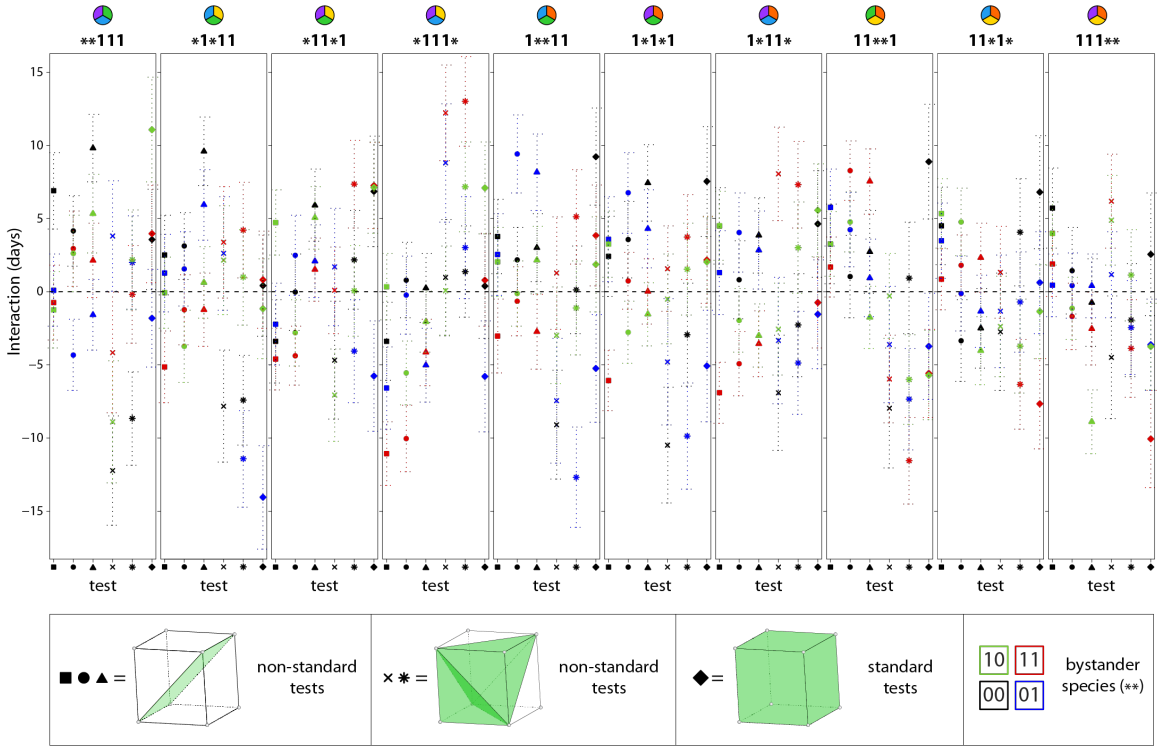

508 **Figure 5. Interactions between bacteria that impact fly lifespan depend on the context of bystander species.** (A)
509 For the fly lifespan trait, the pairwise interaction was calculated between each pair of species for each set of
510 possible bystander species. For each test, indicated by *e.g.* 11***, the '1's indicate the species for which the
511 interaction test is calculated and the '*'s indicate the possible bystander species. The binary code (*e.g.* '101') in the
512 legend indicates which of the three possible bystanders is present. For instance '000' indicates no bystanders and
513 is shown by a black point. Note the interactions change depending on the bystanders present. (B) For the fly

514 lifespan trait, the four different three-way interactions were calculated with each possible set of bystander species.
515 Interactions between sets of three species (equations *g*=square, *i*=circle, *k*=triangle, *m*=plus, *n*=ex ('x'), and
516 u_{111}=diamond in Math Supplement) are compared to determine (i) whether context of other species changes
517 interactions and (ii) whether additive non-standard tests can describe cases of non-additive standard tests. Each of
518 the 10 combinations of three species (denoted in panel titles as "k", "l", and "m") is compared along with the four
519 variants of bystander species (denoted in the panel titles as "*", and shown by the different colored symbols). The
520 differences between the colors for a given interaction test indicate that bystanders change interactions. Error bars
521 indicate propagated S.E.M.

522 Relevant equations (from Math Supplement) are:

523 $g = w_{000} - w_{100} - w_{011} + w_{111}$ (squares), a non-standard test;

524 $i = w_{000} - w_{010} - w_{101} + w_{111}$ (circles), a non-standard test;

525 $k = w_{000} - w_{001} - w_{110} + w_{111}$ (triangles), a non-standard test;

526 $m = w_{001} + w_{010} + w_{100} - w_{111} - 2w_{000}$ (pluses), a non-standard test;

527 $n = w_{110} + w_{101} + w_{011} - w_{000} - 2w_{111}$ (exes), a non-standard test;

528 $u_{111} = w_{111} - (w_{110} + w_{101} + w_{011}) + (w_{100} + w_{010} + w_{001}) - w_{000}$ (diamonds), the standard 3-way test.

529

530 **Microbial diversity increases in the intra-host environment**

531 To what extent do these microbiome-host interactions originate from direct ecological interactions
532 between bacteria versus through interactions depending on the host? To examine the microbial ecology,
533 we first applied the epistasis framework to total CFUs count data to determine interactions between
534 bacterial species. Significant positive and negative interactions of 2, 3, 4 and 5 species occur (Fig. 4D). As
535 with the fly physiology interactions, the bacterial interactions show significant context-dependence (Fig.
536 S12A,D), indicating that bystander species change interactions.

537

538 In order for specialized microbiome communities (rather than just host-microbe pairs) to evolve with
539 their host, there might be a correspondence between the factors shaping the bacterial community and
540 the bacterial community's impact on the host. We observed evidence that two individual species impact
541 lifespan and fecundity to a small but significant extent (Figs. 3D,E), which would not on its own explain
542 the whole microbiome communities that are associated with fruit flies (29, 30). We next asked whether
543 their interactions were correlated between the different phenotypes we measured (CFUs, development,
544 fecundity and lifespan; Fig. S13). Focusing on the statistically significant interactions, there is a strong
545 correlation between the interaction strengths for these different phenotypes (Fig. S13D), indicating that
546 the microbial interactions that change microbiome abundance also change fly physiology. This
547 relationship is notably in contrast to the relationship between the individual bacterial abundances and
548 fly physiology phenotypes, where only two weak linkages were established and for only two species
549 (Figs. 3D,E, S6-7).

550

551 ***In vitro* interactions do not support community diversity**

552 We next investigated the nature of the microbial ecology interactions. First, we asked what role the host
553 plays in the bacterial ecology by examining them outside the host. We inoculated the 32 bacterial
554 combinations into liquid growth media and passaged these cultures to fresh media three times at the
555 48-hour time point (when OD has stabilized). We used three rich growth media formulated to optimize
556 (i) *Lactobacillus* growth (MRS), (ii) *Acetobacter* growth (MYPL), and (iii) fly health (YG). In agreement
557 with previous reports (31), we found that *in vitro* culture supported only low diversity (Fig. 6A), with a
558 maximum of two species coexisting in the three rich media types. However, when we compare the same
559 combinations in the guts of flies *in vivo*, high diversity was maintained, up to the complete five species

community (Fig. 6A). This observation indicates that additional factors in the fly environment support microbial diversity. Microbial growth and persistence on food in the fly vial are an obvious factor, but as previously discussed (Fig. S5) we found that flies remain stably associated with their complete microbial community without ingesting microbes from the food. Thus, bacterial persistence inside the fly gut is influenced by the host gut environment. If the effect of the host environment was to segregate the bacterial species so that they do not compete, we would expect to detect no interaction between species. However, our epistasis calculations for CFUs indicate that significant interactions do occur, and they are predominantly negative, particularly at higher diversity (Fig. 4D).

Microbial community interactions promote stability

To further dissect these interactions in the context of the gut community ecology, we used the microbiome abundance data (Figs. 3B, S5) to calculate the pairwise correlations in species abundances as a function of the total number of species present in the gut (Fig. 6B). Correlations became more negative for individual species pairs as diversity increased (p=0.03, n=10 species pairs, Kendall's Tau and Wilcoxon signed rank; see Math Supplement, Sections 9.3-9.4). Weakly negative interactions in an ecosystem should promote stability and thus the maintenance of diversity granted that the interactions between species tend to be asymmetric (32). This relationship between interaction strength and symmetry is intuitive: negative interactions tend to prevent a system from leaving equilibrium. In the symmetric case, higher strength interactions increase the rate of return to equilibrium. However, for asymmetric interactions, high interaction strength favors overshoot of the equilibrium, preventing stability. Thus the stable system has weakly negative asymmetric interactions which both prevent population explosions and also dampen oscillations.

To ask whether these interactions in the fly gut are symmetric, we first calculated the directional interactions (*i.e.* A→B *vs*. B→A) based on our CFU count data. We used Paine's classic approach (33) to directly calculate interaction strength at high and low diversity (Figs. 6C, S14; see Math Supplement, Section 9.1). Interaction strength is calculated as the change in abundance of one species when a second species is removed. Thus, the general mathematical approach is related to the non-standard tests (Figs 4, 5). We rescaled Paine's equation to give a symmetric range

$$M_{ij} = \log_2\left(1 + \frac{y_i^{+j} - y_i^{-j}}{y_i^{-j}}\right)$$

where M_{ij} specifies the asymmetric interaction matrix giving the effect of species j on i. y_i^{+j} indicates the abundance of species i when j is present, and y_i^{-j} indicates the abundance of species i when j is absent. As in Paine's approach, we bootstrapped the data set to calculate the mean and standard error of the interactions (see Math Supplement, Section 9.1). To corroborate the general patterns of interactions, we used an alternate approach to calculate the asymmetric interaction matrix by implementing the classic generalized Lotka-Volterra model to the data (see Math Supplement, Section 9.2). In agreement with the correlation analysis (Fig. 6B), both methods showed that bacterial interactions are generally positive when only two species are present but that interactions are more negative at higher diversity, indicating that stability is favored by diversity.

In order to calculate the asymmetry in the interaction network, we used the approach of Bascompte *et al* (34), where asymmetry of interactions is indexed from 0 (perfectly symmetric) to 2 (exactly opposite).

$$AS_{ij} = \frac{|M_{ij} - M_{ji}|}{\max(|M_{ij}|, |M_{ji}|)}$$

where the asymmetry index between species i and j, AS_{ij}, is calculated from the terms of the directional interaction matrix, M. For the low diversity case the mean asymmetry is 1.04 (SD = 0.13), and for the high diversity case the mean asymmetry is 0.77 (SD = 0.08) (see Math Supplement, Section 9.1). Thus the interaction matrix is significantly asymmetric at both low and high diversity, favoring stability at higher diversity. High strength asymmetric interactions at low diversity are destabilizing to an equilibrium, suggesting that additional stabilizing mechanisms, such as host immunity, might mitigate the feedbacks (35). However, when four species are present, interactions are typically negative and weaker (Figs. 6C, S14), which would tend to stabilize this diversity. Thus, these stabilizing interactions are an emergent property of increased diversity, consistent with the recent theoretical prediction that higher-order interactions support diversity (36). Taking the epistatic interactions (Figs. 4, S12) and the directional interactions (Figs. 6, S14) together, we uncovered both significant positive and negative high-order interactions by both standard and non-standard tests (Math Supplement), indicating that the biological interactions determining the bacterial community in the fly gut involve more than just pairs of species (36) and that they generally become weaker and more negative as diversity increases, which would tend to favor stability.

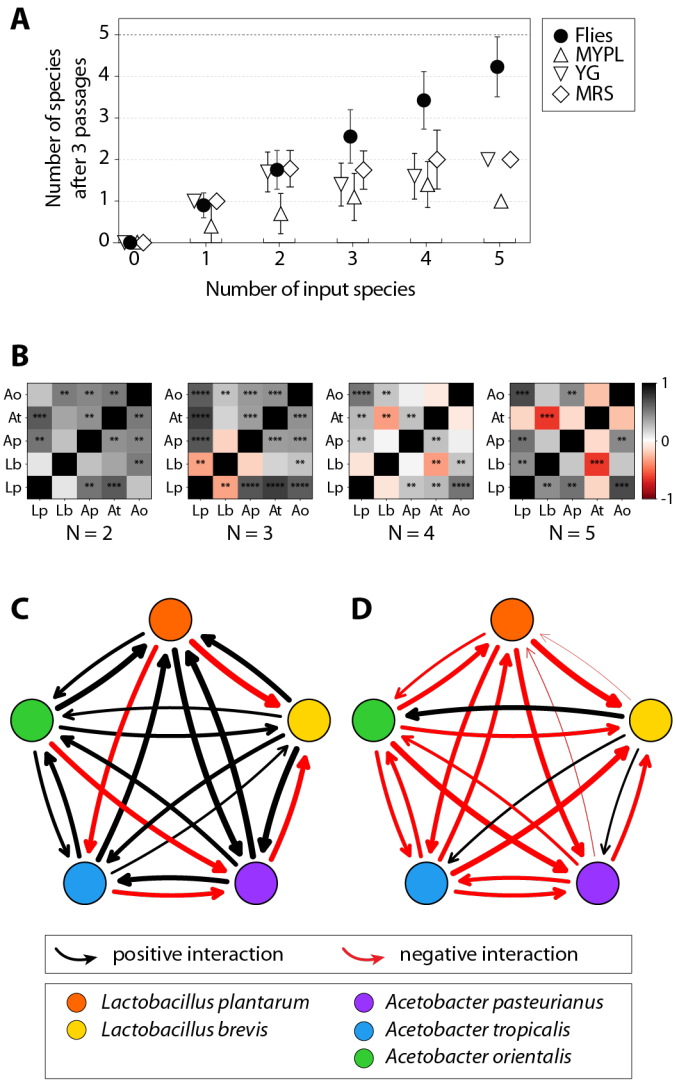

Figure 6. Microbiome interactions stabilize diversity in the fly gut. (**A**) Microbial diversity is maintained inside the fly gut to a greater degree than in liquid co-culture. The number of species detected as a function of the number inoculated shows an increase in flies but a plateau at N=2 species *in vitro*. 24 flies per bacterial treatment were continuously fed their bacterial treatment (32 total treatments) for 10 days before being flipped to fresh, germ-free food daily for 5 days. Individual flies were then crushed, plated and enumerated as CFUs (filled circles; see Fig. S5C,D). The same bacterial treatments were inoculated (3-6 replicates) into three rich media types (MRS, MYPL, and YG [open triangle and diamond markers; see Methods]) that are similar in composition to fly food, passaged three times at 48-h intervals, and assayed by plating after the third passage. Error bars S.E.M. (**B**) Pairwise correlations in abundance for the 5 species of bacteria in fly guts with totals of 2, 3, 4, and 5 species present. More positive correlations are apparent at low diversity, whereas more negative correlations occur as diversity increases (p=0.03; see Math Supplement, Section 9.3). Direct calculation of interaction strength (33) at (**C**) low (1 to 2-species) and (**D**) high (4 to 5-species) diversity based on CFU abundance data (see Figs. 3B, S5) revealed asymmetric interactions that decrease in strength at higher diversity (see Math Supplement, Section 9.1; Fig. S14). Consistent with the correlations in **B**, more negative interactions occur in more diverse guts.

617 # Discussion

618 **Microbiome interactions mediate a life history tradeoff between lifespan and fecundity**

619 Overall, we found that interactions (and not just individual species) in the fruit fly gut microbiome
620 structure both the fitness of the fly and the stability of the microbiome (Fig. 4). The magnitudes of these
621 interactions are equivalent to the effects of individual species. Thus, microbiome interactions (and not
622 just individual species) can be a major driver of evolution. While there are clear examples of mutually
623 beneficial associations between single bacteria and their hosts (37), it has remained less clear how or
624 why a complex community would persist with its host through evolutionary time. Our results show that
625 the stabilizing community interactions within the microbiome are tied to host fitness traits (Fig. S13).
626 Propagated over evolutionary time, this linkage could give rise to stable and diverse host-microbiome
627 units (a.k.a. holobionts (38)).

628

629 **Microbiome effects on lifespan are tied to tradeoffs with reproduction**

630 Many studies have documented changes in fly lifespan as a function of various factors including diet,
631 host genetics, and microbiome composition (3, 28, 39, 40). Our study links changes in lifespan to a life
632 history tradeoff with total fecundity. Furthermore, we found that interactions in the microbiome
633 mediate these tradeoffs. Interestingly, mid-life removal of the microbiome can break the life history
634 tradeoff by extending lifespan, but for certain bacterial associations (*Ao* and *Ao*+*Lp*+*Lb*), this lifespan
635 extension is not possible due to hysteresis in host physiology. We found that this hysteresis can
636 originate during early adult association with *Ao*. However, interaction with *Lp* was able to break the
637 hysteresis. *Acetobacter* and *Lactobacillus* species have been shown to individually impact fly physiology
638 through host nutrient sensing and insulin signaling (41, 42). Our results agree with these previous
639 findings. However, as we quantified the complete microbiome interaction landscape for fly fitness, we
640 found that the microbial community additionally impacts physiological tradeoffs in the host. Thus, our
641 study suggests that microbiome composition and the timing of association with the microbiome can
642 have major impacts on lifespan and life history tradeoffs (43). In a paper submitted concurrently with
643 this one, Walters *et al* show the consequences of this tradeoff for ecology and evolution of flies in the
644 wild (44).

645

646 **The *Drosophila* gut microbiome serves as an effective combinatorial microbiome model**

647 One of the major challenges in host-microbiome science is the complexity of most host-associated
648 microbiomes. The genetic model organism, *Drosophila melanogaster*, has a naturally low diversity
649 microbiome, which facilitates the study of complexity. The core members of the stable lab fly microbiota
650 in our lab, constitute only five species, which yields a total of only 32 combinations of bacteria. Under
651 the rearing conditions in our lab, we find that the five-member community stays stably associated with
652 the fly even with daily transfer to fresh food. This result is in contrast to previously published literature
653 (23). We note that a major difference in our experimental conditions is that we specifically leave out the
654 microbial growth inhibitor methylparaben, which is common to most standard fly media (25).

655 Regarding model suitability, one major question is whether such a simple system with just five species
656 can recapitulate the complex phenotypes associated with higher diversity microbiomes such as humans
657 and plants. The fact that we observe emergent properties in this simple and tractable five species
658 community makes it an attractive model for studies of microbiome complexity. Through our complete
659 combinatorial dissection of the fly gut microbiome, we have demonstrated a rich host-microbiome
660 interaction landscape.

661

662 **Quantifying microbiome interactions using mathematical principles from genetic epistasis**

663 An open challenge in microbiome complexity is how one should quantify microbiome interactions. A
664 large body of work has developed the concept of epistasis to measure genetic interactions and account
665 for different network structures (27, 45-47). Here we applied a mathematical framework commonly
666 used in genetics ((18, 48) Box 1; Math Supplement). In this framework, interactions are quantified by
667 two types of formulas, called interaction coordinates and circuits. The interaction coordinates quantify
668 basic linear interactions between species. These interaction coordinates then serve as the basis vectors
669 for the complete interaction space, which is traversed by 'circuits'. These formulas allow us to compare
670 phenotypes of different bacterial communities using a combinatorial approach (Fig 4-5, S12; see Math
671 Supplement). For each formula we also analyzed how these interactions depend upon the context of
672 other species present as bystanders (Fig. 5, S12). While there is clearly more complexity in a microbial
673 genome than in a single gene, epistasis has been applied broadly to measure genetic interactions in
674 quantitative trait locus (QTL) studies of multicellular organisms, such as chickens and rice (47). In these
675 studies, epistasis measures the degree to which the phenotype of a genotype cannot be predicted by
676 the sum of its component single locus phenotypes.

677 Our application of these general formulas to calculate interactions serves as a starting point to quantify
678 the complexity of the microbiome as the deviation from additivity. If two bacterial species cause
679 phenotypes a and b respectively in their host, then we predict that having both species together will
680 cause phenotype $a + b$. The difference between the measured phenotypes for the single and double
681 associations is the strength of the interaction. That is, an interaction is the degree to which the whole is
682 different from the sum of its parts. Complexity arises as interactions make systems behave differently
683 from the sum of their parts. Thus, this simple metric allows us to quantify the complexity of the
684 microbiome.

685 Based on our empirical results, we argue that interactions rather than just individual species may be
686 fundamental building blocks of microbiome communities. Our mathematical approach, based on
687 interaction coordinates and circuits provides a natural framework with which to explore the interaction
688 space.

689

690 **Persistence of microbiome diversity**

691 Gut microbiomes support high diversity, which facilitates complexity in the microbiome-host
692 relationship due to the increased number of potential interactions. A classic problem in ecology is how
693 this species diversity persists despite positive feedbacks that tend to destabilize the community (49).
694 Ecological models suggest that specific patterns of negative species interactions can dampen positive
695 feedbacks to produce stable communities (36, 49). Two related patterns of stabilizing interactions have
696 been proposed: (i) sufficient competition between pairs of bacteria (49), and (ii) higher-order (more
697 than pairwise) negative interactions that are emergent under higher diversity (36). Our results (Figs. 4-6)
698 are consistent with emergent higher-order interactions maintaining microbiome diversity as we observe
699 a context-dependence of interactions, with the sign of the interactions shifting to more negative (and
700 thus more stable) as diversity increases.

701

702 **Evolution of specialized host-microbiome units**

703 From an evolutionary perspective, previous reports document host-specialized microbiomes with a
704 phylogenetic signature and correlated fitness consequences of this co-adaptation (1, 50-52). A major
705 question is how these complex and specialized communities arise and how the fate of these
706 communities can be tied to that of their host. While simple pairwise obligate symbioses such as the
707 aphid-*Buchnera* association (37) have obvious benefits to both bacterium and host, it is less clear why

708 non-obligate, complex communities persistently colonize animal guts. One hypothesis would be that
709 each individual bacterial species confers a direct benefit to the host. An alternative hypothesis would be
710 that interactions between species benefit the host. We found evidence for both hypotheses, but
711 evidence that individual species impact the host was weak in more diverse microbiomes (Fig. 2).
712 Interactions between species tended to drown out the phenotypes of individual species. Importantly,
713 the same bacterial interactions that drive microbiome abundance also drive host fitness traits (Fig. S13).
714 This relationship indicates that microbial interactions shape the microbiome community structure and
715 that this structure similarly shapes host fitness, linking a diverse microbial community with its host and
716 providing the potential for co-evolution of specialized host-microbiome units.
717

Acknowledgments

The National Science Foundation Graduate Research Fellowship supported EWJ under Grant No. 1650114. The Royal Society of New Zealand partially supported AG through Rutherford Discovery Fellowship, project RDF-17-UOO-007. The David and Lucile Packard Foundation and the Institute for Collaborative Biotechnologies supported JMC through grant W911NF-09-0001 from the U.S. Army Research Office to JMC. The NIH Director's Early Independence award (1DP5OD017851-01) and the UC Berkeley MCB Dept's William Bowes Research Fellowship to WBL supported ALG, VZ, BO, and WBL**.** The content of the information does not necessarily reflect the position or the policy of the Government, and no official endorsement should be inferred. The funders had no role in study design, data collection and analysis, decision to publish, or preparation of the manuscript.

Materials and Methods

Fly stock maintenance: *Wolbachia*-free *Drosophila melanogaster* Canton-S flies were reared on cornmeal-based medium (6.67% cornmeal, 2.7% active dry yeast, 1.6% sucrose, 0.75% sodium tartrate, 0.73% ethanol, 0.68% agar, 0.46% propionic acid, 0.09% methylparaben, 0.06% calcium chloride, and 0.01% molasses). Fly stocks were maintained at 25 ˚C, 60% humidity, and 12:12 h light:dark cycles. Fly stocks were tested for the presence of known RNA viruses by RT-PCR and were virus-free (17). Germ-free fly stocks were kept in sterile conditions over multiple generations to reduce heterogeneity due to parental nutrition derived from microbiome variability.

Bacteria strains: *Lactobacillus plantarum*, *L. brevis*, *Acetobacter pasteurianus*, *A. tropicalis*, and *A. orientalis* bacteria were isolated from *D. melanogaster* flies in our lab. Bacteria were grown overnight in MRS medium in a shaker set at 30 ˚C. The bacteria were resuspended at a concentration of 10^8 cells/mL in sterile phosphate-buffered saline (PBS) for fly gnotobiotic preparations (16) so that constant numbers of CFUs were inoculated per fly vial. The 32 combinations of the 5 bacterial strains were mixed using a Beckman Coulter Biomek NXP workstation to standardize the inoculum. Vials were swabbed to ensure correct bacterial species were present without contaminants.

Germ-free fly preparation: *Wolbachia*-free and virus-free *Drosophila melanogaster* Canton-S flies reared on a cornmeal-based medium were transferred to embryo collection cages and allowed to acclimate in the cage for at least one day before egg collection. On the morning of egg collection, a yeast paste was added on a grape juice agar plate. Flies were left to lay eggs on this grape juice agar plate for 5-6 h. Eggs were then collected into a 400 μm cell strainer. In a biosafety cabinet, fly eggs were rinsed twice in 10% bleach (0.6% sodium hypochlorite) for 2.5 min each, once in 70% ethanol for 30 s, and three times in sterile dH_2O for 10 s each. Approximately 50 eggs were transferred using a sterile cotton swab to individual vials containing sterile fly medium (10% filter-sterilized glucose, 5% autoclaved active dry yeast, 1.2% autoclaved agar, 0.42% filter sterilized propionic acid). The resulting adults were maintained germ-free for at least three generations to mitigate any parental effects.

Adult gnotobiotic fly preparation: Germ-free mated flies 5-7 days post-eclosion were sorted into 10% glucose, 5% active dry yeast medium inoculated with a defined mixture of bacteria. Flies thus treated have been shown to have less variation in physiology and gut morphology (20). Inoculating in the adult phase allowed us to separate developmental differences from effects on adult flies. Each vial contained a total of $5x10^6$ CFUs (50 μL of 10^8 bacteria/mL in 1x PBS). Ten female and ten male flies were

764 transferred into each vial. Gnotobiotic flies were transferred to freshly inoculated medium every 3 days
765 for the duration of the concurrent lifespan-fecundity-development experiment (see following sections).
766
767 **For the bacterial ecology calculations** (Fig. 6), two different treatments were applied after an initial 10
768 days of inoculation where flies were inoculated as described in 'Adult gnotobiotic fly preparation.' Every
769 three days the remaining live flies were transferred to fresh food vials inoculated with $5x10^6$ CFUs/vial
770 (as with the initial inoculation) in order to reduce the effects of microbial interactions on the fly media.
771 Vial swabs were performed to check that all inoculated species were still present on the third day. In the
772 first treatment (N=24 flies per bacterial treatment), flies were immediately subjected to bacterial load
773 quantification on the 10th day of inoculation (see 'Bacterial load counts' section). This experiment lets us
774 evaluate the load and relative abundance of bacteria during the fly fitness experiment.
775
776 A second treatment was undertaken to measure the steady state of bacterial population sizes in the
777 absence of new colonization. After the initial 10 days of inoculation, these flies were transferred daily to
778 fresh germ-free food for 5 days before subsequent bacterial load quantification (Fig S5C).
779
780 **Check for contamination and correct colonization:** All fly work including media preparation and
781 transfers to fresh food was performed in a tissue culture hood using sterile technique. Contamination
782 was assessed by two methods. First, groups of 10 flies were crushed and plated to determine whether
783 they were colonized. Correct colonization was determined by colony morphology on MRS and MYPL
784 media and by 16S PCR followed by Sanger sequencing to confirm species identities. Whole fly DNA
785 extracts were also checked by PCR using both 16S and Wolbachia-specific primers. We perform these
786 tests every two weeks to maintain our gnotobiotic flies. During the fitness experiment, the correct
787 colonization was checked by swabbing the old vials after adults were transferred to fresh media.
788
789 **PCR for fly bacteria**
790 We used PCR to test for correct bacterial association and to ensure that our flies remained *Wolbachia*-
791 free. 16S universal primers to the V4 region of the rRNA gene were used to check for proper bacterial
792 association (16S V4 Forward: 5'- GTG TGC CAG CMG CCG CGG TAA; 16S V4 Reverse: 5'- CCG GAC TAC
793 HVG GGT WTC TAA T). PCR reaction mix and cycling parameters were as follows:
794 KAPA2G Robust HotStart Kit, 15uL reaction: 3uL 5X KAPA2G Buffer B; 0.3uL dNTP mix; 0.12uL KAPA2G;
795 Robust HotStart DNA Polymerase ; 0.5uL 16S V4 Forward primer; 0.5uL 16S V4 Reverse primer ; 1uL
796 template DNA ; 9.58uL dH_2O.
797 Cycling Conditions: Initial denaturation: 98C – 45 seconds; 36 cycles: 98C – 15 s, 58C – 15 s, 72C – 15 s;
798 Final Extension: 72C – 5 min; Hold at 4C.
799 *Wolbachia*-specific primers were used to check for infection every month (Wsp 81F: 5'-TGG TCC AAT
800 AAG TGA TGA AGA AAC; Wsp 691R: 5'-AAA AAT TAA ACG CTA CTC CA). The same reaction mix and
801 cycling parameters were used with the exception that denaturation, annealing, and polymerization
802 steps were all extended to 1 minute each.
803 Standard Sanger sequencing was performed to validate contamination results.
804
805 **Concurrent lifespan assay, fecundity (pupae counts), fly development**: We measured all host fitness
806 phenotypes concurrently in mixed sex populations in order to mimic more natural conditions. To
807 measure the lifespan of flies on each combination of bacteria, we recorded the number of flies living and
808 number of flies dead daily until the entire population was dead. Dead flies were removed as the vials
809 were flipped. Average daily female fecundity was assessed by counting the total number of pupae in
810 each vial after the adults were flipped to a fresh vial. In tests, we found that greater than 99% of pupae
811 eclosed into adults and therefore used pupae counts as a proxy for adults. Due to the variable

812 development times involved, vials were monitored daily for 14 days after removing the adults. To
813 determine development times, we counted the day when the first adult emerged from each vial. We
814 chose this metric because adults were housed in the same vial for 3 days and therefore the start of
815 development was not synchronized.
816
817 **Development Assays:** In the experiments presented in Fig. S9, development times were assessed for
818 each egg introduced to the vial. Eggs were first dechorionated and sterilized as described in *Germ-Free*
819 *Fly Preparation* above. Eggs were then suspended in 1x PBS with 0.1% TritonX to facilitate pipetting of
820 the eggs. Roughly 30 eggs (and always >20 eggs) were pipetted into the recipient vial. Timing of
821 pupation and eclosion in vials in which flies had previously developed were assayed at 1-day intervals for
822 non-heat-killed (blue dots) and heat-killed (red dots) preparations. For the germ-free eggs inoculated
823 with fresh bacteria (Fig. S9 black points), development timing was assessed at ~3-h intervals.
824
825 **Bacterial load counts from flies:** To assess the number of bacterial CFUs per fly (Figs. 3B, S5), flies were
826 shaken in 70% ethanol for 5 s, rinsed in ddH_2O for 5 s, and put into the well of a 96-well plate containing
827 100 μL PBS and 80 μL 0.5 mm glass beads (Biospec). Plates were heat sealed with aluminum sealing film
828 (E&K Scientific), then bead beaten for 60 s at maximum speed in a MiniBeadBeater-8 (Biospec)
829 converted to hold a 96-well plate using a custom-built attachment. Plates were then pinned with a 96-
830 pin replicator (Boekel) in three technical replicates per fly onto selective media that allowed us to
831 visually distinguish each bacterial species. Selective media were: MRS (Difco) with X-gal, which grows
832 only *Lp* (yellowish-white colonies) and *Lb* (blue colonies); MYPL with 5 mg/L tetracycline, which grows
833 only *Ap* (rounder, thicker, browner colonies) and *Ao* (flat colonies with ruffled borders); and MYPL with
834 50 mg/L gentamycin, which grows only *At* and *Ao*. Plates were grown at 30˚C. A standard curve was
835 constructed for each strain to calculate CFUs from the observed bacterial counts (Fig. S15).
836
837 **Bacterial load counts from food:** To assess the bacterial load in fly food (Fig S8), a similar protocol was
838 followed as for the whole flies. A 96-well plate containing 100 μL PBS and 80 μL 0.5 mm glass beads
839 (Biospec) was prepared. This plate was placed on an analytical balance. A small metal spatula was then
840 dipped into the fly food to gather ~10 mg of food. The food was scraped into a well of the plate and
841 weighed. The spatula was sterilized in 70% ethanol and a flame between samples. Three samples were
842 taken from separate regions of each fly vial and two separate biological replicates were made for each
843 bacterial treatment. The plate was then heat sealed, bead beaten for 60 s, replica pinned onto selective
844 media, and scored (as was done in making the bacterial counts from flies).
845
846 ***In vitro* passaging assay:** Each bacterial combination was made in 1x PBS and 5 µL of 10^7 CFUs/mL was
847 inoculated in triplicate into three rich media in 96 well plates: MRS, MYPL, and YG. YG is 50% diluted fly
848 food without agar: 5% glucose, 2.5% boiled baker's yeast, and 0.21% proprionic acid. The yeast sediment
849 has been removed by centrifugation. Culture volume was 150 µL per well. The cultures were allowed to
850 grow for 48 hours at 25˚C under constant shaking. Cells were then passaged to fresh media in 96 well
851 plates by diluting each well 10 fold and then replica pinning (Boekel 96 pin tool) to the fresh plate, which
852 delivers ~2µL. A total of three passages were made, and the final passage was replica pinned onto
853 selective agar, allowing discrimination of the 5 species' presence/absence. Selective agar were the
854 following: MRS + Xgal grows *Lp* and *Lb* and *Lb* turns blue while *Lp* is yellowish white. MYLP + 10 µg/mL
855 gentamycin grows *At* and *Ao*. MYPL + 5 µg/mL tetracycline grows *Ap* and *Ao*. *Ao*'s colony morphology is
856 distinctive and can be distinguished by eye.
857
858 **Fly activity assay**: Gnotobiotic flies were prepared as previously described. Ten females and ten male
859 flies were sorted into each vial. Each vial was flipped every 3 days into medium inoculated with the

required bacterial mixture. After the 9th day (the third flip), gnotobiotic flies were flipped into a vial containing sterile gnotobiotic fly medium (10% glucose, 5% yeast, 1.2% agar, and 0.42% propionic acid). These vials were placed into the LAM25 (Locomotor Activity Monitor; Trikinetics) kept at 25 ˚C, 60% humidity, and 12:12 h light:dark cycles and monitored for 7 days.

Fitness calculations: We estimated fitness for each bacterial treatment using a Leslie matrix (1,000 replicates per treatment). For each replicate Leslie matrix, we randomly sampled from the experimental replicates of development time, fecundity and lifespan. Female fecundity was counted as zero until the day of adult emergence. Thereafter, the fecundity was filled from the data by random sampling of the 5 replicate vials for each time point.
The diagonal was filled with '1's corresponding to the development time. After development, the adult survival data were used by randomly sampling the 5 adult survival-probability replicates for each day. The remaining values in the matrix were zeros. We then calculated the dominant eigenvalue of the matrix for each of the 1,000 replicate samplings, yielding a range of fitness estimates. This fitness value, λ, corresponds to the daily fold expansion of the population, $N_{t+1} = \lambda N_t$, under ideal conditions.

Statistical analyses: All statistics were calculated using R (v.3.3.3) (53) unless otherwise noted. Survival data average curves were calculated as the cumulative proportion of the population that died over time. A 3-parameter Gompertz function with an upper limit of 1 was selected using the 'drc' package(54) in R, $N(t) = N_0 e^{-e^{-a(t-b)}}$, where $N(t)$ is the proportion of the population surviving as a function of time (Fig. S1). Model selection using the Akaike information criterion was applied to pick the best function. The same approach was applied to fit the fecundity data (Fig. S4), resulting in a 3-parameter Gompertz, $f(t) = f_0 e^{-e^{-a(t-b)}}$.

The Shapiro-Wilk test was used to determine if data were consistent with a normal distribution. For correlation tests, Pearson correlations were used where the data were consistent with a normal distribution. Spearman correlations were used where the data were inconsistent with a normal distribution.

References

1. Moeller AH*, et al.* (2016) Cospeciation of gut microbiota with hominids. *Science* 353(6297):380-382.

2. Steinfeld HM (1927) Length of life of Drosophila melanogaster under aseptic conditions. *Dissertation thesis*:1-23.

3. Clark RI*, et al.* (2015) Distinct Shifts in Microbiota Composition during Drosophila Aging Impair Intestinal Function and Drive Mortality. *Cell Reports*:1-13.

4. Smith P*, et al.* (2017) Regulation of life span by the gut microbiota in the short-lived African turquoise killifish. *eLife* 6.

5. Travers LM, Garcia-Gonzalez F, & Simmons LW (2015) Live fast die young life history in females: evolutionary trade-off between early life mating and lifespan in female Drosophila melanogaster. *Scientific Reports*:1-7.

902 6. Roff DA & Fairbairn DJ (2007) The evolution of trade-offs: where are we? *Journal of Evolutionary*
903 *Biology* 20(2):433-447.

904 7. Stearns SC (1989) Trade-offs in life-history evolution. *Functional Ecology*:259-268.

905 8. van Noordwijk AJ & de Jong G (1986) Acquisition and Allocation of Resources: Their Influence on
906 Variation in Life History Tactics *American Naturalist* 128(1):137-142.

907 9. Cho I & Blaser MJ (2012) Applications of Next-Generation Sequencing: The human microbiome:
908 at the interface of health and disease. *Nature Reviews Genetics* 13(4):260-270.

909 10. Degnan PH, Taga ME, & Goodman AL (2014) Vitamin B12 as a Modulator of Gut Microbial
910 Ecology. *Cell Metabolism* 20(5):769-778.

911 11. Seth EC & Taga ME (2014) Nutrient cross-feeding in the microbial world. *Frontiers in*
912 *microbiology* 5:350.

913 12. Rolig AS, Parthasarathy R, Burns AR, Bohannan BJM, & Guillemin K (2015) Individual members of
914 the microbiota disproportionately modulate host innate immune responses. *Cell Host & Microbe*
915 18(5):613-620.

916 13. Ryu JH*, et al.* (2008) Innate immune homeostasis by the homeobox gene caudal and commensal-
917 gut mutualism in Drosophila. *Science* 319(5864):777-782.

918 14. Wong CNA, Ng P, & Douglas AE (2011) Low-diversity bacterial community in the gut of the
919 fruitfly Drosophila melanogaster. *Environmental Microbiology* 13(7):1889-1900.

920 15. Chandler JA, Lang JM, Bhatnagar S, Eisen JA, & Kopp A (2011) Bacterial communities of diverse
921 Drosophila species: ecological context of a host-microbe model system. *PLoS Genetics*
922 7(9):e1002272.

923 16. Newell PD & Douglas AE (2013) Interspecies Interactions Determine the Impact of the Gut
924 Microbiota on Nutrient Allocation in Drosophila melanogaster. *Applied and Environmental*
925 *Microbiology* 80(2):788-796.

926 17. Obadia B*, et al.* (2017) Probabilistic Invasion Underlies Natural Gut Microbiome Stability. *Current*
927 *Biology* 27(13):1999-2006.e1998.

928 18. Beerenwinkel N, Pachter L, & Sturmfels B (2007) Epistasis and shapes of fitness landscapes.
929 *Statistica Sinica*.

930 19. Bordenstein SR & Theis KR (2015) Host Biology in Light of the Microbiome: Ten Principles of
931 Holobionts and Hologenomes. *PLoS Biology* 13(8):e1002226.

932 20. O'Brien LE, Soliman SS, Li X, & Bilder D (2011) Altered modes of stem cell division drive adaptive
933 intestinal growth. *Cell* 147(3):603-614.

934 21. Chippindale AK, Leroi AM, Kim SB, & Rose MR (1993) Phenotypic plasticity and selection in
935 Drosophila life-history evolution. I. Nutrition and the cost of reproduction. *Journal of*
936 *Evolutionary Biology*:1-23.

937 22. Leslie PH (1945) On the use of matrices in certain population mathematics. *Biometrika* 33:183-
938 212.

939 23. Blum JE, Fischer CN, Miles J, & Handelsman J (2013) Frequent Replenishment Sustains the
940 Beneficial Microbiome of Drosophila melanogaster. *mBio* 4(6):e00860-00813.

941 24. Wong AC-N, Chaston JM, & Douglas AE (2013) The inconstant gut microbiota of Drosophila
942 species revealed by 16S rRNA gene analysis. *The ISME Journal* 7(10):1922-1932.

943 25. Obadia B, Keebaugh ES, Yamada R, Ludington WB, & Ja WW (2018) Diet influences host-
944 microbiota associations in Drosophila. *Proceedings of the National Academy of Sciences*.

945 26. Fischer C*, et al.* (2017) Metabolite exchange between microbiome members produces
946 compounds that influence Drosophila behavior. *eLife* 6.

947 27. Weinberger ED (1991) Fourier and Taylor series on fitness landscapes. *Biological cybernetics*:1-
948 10.

949 28. Yamada R, Deshpande SA, Bruce KD, Mak EM, & Ja WW (2015) Microbes Promote Amino Acid
950 Harvest to Rescue Undernutrition in Drosophila. *Cell Reports* 10(6):865-872.

951 29. Adair KL, Wilson M, Bost A, & Douglas AE (2018) Microbial community assembly in wild
952 populations of the fruit fly Drosophila melanogaster. *The ISME Journal*:1-14.

953 30. Martinson VG, Douglas AE, & Jaenike J (2017) Community structure of the gut microbiota in
954 sympatric species of wild Drosophila. *Ecology Letters* 26:32.

955 31. Friedman J, Higgins LM, & Gore J (2017) Community structure follows simple assembly rules in
956 microbial microcosms. *Nature Ecology & Evolution* 1:1-7.

957 32. Gellner G & McCann KS (2016) Consistent role of weak and strong interactions in high- and low-
958 diversity trophic food webs. *Nature Communications* 7:11180-11180.

959 33. Paine RT (1992) Food-web analysis through field measurement of per capita interaction
960 strength. *Nature* 355:73-75.

961 34. Bascompte J, Jordano P, & Olesen JM (2006) Asymmetric coevolutionary networks facilitate
962 biodiversity maintenance. *Science (New York, NY)* 312(5772):431-433.

963 35. May RM (1972) Will a large complex system be stable? *Nature* 238(5364):413-414.

964 36. Grilli J, Barabás G, Michalska-Smith MJ, & Allesina S (2017) Higher-order interactions stabilize
965 dynamics in competitive network models. *Nature* 548:210-214.

966 37. Douglas AE (2011) Lessons from studying insect symbioses. *Cell Host & Microbe* 10(4):359-367.

967 38. Rosenberg E & Zilber-Rosenberg I (2018) The hologenome concept of evolution after 10 years.1-
968 14.

969 39. Ja WW, Carvalho GB, Madrigal M, Roberts RW, & Benzer S (2009) The *Drosophila* G protein-
970 coupled receptor, Methuselah, exhibits a promiscuous response to peptides. *Protein Sci*
971 18(11):2203-2208.

972 40. Brummel T, Ching A, Seroude L, Simon AF, & Benzer S (2004) Drosophila lifespan enhancement
973 by exogenous bacteria. *Proceedings of the National Academy of Sciences* 101(35):12974-12979.

974 41. Storelli G*, et al.* (2011) Lactobacillus plantarum Promotes Drosophila Systemic Growth by
975 Modulating Hormonal Signals through TOR-Dependent Nutrient Sensing. *Cell metabolism*
976 14(3):403-414.

977 42. Shin SC*, et al.* (2011) *Drosophila* microbiome modulates host developmental and metabolic
978 homeostasis via insulin signaling. *Science* 334(6056):670-674.

979 43. Chippindale AK, Leroi AM, Kim SB, & Rose MR (1993) Phenotypic plasticity and selection in
980 *Drosophila* life-history evolution. I. Nutrition and the cost of reproduction. *J Evol Biol* 6:171-193.

981 44. Walters AW*, et al.* (2018) The microbiota influences life history tradeoffs in Drosophila
982 melanogaster. *in review*.

983 45. Pumir A & Shraiman B (2011) Epistasis in a Model of Molecular Signal Transduction. *PLoS*
984 *computational biology* 7(5):e1001134.

985 46. Sailer ZR & Harms MJ (2017) High-order epistasis shapes evolutionary trajectories. *PLoS*
986 *computational biology* 13(5):e1005541.

987 47. Carlborg Ö & Haley CS (2004) Epistasis: too often neglected in complex trait studies? *Nature*
988 *reviews Genetics* 5(8):618-625.

989 48. Beerenwinkel N, Pachter L, Sturmfels B, Elena SF, & Lenski RE (2007) Analysis of epistatic
990 interactions and fitness landscapes using a new geometric approach. *BMC evolutionary biology*
991 7(1):60.

992 49. Coyte KZ, Schluter J, & Foster KR (2015) The ecology of the microbiome: Networks, competition,
993 and stability. *Science* 350(6261):663-666.

994 50. Ramalho MO, Bueno OC, & Moreau CS (2017) Species-specific signatures of the microbiome
995 from Camponotus and Colobopsis ants across developmental stages. *PLoS One*
996 12(11):e0187461.

997 51. Kwong WK*, et al.* (2017) Dynamic microbiome evolution in social bees. *Science Advances*
998 3(3):e1600513.

999 52. Brucker RM & Bordenstein SR (2013) The Hologenomic Basis of Speciation: Gut Bacteria Cause
1000 Hybrid Lethality in the Genus Nasonia. *Science* 341(6146):667-669.

1001 53. team Rc (2017) R: A language and environment for statistical computing. (R Foundation for
1002 Statistical Computing, Vienna, Austria).

1003 54. Ritz C, Baty F, Streibig JC, & Gerhard D (2015) Dose-Response Analysis Using R. *PLoS One*
1004 10(12):e0146021.
1005

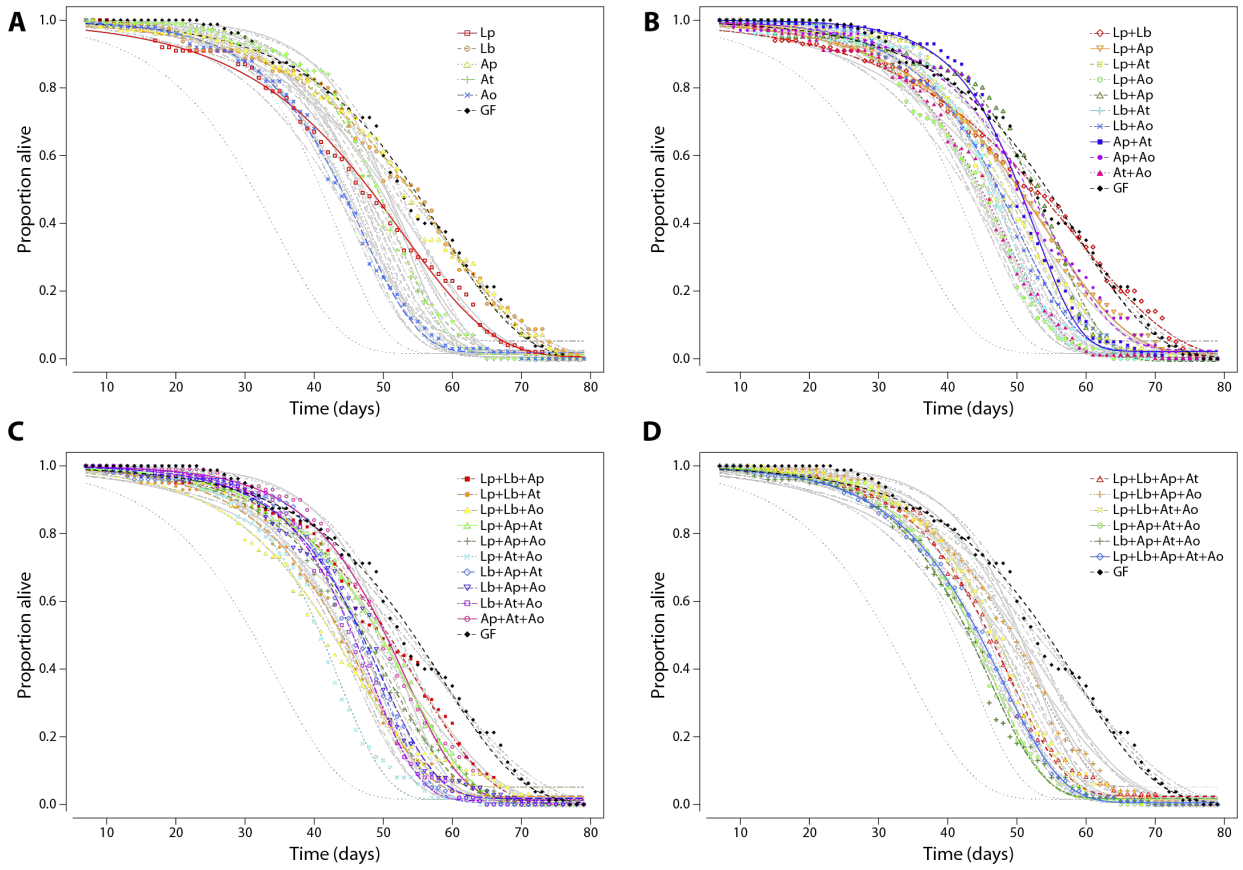

Figure S1. Curve fits to raw lifespan data aggregated from all 5 experimental replicates for each bacterial combination. Curve fits to a 3-parameter Gompertz distribution with an upper limit at one are depicted (see Methods). Bacterial combinations are grouped by the number of species. (**A**) Single species and germ-free flies. (**B**) Species pairs and germ-free flies. (**C**) Species trios and germ-free flies. (**D**) Species 4-way combinations, 5-way combination, and germ-free flies. All curves are displayed in grayscale as a reference.

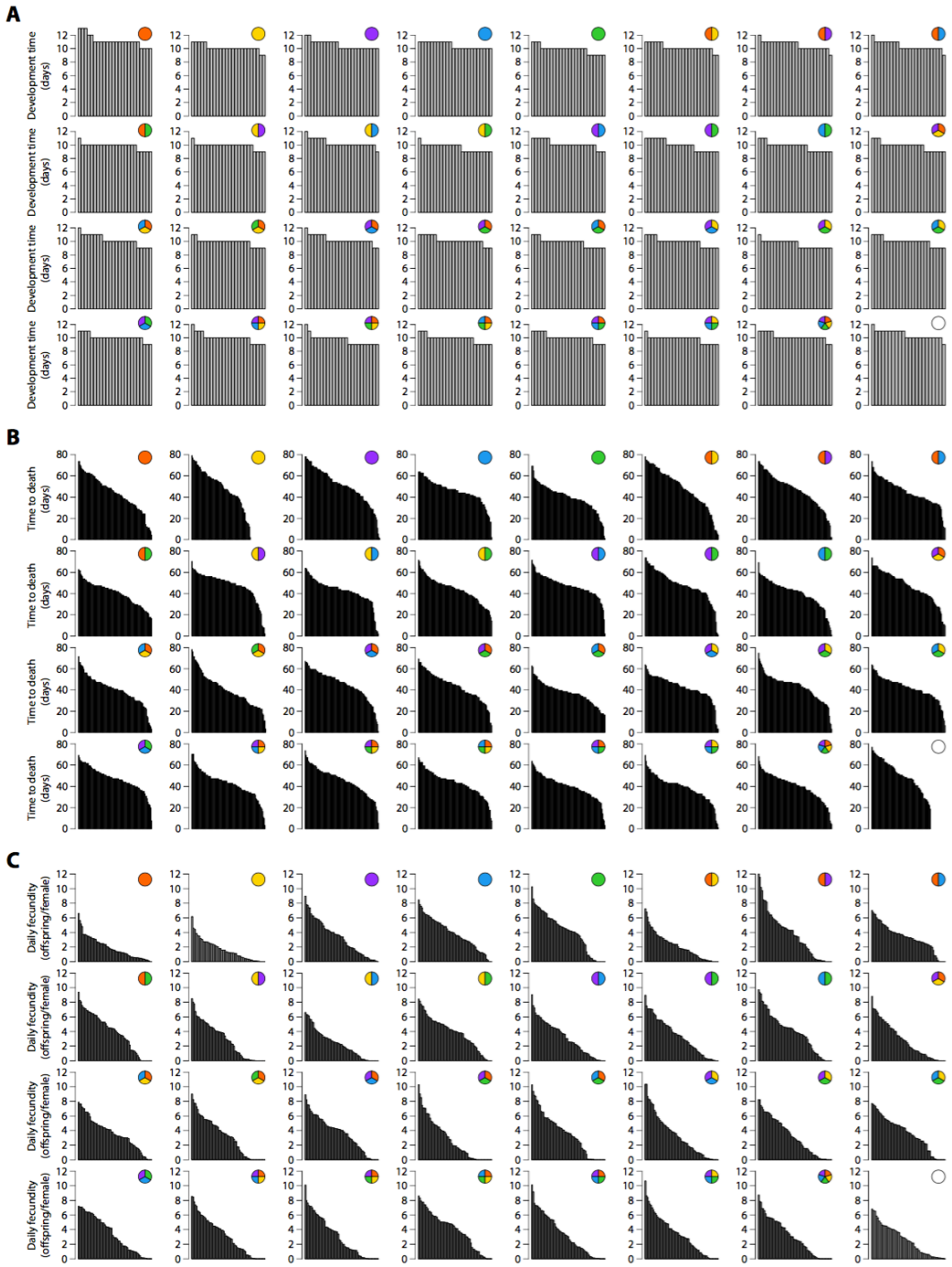

Figure S2. Raw data from development rate, fecundity, and time to death. (**a**) Raw data for development time by microbial treatment. Each bar within a treatment is the fastest-developing fly within a vial. (**b**) Raw data for time to death by microbial treatment. Each bar represents the lifespan of an individual fly. Male and female flies are aggregated because no statistically significant difference was detected between male and female lifespans in these mixed-sex experiments. (**c**) Raw data for fecundity per day per female by treatment. Each bar represents the total fecundity measured from a single fly vial normalized to the number of adult female flies.

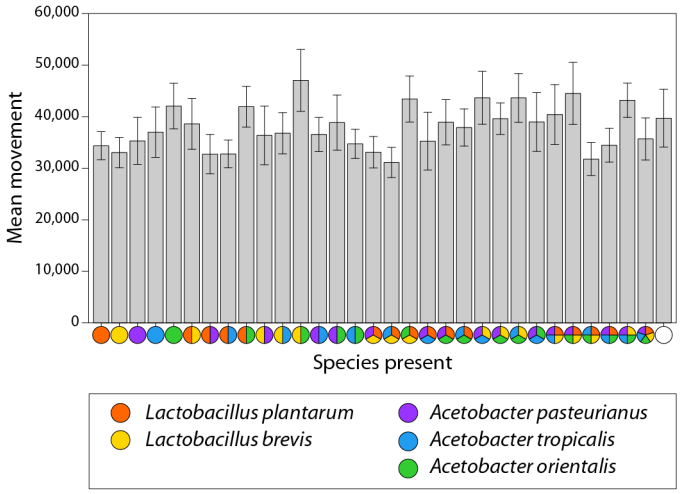

Figure S3. Average fly activity is unrelated to the fitness phenotypes. Fly movement is associated with overall metabolism, including food intake and energy expenditure. To search for behavior changes underlying the physiological differences in our bacterial treatments, we examined changes in fly motility for each bacterial treatment (n=32) in 5 replicate trials (n=20 flies per trial) using the LAMS (Trikinetics) population-based motility assay. Error bars show standard error of the mean. Trials were carried out for 7 days. Flies were flipped into fresh vials and placed in the activity-monitoring device. The first 24 h of data were removed to allow for fly acclimation to the new vial. Overall, we found no significant differences between bacterial combinations nor were there any correlations in the mean values with the other physiological data.

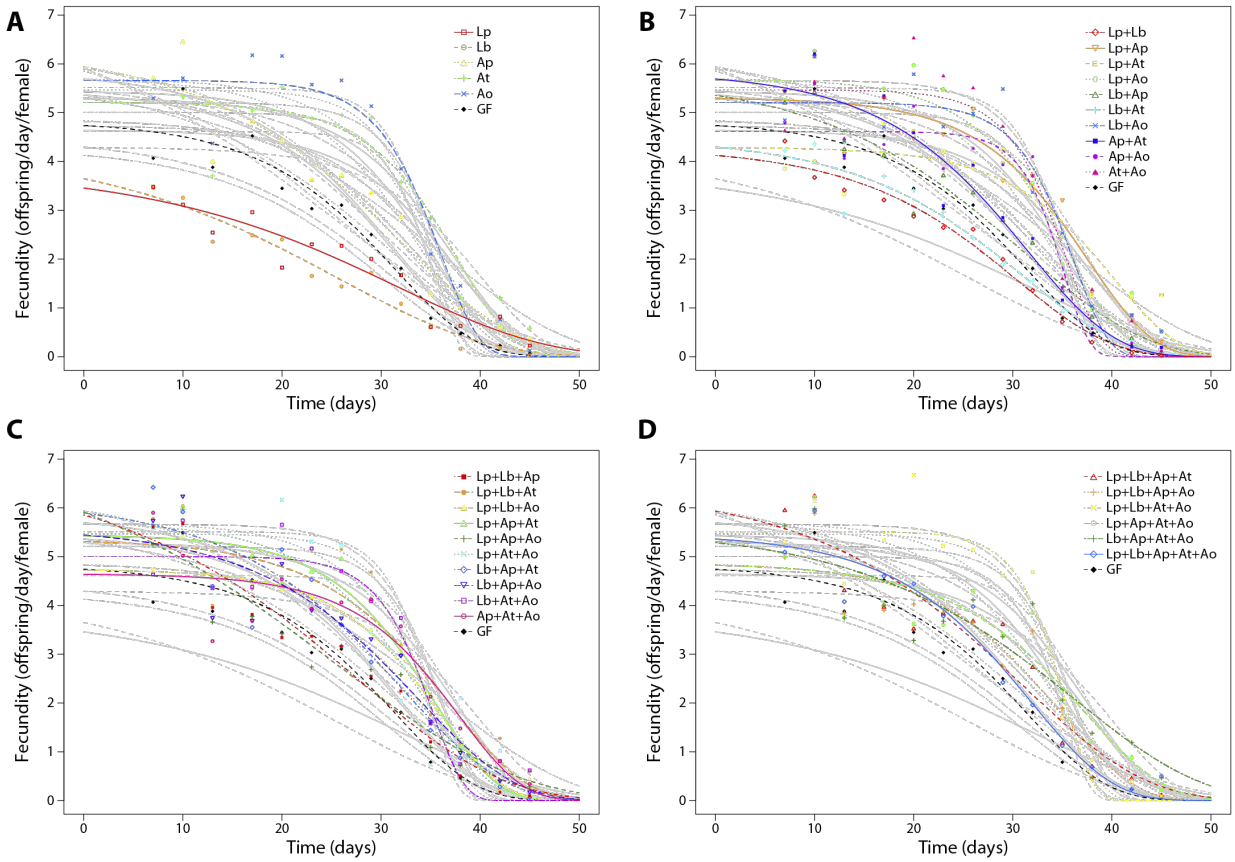

Figure S4. Curve fits to raw fecundity data aggregated from all 5 experimental replicates for each bacterial combination. Curve fits to a 3-parameter Gompertz distribution are depicted (see Methods). Bacterial combinations are grouped by the number of species. (**A**) Single species and germ-free flies. (**B**) Species pairs and germ-free flies. (**C**) Species trios and germ-free flies. (**D**) Species 4-way combinations, 5-way combination, and germ-free flies. All grayscale curves are kept as a reference.

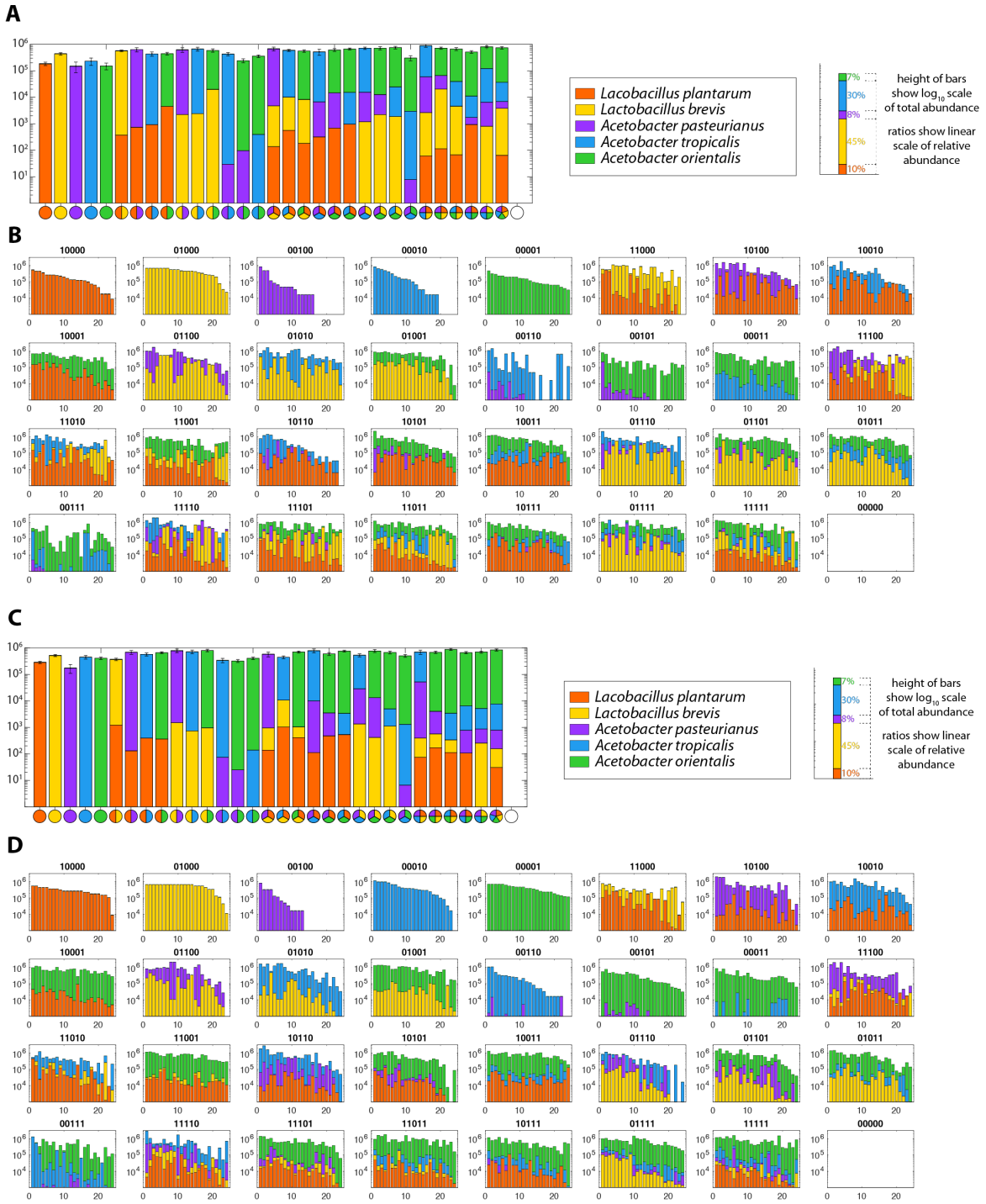

Figure S5. Raw bacterial abundance counts (CFUs) for each fly with each bacterial combination. Y-axes are CFUs on a $\log_{10}$ scale. The relative abundance of individual species is indicated by ratios on a linear scale. (**A**) Average CFUs for each bacterial combination where flies were fed defined bacteria continuously for 10 days and then crushed and CFUs enumerated. (**B**) Individual fly data for the same experiment represented in **A**. X-axes indicate the 24 individual flies. (**C**) Average CFUs for each bacterial combination. The experiment is identical to **A** with one difference: after the initial 10 days of inoculation, flies were transferred daily to fresh food for 5 days. Note that there are subtle differences between **A** and **C**. (**D**) Individual fly data for the same experiment represented in **C**. X-axes indicate the 24 individual flies.

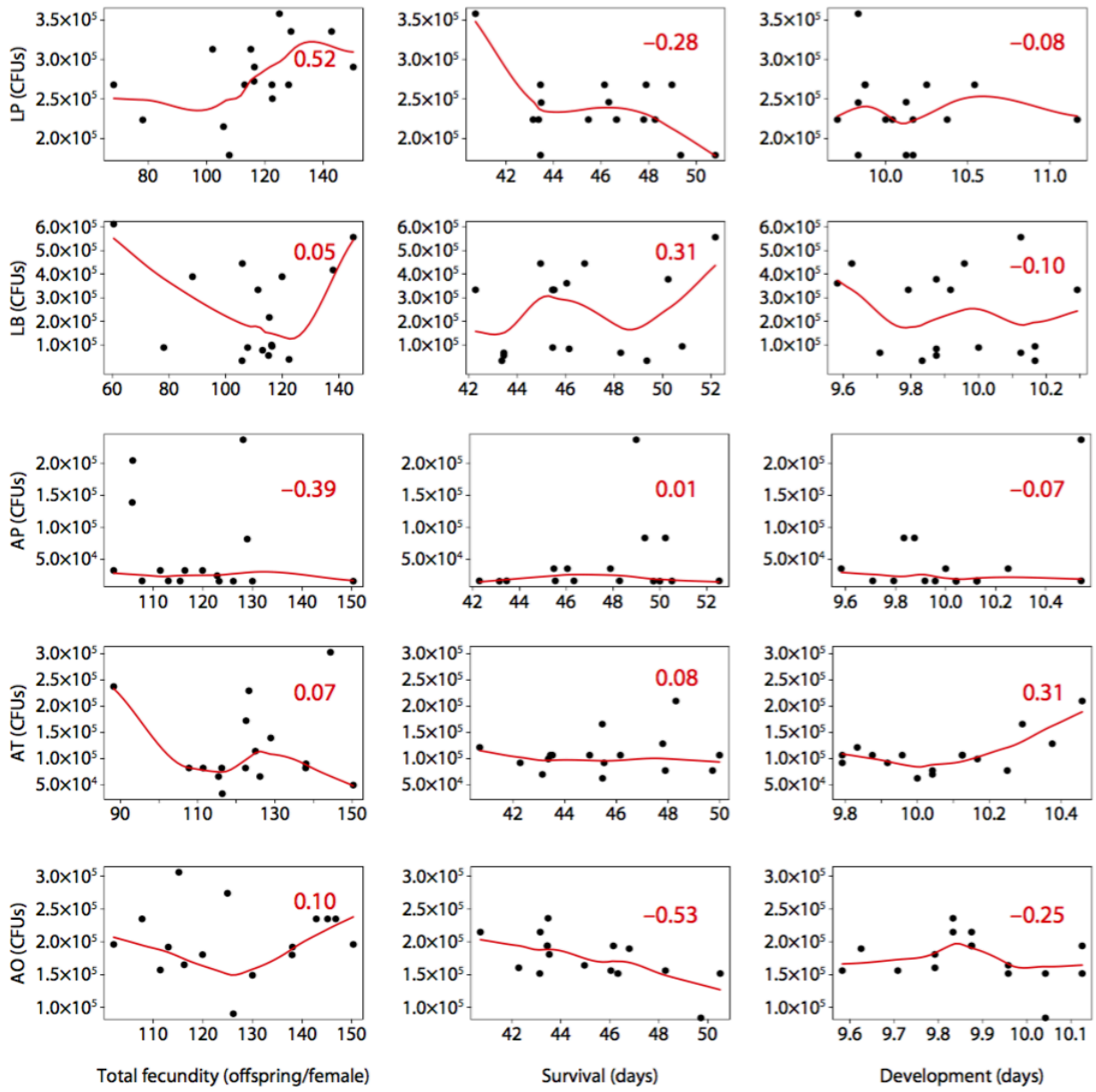

CFUs species fitness correlations plots

	Lp		Lb		Ap		At		Ao	
	r	p	r	p	r	p	r	p	r	p
TotalFecundity	**0.52**	**0.04**	0.05	0.86	-0.39	0.13	0.07	0.80	0.10	0.71
TimeDeath	-0.28	0.30	0.31	0.25	0.01	0.96	0.08	0.77	**-0.53**	**0.03**
Develop	-0.08	0.78	-0.10	0.71	-0.07	0.80	0.31	0.24	-0.25	0.35
C.V. TotalFecund	-0.21	0.42	-0.18	0.51	-0.22	0.41	0.31	0.24	0.47	0.07
C.V. TimeDeath	0.46	0.08	0.31	0.25	0.14	0.59	0.08	0.77	-0.43	0.10
C.V. Develop	0.14	0.60	0.35	0.19	0.14	0.61	0.34	0.20	0.08	0.77

Figure S6. Fly phenotype correlations with individual bacterial species abundances. Phenotype data from Fig. 2. CFU data from Fig. S5. P-values adjusted for multiple comparisons using Tukey's correction. Table shows Spearman correlations and p-values or each comparison. Coefficient of variation (C.V.) correlations are plotted in Fig. S7.

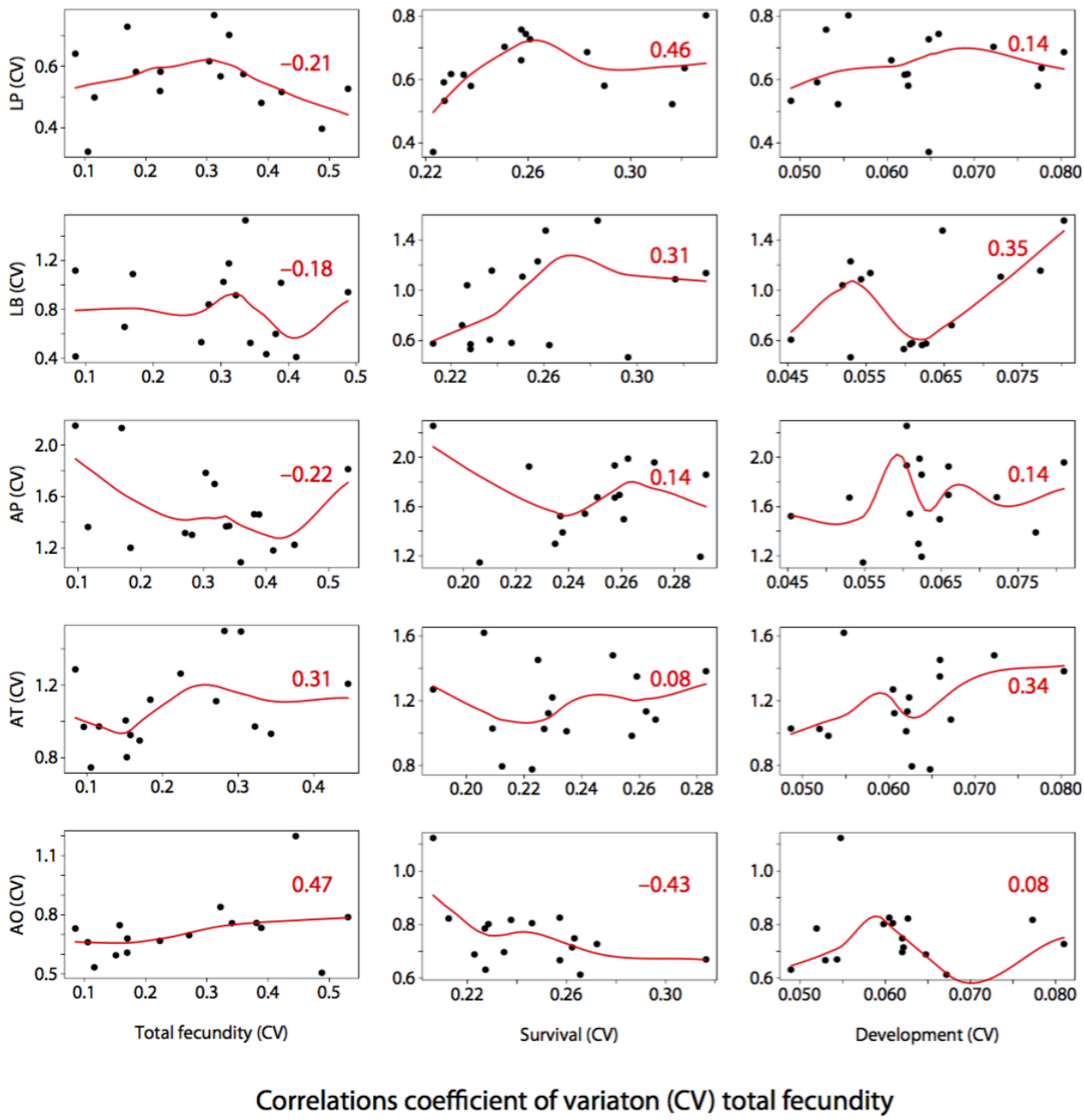

Figure S7. Correlation plots between the coefficient of variation for fly phenotypes and individual bacterial species abundances. None of the correlations are statistically significant (see Table in Fig. S6).

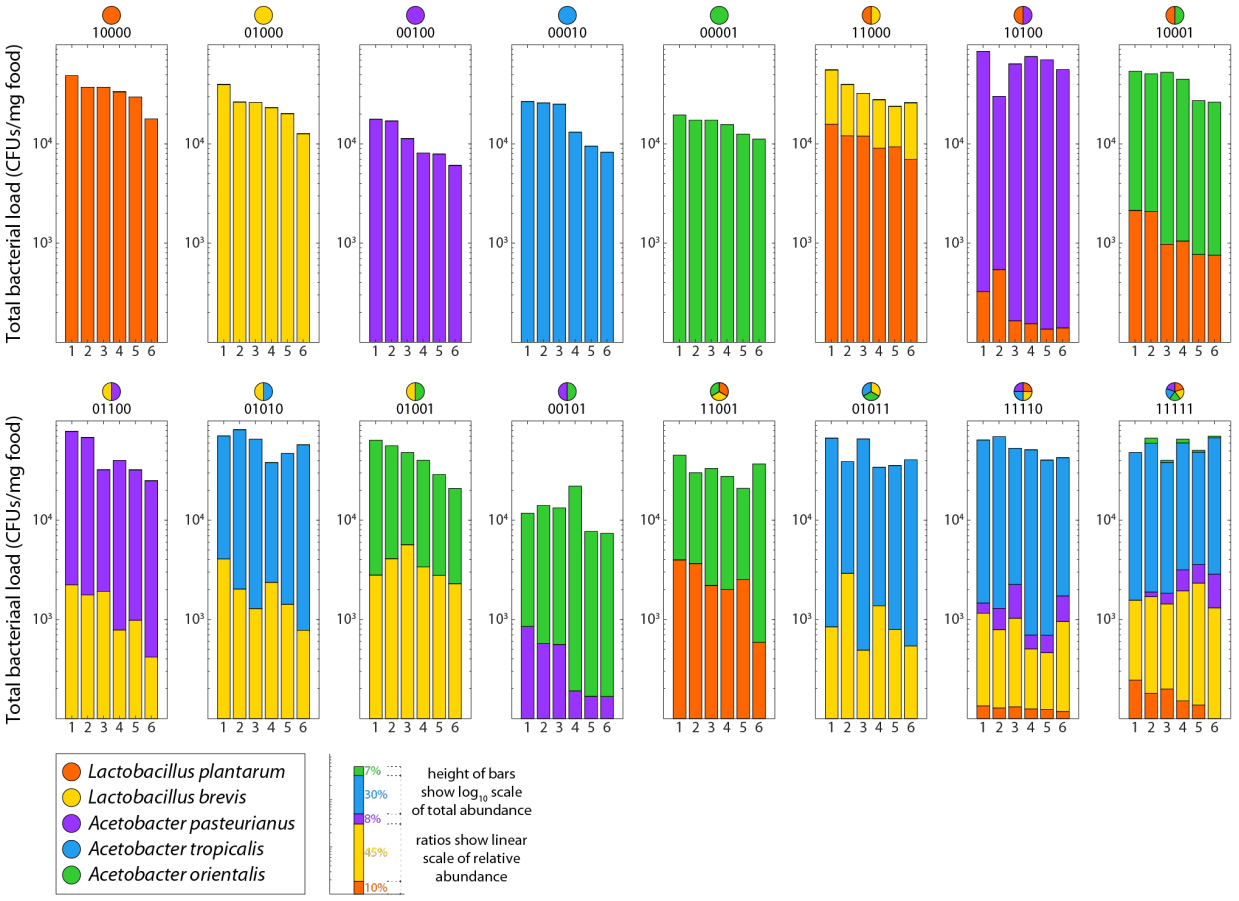

Figure S8. Raw bacterial abundance counts (CFUs) for fly food treatments with 16 selected bacterial combinations. X-axes indicate individual food samples 1 to 6. For each combination, the first three samples are from the first biological replicate, and the last three are from the second biological replicate. Y-axes are total CFUs on a $\log_{10}$ scale. The relative abundance of individual species is indicated by ratios on a linear scale.

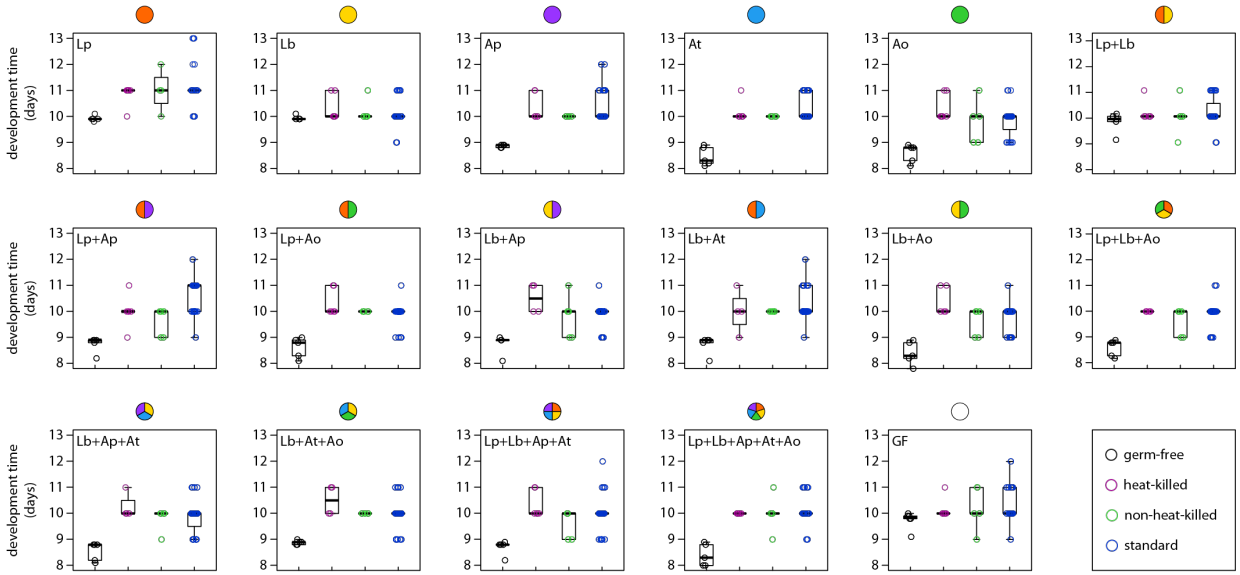

Figure S9. Parental effects and live bacteria influence offspring developmental pace. Sixteen microbial combinations and germ-free flies (indicated in upper left corners of boxes) were tested for their impacts on development time (number of days from embryo laid to adult emergence from pupal case). In the original experiments, the developmental time was measured from embryos that were directly laid by females continuously inoculated with their bacterial combination in the fitness experiment (blue data points in this figure; see also Fig. 1A, 2B). To test the role of parental effects, we experimentally varied the source of the embryos as well as the bacterial treatment. For all treatments (black, purple, green and blue data points), embryos were collected and dechorionated using 10% bleach, washed in 70% ethanol, and pipetted onto food in PBS with 0.1% Triton X detergent to prevent eggs sticking to one another (see Methods). Black points show data for n=20 embryos taken from germ-free mothers. Green points show data where colonized vials (with flies and bacteria) were emptied of all their flies (and larvae) and then n=20 germ-free eggs were introduced. No significant differences were detected in development between standard and non-heat-killed vials (paired sample t-test, $p>0.18$, n=500). Purple points indicate development in vials that were heat-killed at 60˚C for 1 hour in a humid chamber to prevent drying (and tested for sterility) prior to the introduction of germ-free eggs. This treatment significantly increased the development time by 8 hours (paired sample t-test, $p<0.005$, n=178; see main text Fig. 3F). The fastest development times were for eggs introduced to fresh vials inoculated with bacteria but without previous fly occupation. In this treatment (black dots), there was very little variation between treatments except that flies lacking all *Acetobacter* species (Lp, Lb, Lp+Lb, germ-free) were delayed by 1 to 2 days with respect to their cohort. Box and whisker plots: box shows 25th to 75th percentile. Thick bar shows median. Whiskers extend to 1.5x the interquartile range. All data points are also shown with each box. The time resolution for these experiments is 1 day.

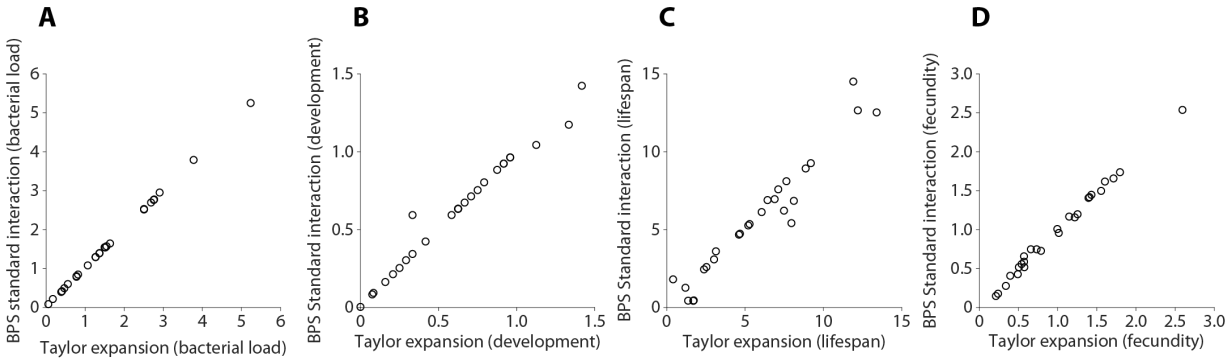

Figure S10. The BPS direct calculations of 'standard interactions' are highly correlated with Taylor expansion linear least squares fitting of interaction coefficients. (A) CFUs in units of colony forming units (r^2=0.99, $p<10^{-30}$, n=26), (B) Development time in units of days (r^2=0.97, $p<10^{-19}$, n=26), (C) Lifespan in units of days (r^2=0.93, $p<10^{-14}$, n=26), and (D) Fecundity in units of viable offspring per female per day (r^2=0.99, $p<10^{-26}$, n=26).

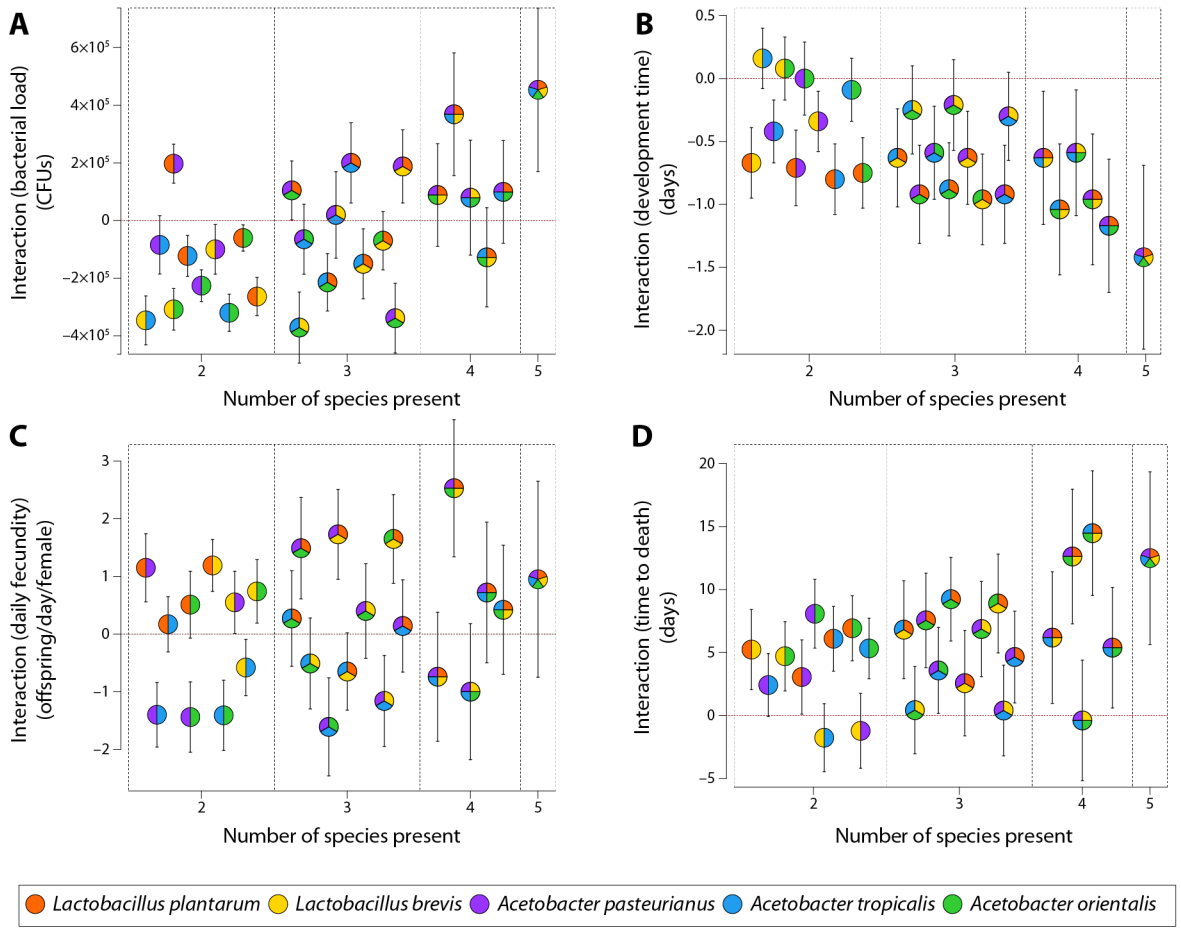

Figure S11. Standard interactions calculated for each phenotype in Fig. 2 and Fig. 3a-d. For all four phenotypes ((**A**) CFUs, (**B**) development time, (**C**) fecundity, (**D**) lifespan) we computed the same 26 standard interactions. In the plots we separated interactions by the number of bacterial species involved (x-axis). The different bacterial combinations are expressed in colors. As general trends, we observe that the same interactions decrease for development time while they increase for time to death, when the diversity of the bacterial species in the microbiome increases (see Fig. S13). See also T-polynomials (Math Supplement). Error bars are the propagated standard error from the raw phenotypes.

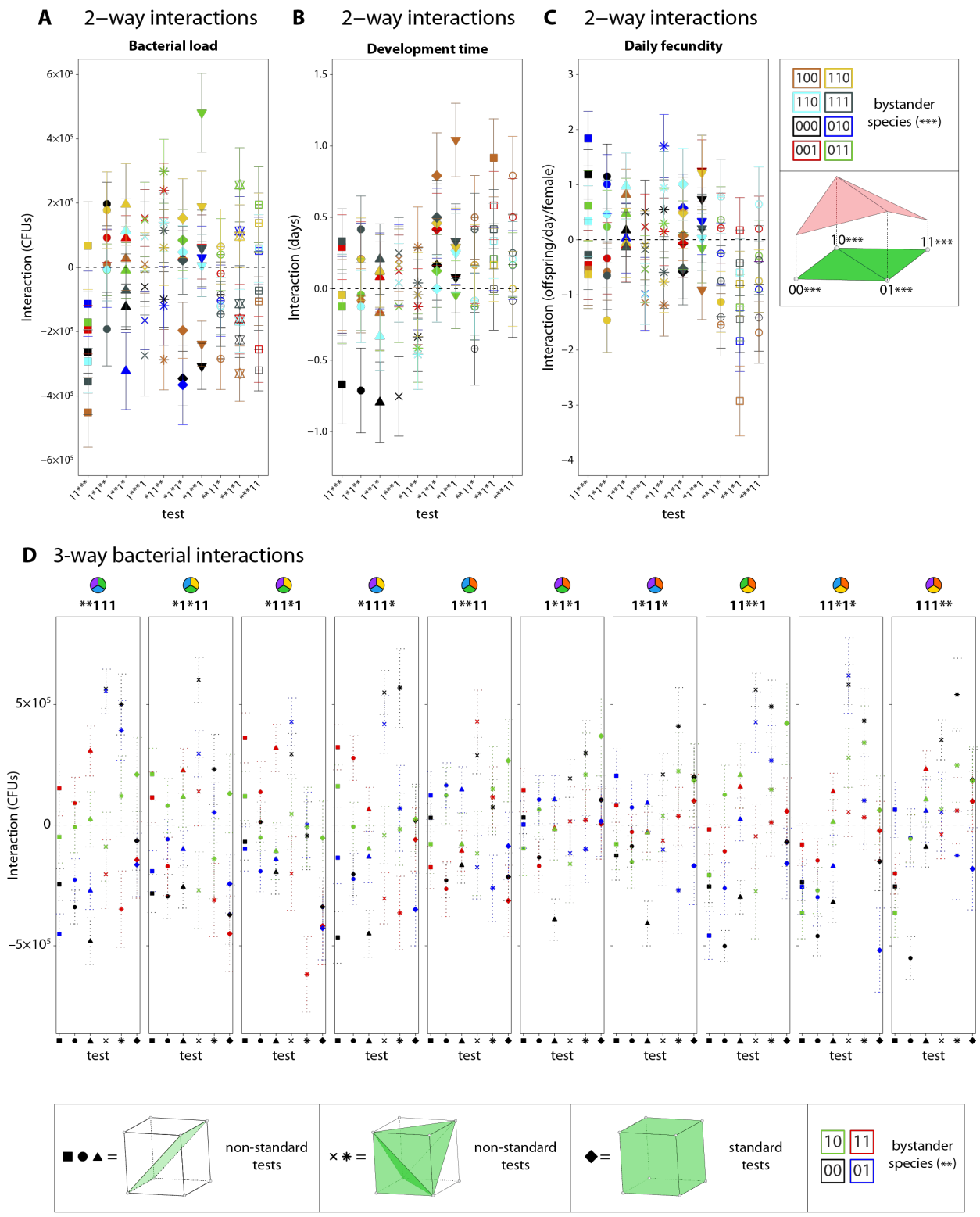
A 2–way interactions
Bacterial load
Interaction (CFUs)
test
B 2–way interactions
Development time
Interaction (days)
test
C 2–way interactions
Daily fecundity
Interaction (offspring/day/female)
test
100 110
110 111
000 010
001 011
bystander species (***)
10***
11***
00***
01***
D 3-way bacterial interactions
**111
*1*11
*11*1
111
1**11
1*1*1
1*11*
11**1
11*1*
111**
Interaction (CFUs)
test
non-standard tests
non-standard tests
standard tests
10 11
00 01
bystander species (**)

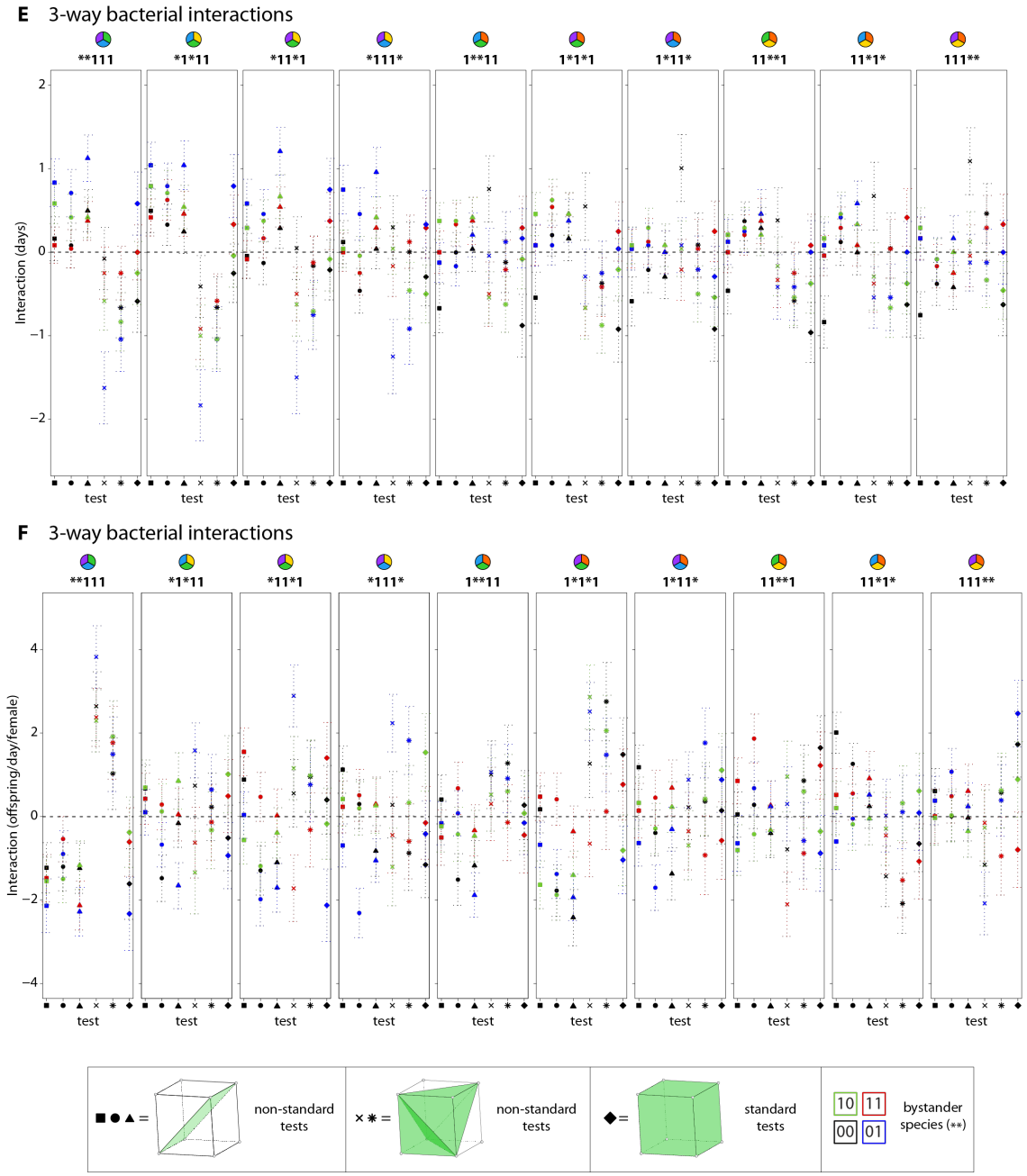

Figure S12. Detailed comparisons of the context-dependence of two-way and three-way interactions depending on bystander species. The pairwise interaction was calculated between each pair of species for each set of possible bystander species as in Fig. 4A for (**A**) bacterial load, (**B**) development time, and (**C**) fecundity. The standard three-way interaction as in Fig. 4B was compared with the related non-standard tests as a function of bystander species present for (**D**) bacterial load, (**E**) development time, and (**F**) fecundity**.** Interactions on the total bacterial load in flies between sets of three species (equations *g*=square, *i*=circle, *k*=triangle, *m*=plus, *n*=ex ('x'), and u_{111}=diamond in Math Supplement) are compared to determine (i) whether additive non-standard tests can

describe cases of non-additive standard tests and (ii) whether context of other species changes interactions (see Main Text).

Relevant equations (from Math Supplement):

$g = w_{000} - w_{100} - w_{011} + w_{111}$ (squares) non-standard test;

$i = w_{000} - w_{010} - w_{101} + w_{111}$ (circles) non-standard test;

$k = w_{000} - w_{001} - w_{110} + w_{111}$ (triangles) non-standard test;

$m = w_{001} + w_{010} + w_{100} - w_{111} - 2w_{000}$ (pluses) non-standard test;

$n = w_{110} + w_{101} + w_{011} - w_{000} - 2w_{111}$ (exes) non-standard test;

$u_{111} = w_{111} - (w_{110} + w_{101} + w_{011}) + (w_{100} + w_{010} + w_{001}) - w_{000}$ (diamonds), the standard test.

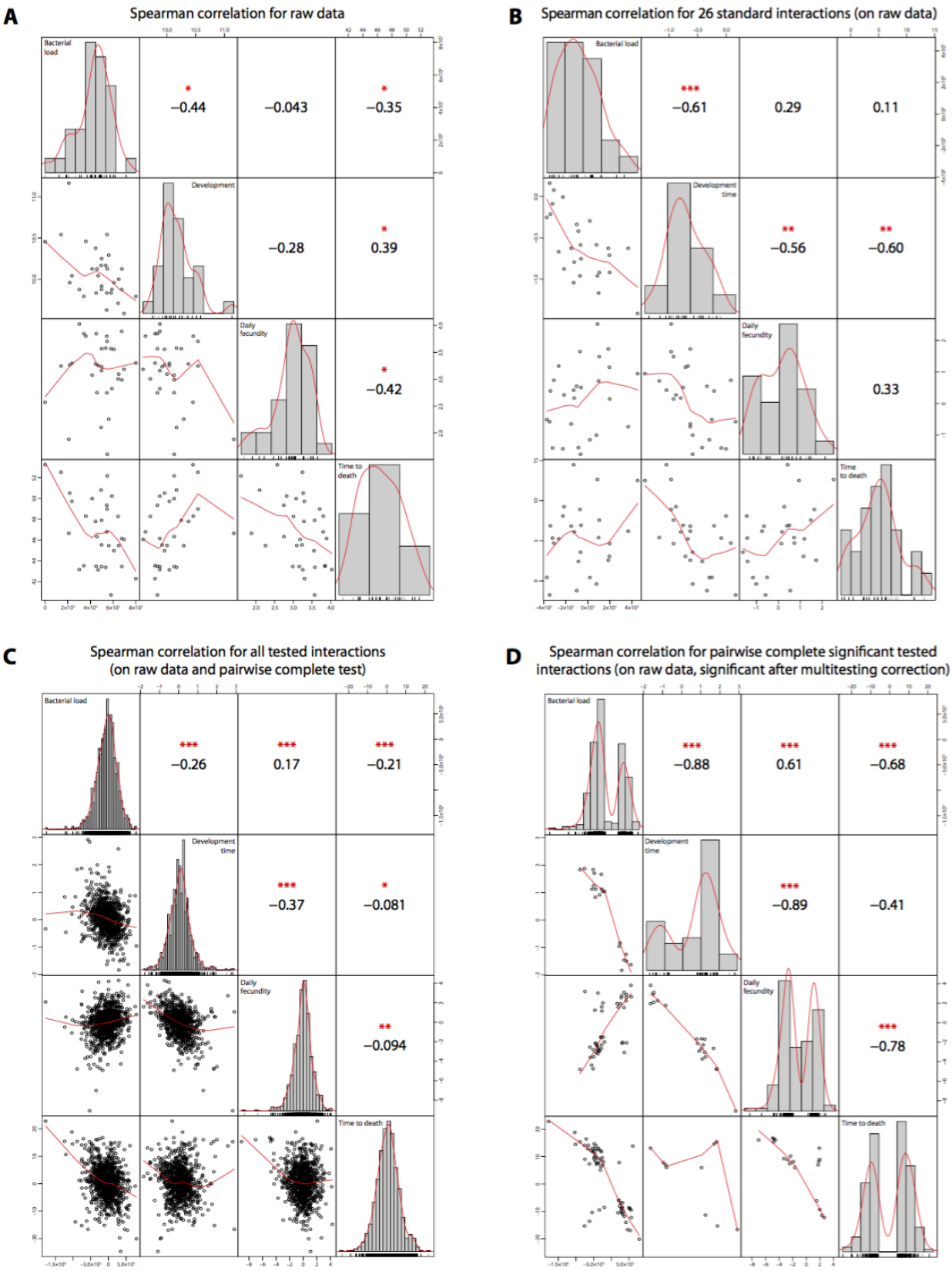

Figure S13. Correlations of raw phenotypes and interactions. (**a**) Raw data correlations between measured host and bacterial phenotypes indicate significant relationships between phenotypes except between fecundity and

development and between fecundity and bacterial load. (**b**) Correlations of all standard interactions between measured host and bacterial phenotypes reveal different relationships than the raw phenotype data (compare with **a**). (**c**) Correlations of interaction strengths for all standard and non-standard tests (26+910=936) highlight significant relationships between all phenotypes. (**d**) Significant interactions have opposite sign between phenotypes except between bacterial load and fecundity, which have the same sign. We observed significant relationships between all phenotypes. Correlations of only significant interactions (where the interaction was significant for both phenotypes) after multiple comparison correction (standard and non-standard tests) between measured host and bacterial phenotypes are shown. Scatter plots appear below the diagonal and histograms are on the diagonal (gray bars = histogram; red line = kernel density function with Gaussian kernel). Correlations are all Spearman coefficients (data were not all normally distributed; Shapiro-Wilk tests). Significance values (*$p<0.005$; **$p<0.001$; ***$p<0.0001$) appear above the diagonal.

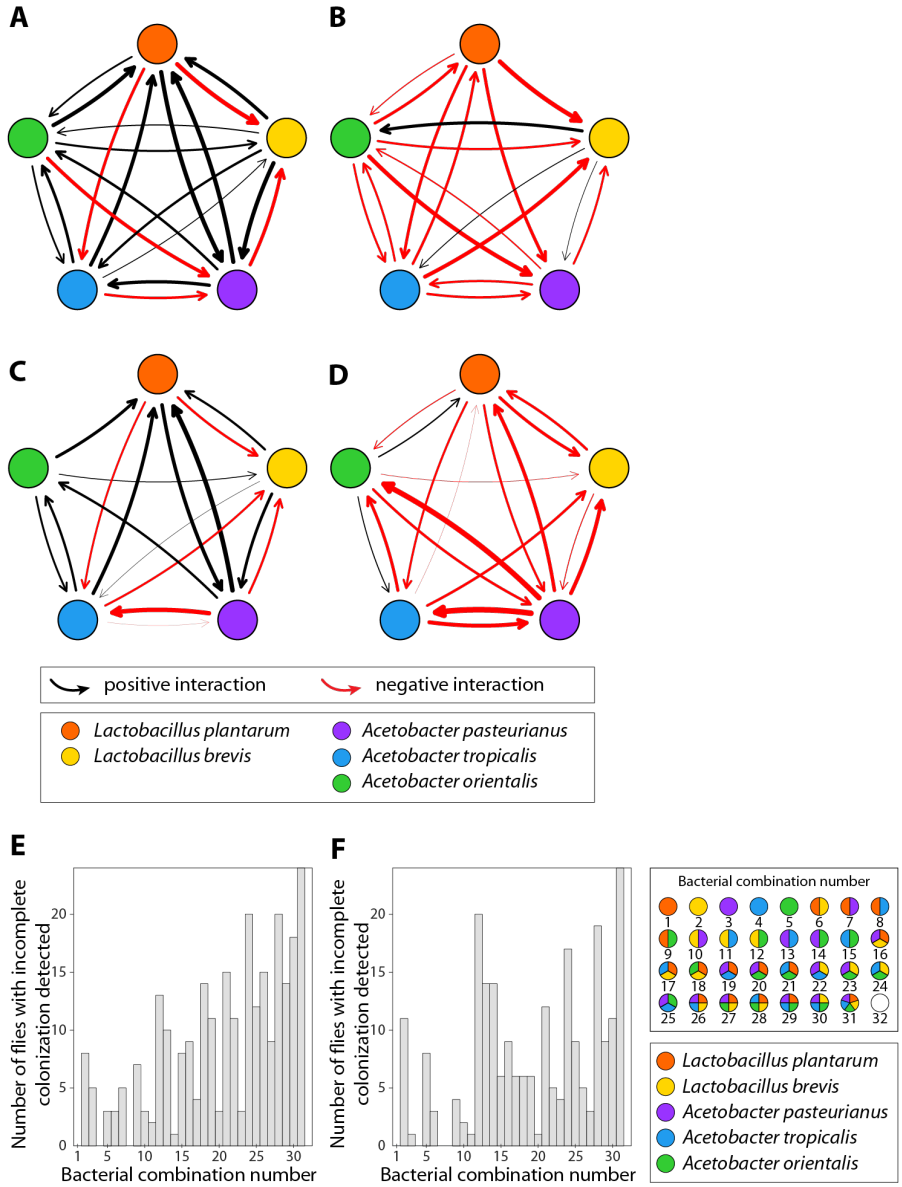

Figure S14. Pairwise bacterial interactions in the fly gut transition from positive to negative as diversity increases. Interaction strength was calculated by fitting the generalized Lotka-Volterra equations for pairwise interactions (see Math Supplement). Mean microbial abundances from Fig S5 were used to fit the equations. (**A**) Interactions calculated by Paine's (33) method for mean CFU abundance data from bacterial combinations with one or two species. (**B**) Interactions calculated by Paine's (33) method for mean CFU abundance data from bacterial combinations with one or two species. (**C**) Interactions calculated using the Lotka-Volterra fitting approach with all individual fly CFU abundance data from bacterial combinations with one or two species. (**D**) Interactions calculated using the Lotka-Volterra fitting approach with all individual fly CFU abundance data from bacterial combinations with 3, 4 or 5 species. (**E**) The number of flies where not all inoculated bacterial species were detected (1,000 CFUs limit of detection) increases as the total species diversity increases when flies were continuously fed bacteria. (**F**) The number of flies where not all inoculated bacterial species were detected (1,000 CFUs limit of detection) increases as the total species diversity increases when flies were daily transitioned to germ-free food for 5 days following an initial 10-day continuous inoculation period. For Fig. 6C,D and S14A,B, flies where not all inoculated bacterial species were detected were eliminated from the analysis.

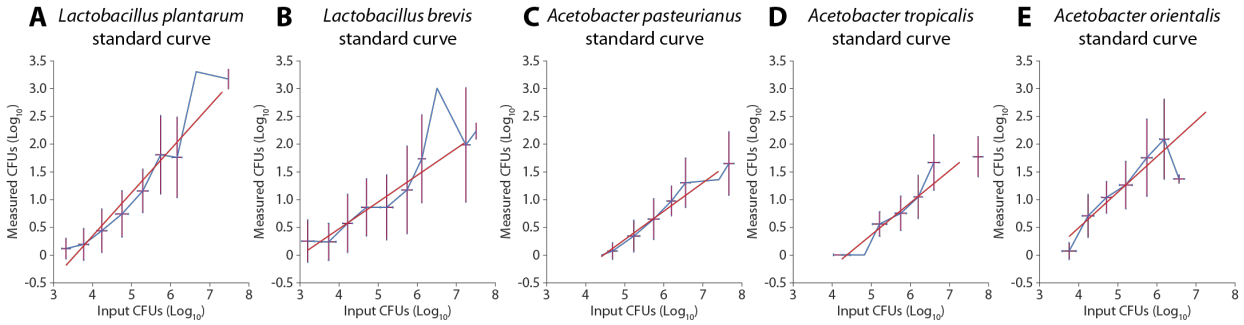

Figure S15. Standard curves used to calculate total CFUs from colony counts (Fig. S5, S8). A standard curve was constructed by plating known concentrations of bacteria on selective medium with a 96-pin replicator as in *Bacterial load counts* (Methods). Counts were fit to a power law curve using the NLINFIT function in MATLAB v2017a.

Math Supplement: Mathematical Framework for Detecting Microbiome Interactions in the Host

May 31, 2018

Contents

1 Availability of code **2**

2 Introduction to Geometric Interactions (Figure 4) **2**

3 Glossary for interactions - Mathematical Terminology **3**

4 Two disjoint families of interactions: standard and non-standard tests **4**
4.1 Standard interactions 4

5 Non-standard interactions **6**
5.1 Interaction coordinates 8
5.2 Circuits 8
5.3 Recursively constructing higher order interactions from lower order interactions 9

6 Significance testing of interactions **11**

7 Supplemental Results of Interaction Testing **12**
7.1 Computed standard interaction tests 12
7.2 Comparing the relative importance of individual bacterial species versus their interactions in determining physiological traits 13
7.3 Results for all computed interactions from Figs. 4, 5, and S12 14

8 Discussion of Interaction Coordinates **16**

9 Pairwise species interactions (Figure 6) **16**
9.1 Bacterial interactions determined by Paine's method (Figure 6C,D, S14A,B) 16
9.2 Bacterial interactions fit by a generalized Lotka-Volterra model (Figure 6c) 17
9.3 Pairwise correlations (Figure 6B) 19
9.4 Determining statistical trends 19

10 Supplements **19**
10.1 Data transformation 19
10.2 Spurious epistasis in the microbiome 21
10.3 Simulated data 21

1 Availability of code

The Python code for computing interactions coordinates and circuits in a system of n-bacterial species is available on Github, see [8]. The code can also be used to compute the magnitude of an interaction as well as the statistical interval in which an interaction is contained if the starting measurements are given as intervals.

2 Introduction to Geometric Interactions (Figure 4)

It is in open question in the microbiome field of how to quantify the many possible interactions between different bacterial species within a microbial community and to measure how these interactions impact host physiology traits. Here, we apply the mathematics of genetic epistasis to the microbiome. We explicitly make an analogy between genetic loci in a genome and bacterial species in a microbiome in order to calculate the interactions between species in a microbiome and their effects on host physiology. The basic assumption is that if two bacterial species have independent effects on the host, their phenotypes will be additive. The interaction is the degree to which this assumption is incorrect.

For an n-genotype system, genetic interactions, *i.e.* epistasis, are commonly described in terms of 'interaction coordinates' and 'circuits' (see work of Beerenwinkel, Pachter, and Sturmfels[2]). Interaction coordinates are equations that calculate the effect of interactions between genetic loci on organismal traits. 'Circuits' use the interaction coordinates as basis vectors and can give a richer description of the complete interaction space (see [2] for details). Circuits can, for instance, ask how much of a three-way interaction can be explained by a two-way interaction between individual species. Beerenwinkel, Pachter, and Sturmfels (BPS) described a formal mathematical framework to quantify interactions between genetic loci in an n-locus system [2]. The combinatorial nature and flexibility of the approach make the BPS framework generalizable to different types of high dimensional interacting systems beyond gene networks. Here we apply the formal framework with its interaction coordinates and circuits to the microbiome.

Besides a graspable biological interpretation, interaction coordinates and circuits also have a geometric interpretation, as these are formulas whose terms can be parametrized by certain sets of vertices on an n-cube and where n is the number of loci considered. These higher order interactions generalize several well-known and widely used notions of gene interaction, including Fourier-Walsh coefficients (see Box 1 in Weinreich, Lan, et al. 2013 [12]). This geometric interpretation is particularly useful, as it facilitates the parametrization of these types of formulas. Different sets of vertices in an n-cube then yield different circuits.

Here, we study interactions of up to five bacterial species, which we have found to be the minimal set of consistently occurring, stably associated species in wild and laboratory *Drosophila melanogaster* fruit flies. In this work, we exploit the combinatorial geometry of the 5-cube. We examine lower dimensional cubes and lift well known lower rank interactions to the higher dimensional space. For instance, we test whether the positive interaction between Ap and Lp stays positive when At is introduced. By this we mean, we compare the formulas of the following type:

$$u_{10100} = w_{00000} + w_{10100} - w_{10000} - w_{00100}$$
$$u_{10110} = w_{00010} + w_{10110} - w_{10010} - w_{00110},$$

where u_{10100} specifies an interaction between the species indicated in binary notation (10100 indicates the first and third species are present; see Fig. 1A and Box 1), and w_{10100} indicates the physiology trait score with the species indicated in binary. Generalizing, we extend the two-way interaction case up to the complete 5-way interactions along with combinatorial associations at intermediate diversity.

Clearly, extracting relevant and biologically meaningful interactions from among the many possible interaction coordinates and circuits must avoid redundant analyses. Therefore, in this paper we focus on the interactions we find biologically interpretable and comparable with other studies (e.g. Newell and Douglas 2014 [9]).

In this Supplement, we give examples of how the mathematical approach applies to other biological systems specifically to bacterial interactions in the gut microbiome and explain how this approach generalizes to n-dimensional systems and to all lower rank interactions inside this system.

3 Glossary for interactions - Mathematical Terminology

The terminology we use is an adaptation of genetic epistasis to the study of interactions among bacterial species in fruit flies. For convenience we include the following intuitive definitions of terms we will repeatedly use later on:

- **n-species system**: a system of n types of bacterial species in the microbiome (present or absent). We refer to a bacterial combination within the n-species system using binary code. For instance, 00000 indicates no species present in a 5-species system, 111 indicates all species present in a 3-species system, and 1010 indicates the first and third species present in a 4-species system. Thus, each unique species is assigned an index with the binary string.

- **n-cube (n dimensional unit hypercube)**: is an n-dimensional generalization of a square (2-cube) or cube (3-cube) whose sides have unit lengths. When n=5, the 5-cube has 32 vertices, 80 edges, 80 square faces, 40 3-cubes and 10 4-cubes, see [4].

- **phenotype**: is a measured, quantitative trait that is associated with a particular bacterial combination. In this work, we consider the number of bacterial CFUs, the development time of a fly from embryo to adult, the fecundity of a female fly, and the lifespan of a fly. We consider each phenotype separately, and we use w to refer generally to any phenotype. The phenotype associated with a specific bacterial combination is given by w_{XXX} where XXX is a binary string of length n referring to a bacterial combination.

- **Interaction coordinates**: are equations that describe the non-additivity of phenotypes associated with sets of species. For instance, if we consider two species, the interaction coordinate is just the degree to which w_{11} cannot be determined from knowing w_{00}, w_{01}, and w_{10}. We use u to refer generally to an interaction coordinate and we associate a specific interaction coordinate with its binary string. For instance, u_{11} indicates the interaction we are considering dependent upon w_{00}, w_{01}, w_{10}, and w_{11}. If $u_{11} = 0$, the phenotypes are completely additive, and we say there is no interaction. More generally, in the n-species system, interaction coordinates are given by linear combinations of the measured traits associated with each bacterial combination.

- **Circuits**: are certain linear combinations of interaction coordinates. In this sense, interaction coordinates form the basis elements for the interaction space, which can be more completely explored using circuits. Many different types of circuits exist, which we classify based on their symmetry groups. We assign a letter to each of these symmetry groups. For instance, the circuit b (described in a later section), is defined as the difference between u_{110} and u_{111} and it asks if the interaction between the first two species changes when the third species is added.

- **Triangulation**: is the local shape of the phenotypic landscape imposed by the interactions between bacterial species (see Box 1 for an example).

- **Standard interactions (or standard tests)**: are 2, 3, 4 and 5-way interactions on all pairs, triples, quadruples and five tuples of species leaving the remaining species absent. An example is u_{11}, described in the definition for 'interaction coordinates'.

- **Non-standard interactions (or non-standard tests)**: are higher-order interactions arising as a generalization of the standard test. For instance, interaction coordinates for the 2, 3 and 4 and 5 species systems can be generalized by allowing the species not present to be occupied by bystanders, whose presence/absence is constant across the species considered in the standard test. Circuit b is an example of a non-standard interaction.

Summary of glossary section In this work, we focus on a 5 species system consisting of 32 bacterial combinations. We encode the different bacterial combinations by a binary string S of lengths 5. Each entry of such a string S represents a bacterial species isolated inside a number of flies guts. For instance, S=00000 describes the germ-free fly, S=11111 describes the fly colonized with all 5 species of bacteria. With this binary notion, each bacterial combination defines a unique vertex of the 5-dimensional cube G. Together

with the 5-cube G, we also consider the following four phenotypes associated with the bacterial combinations: bacterial load (CFUs), development rate, fecundity, and time to death. The phenotypes associated with each bacterial combination in binary notation are denoted simply by w_S.

4 Two disjoint families of interactions: standard and non-standard tests

In the following, we formally define two disjoint families of interaction formulas in the five bacterial species setting. The first family, standard interaction tests, is smaller in size than the second, non-standard interaction tests. Standard interactions allow us to determine whether the phenotype of a group of bacterial species can be predicted from the sum of its parts.

The family of non-standard interactions consists of a large number of different interaction formulas recursively defined. These interactions describe how the interactions of the bacterial groups change according to the presence of additional species [2]. The set of non-standard interactions includes circuits. For instance, one type of non-standard interaction asks how a standard interaction changes in the presence a bystander species.

These two families of interactions we define in this work are new and inspired by [1] and [6] (the second reference for standard tests).

4.1 Standard interactions

Consider the two species interaction formula, given by:

$$u_{11} = w_{00} + w_{11} - w_{01} - w_{10}$$

where w_{00} indicates a phenotype, such as daily fecundity, time to death, CFU or development rate, associated to the bacterial combination 00, which is germ-free. Similarly, w_{11} (both species), w_{01} (one species) and w_{10} (the other species). Biologically, the meaning of this interaction formula is well understood: it compares the phenotype contributions of the two-species association with the single species associations. Geometrically, the summands of u_{11}, which are w_{00}, w_{11}, w_{01} and w_{10}, are indexed by the four vertices of a unit square.

We then consider the following generalizations of u_{11} for the 3-, 4- and 5-species system:

$$u_{111} = w_{000} + w_{011} + w_{101} + w_{110} - w_{100} - w_{010} - w_{001} - w_{111}$$

$$\begin{aligned} u_{1111} = {} & w_{0000} + w_{1100} + w_{0110} + w_{0011} + w_{1010} + w_{0101} + w_{1001} + w_{1111} \\ & - w_{1000} - w_{0100} - w_{0010} - w_{0001} - w_{1011} - w_{1101} - w_{0111} - w_{1110} \end{aligned}$$

$$\begin{aligned} u_{11111} = {} & w_{00000} - w_{00001} - w_{00010} - w_{00100} - w_{01000} - w_{10000} + w_{11000} \\ & + w_{10100} + w_{10010} + w_{10001} + w_{01100} + w_{01010} + w_{01001} + w_{00110} \\ & + w_{00101} + w_{00011} - w_{11100} - w_{11010} - w_{11001} - w_{10110} - w_{10101} \\ & - w_{10011} - w_{01110} - w_{01101} - w_{01011} - w_{00111} + w_{11110} + w_{11101} \\ & + w_{11011} + w_{10111} + w_{01111} - w_{11111}. \end{aligned}$$

In the following, we simply call u_{11} the 2-way interaction, u_{111} the 3-way interaction, u_{1111} the 4-way interaction, and u_{11111} the 5-way interaction. From the given formulas it is clear that these interactions are defined by 4, 8, 16, and 32 terms, respectively. The signs of the terms change according to the definition of the interaction coordinate function given in equation (4). As previous authors have described, this sign change results from a Fourier transform, see [2]. Biologically, one can say that these interactions compare the phenotypes of bacterial combinations when an even number of bacterial species are present versus when an odd number of bacterial species are present (e.g. w_{00} and w_{11} vs w_{01} and w_{10}).

Quantifying the number of interactions within each symmetry group. Examining for example the symmetries of the 5-cube, we can see that there are 10 possible two-way interactions, u_{11}. Similarly there are 10 three-way interactions and five four-way standard interactions. Together, this approach gives:

$$\binom{5}{2} + \binom{5}{3} + \binom{5}{4} + \binom{5}{5} = 26 \tag{1}$$

different standard interactions in a five species system. The number of standard interactions we find in Equation (1) matches the results of [6].

To be explicit, the standard interactions involving two species of bacteria out of five are:

$$\begin{aligned}
u_{00**0} &= w_{00000} + w_{00110} - w_{00010} - w_{00100} \\
u_{**000} &= w_{00000} + w_{11000} - w_{01000} - w_{10000} \\
u_{*0*00} &= w_{00000} + w_{10100} - w_{00100} - w_{10000} \\
u_{0**00} &= w_{00000} + w_{01100} - w_{00100} - w_{01000} \\
u_{*00*0} &= w_{00000} + w_{10010} - w_{00010} - w_{10000} \\
u_{0*0*0} &= w_{00000} + w_{01010} - w_{00010} - w_{01000} \\
u_{00*0*} &= w_{00000} + w_{00101} - w_{00001} - w_{00100} \\
u_{*000*} &= w_{00000} + w_{10001} - w_{00001} - w_{10000} \\
u_{0*00*} &= w_{00000} + w_{01001} - w_{00001} - w_{01000} \\
u_{000**} &= w_{00000} + w_{00011} - w_{00001} - w_{00010}
\end{aligned}$$

These u-interactions arise from the 2-way interaction and always involve two species (indicated with $*$) out of five leaving the other three species absent. Geometrically, these u-interactions involve the four vertices of certain square faces inside a 5-dimensional cube G.

The standard interactions involving three species out of the five will be denoted by u and are obtained from the 3-way interaction. These u-interactions involve the eight vertices of the 3-cubes inside G:

$$\begin{aligned}
u_{00***} &= w_{00000} + w_{00011} + w_{00101} + w_{00110} - w_{00100} - w_{00010} - w_{00001} - w_{00111} \\
u_{***00} &= w_{00000} + w_{01100} + w_{10100} + w_{11000} - w_{10000} - w_{01000} - w_{00100} - w_{11100} \\
u_{**0*0} &= w_{00000} + w_{01010} + w_{10010} + w_{11000} - w_{10000} - w_{01000} - w_{00010} - w_{11010} \\
u_{*0**0} &= w_{00000} + w_{00110} + w_{10010} + w_{10100} - w_{10000} - w_{00100} - w_{00010} - w_{10110} \\
u_{0***0} &= w_{00000} + w_{00110} + w_{01010} + w_{01100} - w_{01000} - w_{00100} - w_{00010} - w_{01110} \\
u_{**00*} &= w_{00000} + w_{01001} + w_{10001} + w_{11000} - w_{10000} - w_{01000} - w_{00001} - w_{11001} \\
u_{*00**} &= w_{00000} + w_{00011} + w_{10001} + w_{10010} - w_{10000} - w_{00010} - w_{00001} - w_{10011} \\
u_{*0*0*} &= w_{00000} + w_{00101} + w_{10001} + w_{10100} - w_{10000} - w_{00100} - w_{00001} - w_{10101} \\
u_{0**0*} &= w_{00000} + w_{00101} + w_{01001} + w_{01100} - w_{01000} - w_{00100} - w_{00001} - w_{01101} \\
u_{0*0**} &= w_{00000} + w_{00011} + w_{01001} + w_{01010} - w_{01000} - w_{00010} - w_{00001} - w_{01011}
\end{aligned}$$

The following five standard interactions arise from the 4-way interaction described by u_{1111} above and involve

four species out of the five, leaving out the remaining bacterial species:

$$
\begin{aligned}
u_{****0} &= w_{00000} + w_{11000} + w_{01100} + w_{00110} + w_{10100} + w_{01010} + w_{10010} + w_{11110} \\
&\quad - w_{10000} - w_{01000} - w_{00100} - w_{00010} - w_{10110} - w_{11010} - w_{01110} - w_{11100} \\
u_{***0*} &= w_{00000} + w_{11000} + w_{01100} + w_{00101} + w_{10100} + w_{01001} + w_{10001} + w_{11101} \\
&\quad - w_{10000} - w_{01000} - w_{00100} - w_{00001} - w_{10101} - w_{11001} - w_{01101} - w_{11100} \\
u_{**0**} &= w_{00000} + w_{11000} + w_{01010} + w_{00011} + w_{10010} + w_{01001} + w_{10001} + w_{11011} \\
&\quad - w_{10000} - w_{01000} - w_{00010} - w_{00001} - w_{10011} - w_{11001} - w_{01011} - w_{11010} \\
u_{*0***} &= w_{00000} + w_{10100} + w_{00110} + w_{00011} + w_{10010} + w_{00101} + w_{10001} + w_{10111} \\
&\quad - w_{10000} - w_{00100} - w_{00010} - w_{00001} - w_{10011} - w_{10101} - w_{00111} - w_{10110} \\
u_{0****} &= w_{00000} + w_{01100} + w_{00110} + w_{00011} + w_{01010} + w_{00101} + w_{01001} + w_{01111} \\
&\quad - w_{01000} - w_{00100} - w_{00010} - w_{00001} - w_{01011} - w_{01101} - w_{00111} - w_{01110}
\end{aligned}
$$

Geometrically, these interactions involve the 16 vertices of the specified 4-cubes inside G. The last standard interaction is simply given by the following expression involving all five species and all 32 fitness values:

$$
\begin{aligned}
u_{*****} &= u_{11111} \\
&= w_{00000} - w_{00001} - w_{00010} - w_{00100} - w_{01000} - w_{10000} + w_{11000} \\
&\quad + w_{10100} + w_{10010} + w_{10001} + w_{01100} + w_{01010} + w_{01001} + w_{00110} \\
&\quad + w_{00101} + w_{00011} - w_{11100} - w_{11010} - w_{11001} - w_{10110} - w_{10101} \\
&\quad - w_{10011} - w_{01110} - w_{01101} - w_{01011} - w_{00111} + w_{11110} + w_{11101} \\
&\quad + w_{11011} + w_{10111} + w_{01111} - w_{11111}.
\end{aligned}
$$

Geometrically, this interaction involves all vertices of G. In Figure 1 below we highlight the regions delimited by the vertices defining the 26 standard interactions described above inside a projection of a five cube G.

For example, in a system with three bacterial species consisting of the following 8 bacterial combinations $G = \{000, 001, 010, 100, 110, 011, 101, 11\}$ there are three standard interactions involving two out of three species:

$$
\begin{aligned}
u_{**0} &= w_{000} + w_{110} - w_{100} - w_{010} \\
u_{*0*} &= w_{000} + w_{101} - w_{100} - w_{001} \\
u_{0**} &= w_{000} + w_{011} - w_{010} - w_{001}
\end{aligned}
$$

together with the 3-way interaction u_{111}, described above.

On the other hand, in an n-species system there are

$$
\sum_{2 \le l \le n} \binom{n}{l} \tag{2}
$$

standard interactions.

5 Non-standard interactions

In the following, we compare the results of the standard tests with the results of the corresponding non-standard tests in a five species system and for various phenotypes. The non-standard tests belong to two different classes, **interaction coordinates**, which are generalizations of the standard interactions, and **circuits**, which are linear combinations of the interaction coordinates. We consider first the interaction coordinates, which specify the basis vectors for the complete interaction space. We then consider the circuits, and we focus on a subset of all possible circuits that have a simple biological meaning. These non-standard tests include higher-order interactions arising by introducing the species not present under the lower dimensional standard tests. For instance, we previously noted that there are 10 possible pairs of species in the

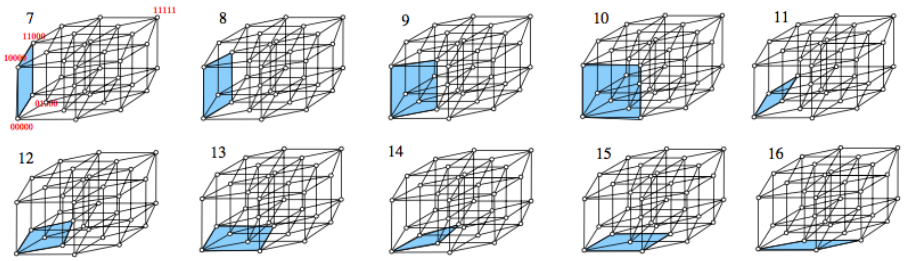

(A) The 10 standard 2-way interactions

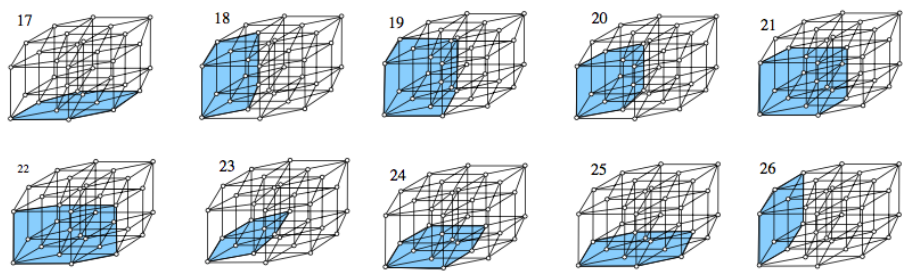

(B) The 10 standard 3-way interactions

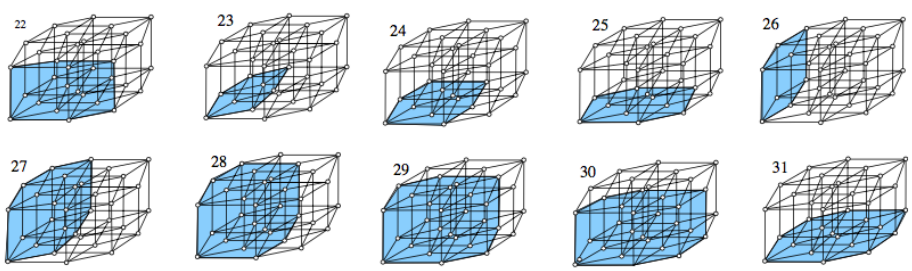

(C) The 5 standard 4-way interactionsl

Figure 1: **Geometric description of the 26 standard interactions**. The highlighted regions inside the projections of the 5-dimensional cube indicate the vertices (indicated by $*$ in the standard interaction formulas) involved in the corresponding interaction. The interaction u_{11111} is defined by all 32 vertices and therefore omitted.

5-species system. For any of these pairs, we can consider how the interaction between the pair changes in the presence of a third, fourth, or fifth species.

In an n-species system there are

$$\sum_{2\leq l\leq n}\binom{n}{l}2^{n-l}(2^l-l-1)+\binom{n}{3}2^{n-3}\cdot 14-\sum_{2\leq l\leq n}\binom{n}{l} \tag{3}$$

different non-standard interactions. Compare with Equation (2) and (6).

In this section, we make precise the notion of interaction coordinates and circuits, see also Glossary [2] for binary systems of n-bacterial species, $\{0,1\}^n$. We first describe these formulas abstractly for arbitrary values of n and later focus on the case where there are only 5 bacterial species.

5.1 Interaction coordinates

For a fixed $n\in\mathbb{N}$, let $j_1,j_2,\ldots,j_n\in\{0,1\}^n$ be a binary strings of lengths n. We view each such string as a vertex of an n-dimensional cube. Let $i=i_1,i_2,\ldots,i_n\in\{0,1\}^n$ be such a binary string with at least two coordinates i_j,i_k being 1. The interaction coordinates u_i can be defined (up to a scalar) in the following way:

$$u_{i_1,i_2,\ldots,i_n}:=\frac{1}{2^n-1}\sum_{j_1=0}^{1}\sum_{j_2=0}^{1}\cdots\sum_{j_n=0}^{1}(-1)^{i_1j_1+i_2j_2+\cdots+i_nj_n}w_{j_1j_2\ldots j_n} \tag{4}$$

where $w_{_}$ are values of a corresponding phenotype and indexed by the vertices of the n-dimensional cube. It then follows, that there are 2^n-n-1 interaction coordinates. Moreover, these coordinates are linearly independent and form a vector space basis of the interaction space.

5.2 Circuits

Certain linear combinations of interaction coordinates give rise to circuits, that is minimal dependency sets of configurations of points in a space of dimension n, see [5]. In the following, the only circuits we will consider are the ones previously presented in the 3-dimensional setting in [2]. As equations, these circuits

can be presented as follows:

$$
\begin{aligned}
a &:= u_{110} + u_{111} = w_{000} - w_{010} - w_{100} + w_{110} \\
b &:= u_{110} - u_{111} = w_{001} - w_{011} - w_{101} + w_{111} \\
c &:= u_{101} + u_{111} = w_{000} - w_{001} - w_{100} + w_{101} \\
d &:= u_{101} - u_{111} = w_{010} - w_{011} - w_{110} + w_{111} \\
e &:= u_{011} + u_{111} = w_{000} - w_{001} - w_{010} + w_{011} \\
f &:= u_{011} - u_{111} = w_{100} - w_{101} - w_{110} + w_{111} \\
\\
g &:= u_{110} + u_{101} = w_{000} - w_{011} - w_{100} + w_{111} \\
h &:= u_{110} - u_{101} = w_{001} - w_{010} - w_{101} + w_{110} \\
i &:= u_{110} + u_{011} = w_{000} - w_{010} - w_{101} + w_{111} \\
j &:= u_{110} - u_{011} = w_{001} - w_{011} - w_{100} + w_{110} \\
k &:= u_{101} + u_{011} = w_{000} - w_{001} - w_{110} + w_{111} \\
l &:= u_{101} - u_{011} = w_{010} - w_{011} - w_{100} + w_{101} \\
\\
m &:= -u_{011} - u_{101} - u_{110} - u_{111} = w_{001} + w_{010} + w_{100} - w_{111} - 2w_{000} \\
n &:= -u_{011} - u_{101} - u_{110} + u_{111} = w_{011} + w_{101} + w_{110} - w_{000} - 2w_{111} \\
o &:= u_{011} + u_{101} - u_{110} - u_{111} = w_{010} + w_{100} + w_{111} - w_{001} - 2w_{110} \\
p &:= u_{011} + u_{101} - u_{110} + u_{111} = w_{000} + w_{011} + w_{101} - w_{110} - 2w_{001} \\
q &:= u_{011} - u_{101} + u_{110} - u_{111} = w_{001} + w_{100} + w_{111} - w_{010} - 2w_{101} \\
r &:= u_{011} - u_{101} + u_{110} + u_{111} = w_{000} + w_{011} + w_{110} - w_{101} - 2w_{010} \\
s &:= -u_{011} + u_{101} + u_{110} + u_{111} = w_{000} + w_{101} + w_{110} - w_{011} - 2w_{100} \\
t &:= -u_{011} + u_{101} + u_{110} - u_{111} = w_{001} + w_{010} + w_{111} - w_{100} - 2w_{011}.
\end{aligned}
$$

Linear combinations of these circuits, which we do not consider here, yield more interactions contained in the interaction space.

Biological and geometric interpretations of these circuits follow from the descriptions given in [2, §.3] for the genetic setting. For instance, circuits m to t relate the three-way interactions to the total two-way interactions. Examining the equation for m, we see that it is equal to the sum of the phenotype terms for each of the single species combinations minus the sum of the three-species association and the germ free flies. Similarly in n, the sum of the two-species combinations is compared to the sum of the three-species combination and the germ free flies. The biological interpretation is that m tells us whether the single species associations predict the three-species combination, and n tells us whether the two-species associations predict the three-species combination. Of note, the signs of the circuits m to t do not have a two-locus interpretation, making them truly of higher-order.

5.3 Recursively constructing higher order interactions from lower order interactions

We now describe interaction coordinates in lower dimensional cubes and how the circuits a-t extend to interaction formulas in higher dimensional cubes. In light of the data analyzed in this paper, we focus on the case of five bacterial species. However, the approach we present here easily extends to systems with n-bacterial species. See discussion at the end of this section.

For instance, the two-way interaction

$$u_{11} = w_{00} + w_{11} - w_{01} - w_{10}$$

extends to the following $80 = 10 \cdot 2^3$ different interaction formulas in a five species system.

$$
\begin{aligned}
\alpha_{**klm} &= w_{00klm} + w_{11klm} - w_{01klm} - w_{10klm} \\
\alpha_{*k*lm} &= w_{0k0lm} + w_{1k1lm} - w_{0k1lm} - w_{1k0lm} \\
\alpha_{*kl*m} &= w_{0kl0m} + w_{1kl1m} - w_{0kl1m} - w_{1kl0m} \\
\alpha_{*klm*} &= w_{0klm0} + w_{1klm1} - w_{0klm1} - w_{1klm0} \\
\alpha_{k**lm} &= w_{k00lm} + w_{k11lm} - w_{k01lm} - w_{k10lm} \\
\alpha_{k*l*m} &= w_{k0l0m} + w_{k1l1m} - w_{k0l1m} - w_{k1l0m} \\
\alpha_{k*lm*} &= w_{k0lm0} + w_{k1lm1} - w_{l0lm1} - w_{k1lm0} \\
\alpha_{kl**m} &= w_{kl00m} + w_{kl11m} - w_{kl01m} - w_{kl10m} \\
\alpha_{kl*m*} &= w_{kl0m0} + w_{kl1m1} - w_{kl0m1} - w_{kl1m0} \\
\alpha_{klm**} &= w_{klm00} + w_{klm11} - w_{klm01} - w_{klm10},
\end{aligned}
\tag{5}
$$

where $**$ indicates two species out of five. The remaining indices k, l, m are then either 0 or 1, and all possible 2^3 combinations are allowed. Similarly, extending to the five species system, the four interaction coordinates u_{111}, $u_{110}, u_{011}, u_{101}$ are defined by (4) above in the following fashion:

$$
\begin{aligned}
\beta_{***kl} &= \sum_{j_1=0}^{1}\sum_{j_2=0}^{1}\sum_{j_3=0}^{1}(-1)^{*j_1+*j_2+*j_3} w_{j_1j_2j_3kl} \\
\beta_{**k*l} &= \sum_{j_1=0}^{1}\sum_{j_2=0}^{1}\sum_{j_4=0}^{1}(-1)^{*j_1+*j_2+*j_4} w_{j_1j_2kj_4l} \\
\beta_{**kl*} &= \sum_{j_1=0}^{1}\sum_{j_2=0}^{1}\sum_{j_5=0}^{1}(-1)^{*j_1+*j_2+*j_5} w_{j_1j_2klj_5} \\
\beta_{*k*l*} &= \sum_{j_1=0}^{1}\sum_{j_3=0}^{1}\sum_{j_5=0}^{1}(-1)^{*j_1+*j_3+*j_5} w_{j_1kj_3lj_5} \\
\beta_{*kl**} &= \sum_{j_1=0}^{1}\sum_{j_4=0}^{1}\sum_{j_5=0}^{1}(-1)^{*j_1+*j_4+*j_5} w_{j_1klj_4j_5} \\
\beta_{k*l**} &= \sum_{j_2=0}^{1}\sum_{j_4=0}^{1}\sum_{j_5=0}^{1}(-1)^{*j_2+*j_4+*j_5} w_{kj_2lj_4j_5} \\
\beta_{kl***} &= \sum_{j_3=0}^{1}\sum_{j_4=0}^{1}\sum_{j_5=0}^{1}(-1)^{*j_3+*j_4+*j_5} w_{klj_3j_4j_5} \\
\beta_{*k**l} &= \sum_{j_1=0}^{1}\sum_{j_3=0}^{1}\sum_{j_4=0}^{1}(-1)^{*j_1+*j_3+*j_4} w_{j_1kj_3j_4l} \\
\beta_{k**l*} &= \sum_{j_2=0}^{1}\sum_{j_3=0}^{1}\sum_{j_5=0}^{1}(-1)^{*j_2+*j_3+*j_5} w_{kj_2j_3lj_5} \\
\beta_{k***l} &= \sum_{j_2=0}^{1}\sum_{j_3=0}^{1}\sum_{j_4=0}^{1}(-1)^{*j_2+*j_3+*j_4} w_{kj_2j_3j_4l}.
\end{aligned}
$$

As before, the notation $***$ indicates three species out of five. The remaining indices k, l are assumed to be fixed and either $kl = 00, kl = 01, kl = 11$ or $kl = 10$. The biological significance of these interactions is examined in the main text Figs. 5 and S12.

We also extend the circuits *a*-*t* to the five species setting. To do this, it is enough to consider the circuit formulas *a*-*t* given above, and replace the u_{i_1,i_2,i_3} with the corresponding extended interaction coordinates.

Similarly one also extends the $2^4 - 5 = 11$ interaction coordinates $u_{i_1,\ldots,i_4}$ defined by equation (4) and $n = 4$.

Thus in a 5-species system, there are

$$\sum_{2 \leq l \leq 5} \binom{5}{l} 2^{5-l}(2^l - l - 1) = 376$$

interaction coordinates together with

$$\binom{5}{3} 2^{5-3} \cdot 20 = 800$$

possible extensions of the circuits a-t. Notice however that the circuits a-f are two way interactions extended to the three species setting, hence only the circuits g-t provide new possible extended circuits. It follows, that only 560 of these extended circuits are different among each other and disjoint from the previous interaction coordinates. Thus, together this approach yields 936 different extended interaction coordinates and circuits.

In an n-species system, the approach described above gives

$$\sum_{2 \leq l \leq n} \binom{n}{l} 2^{n-l}(2^l - l - 1) + \binom{n}{3} 2^{n-3} \cdot 14 \tag{6}$$

different extended interaction coordinates together with the disjoint set of all possible and different extensions of the circuits g-t. As for the five species setting, in equation (6) we omit the circuits a-f.

The biological and geometric interpretation of the interactions enumerated in equation (6) can be deduced from the lower dimensional interpretations given in [2], for the three species case $\{0, 1\}^3$. Clearly, more interactions might be obtained by considering linear combinations of the above formulas.

6 Significance testing of interactions

Despite the standard and non-standard interactions being disjoint families, the two sets of interactions are not statistically independent as they derive from the same underlying data sets. In order to determine whether an interaction is non-zero, we took the uncertainty in the phenotype measurements into account and devised a statistical test as follows. Since the phenotype measurements come with their standard errors, we computed the corresponding propagation of error for each interaction (standard and non-standard). This error was determined by taking the square root of the sum of squares of the standard errors involved in each interaction formula. For example, for u_{11}, the propagated standard error $s(u_{11})$ is

$$s(u_{11}) = \sqrt{s_{00}^2 + s_{11}^2 + s_{01}^2 + s_{10}^2}$$

where s_{00} denotes the standard error of w_{00}, etc.

Moreover, if different formulas give rise to the same interaction term, we considered only the formula yielding the smallest propagation of error, that is, the formula involving the least number of operations. For instance, each interaction term $a, \ldots, t$ can be defined in two ways, one involving a difference between interaction coordinates and a direct way by canceling out the redundant phenotypes in the formula. The direct way involves less operations, and therefore a smaller propagated error.

We then determined significant interactions in the following way. We assumed that each interaction formula comes from a Gaussian distribution with mean 0 and standard deviation given by the propagated error. For each interaction u, we performed a two-sided null hypothesis test. The null hypothesis states that the true value of the interaction is $u = 0$, versus the alternative hypothesis that $u \neq 0$. We then considered an interaction statistically significant if the p-value was below 0.05. This means, that if the null hypothesis was true, the probability of obtaining the result of the interaction u we computed would be 5%.

To account for the multiple comparisons, we corrected all the above p-values using the Benjamini-Hochberg procedure. In this way, we are able to control the false discovery rate at 5%; that is, we eventually considered an interaction statistically significant if the corrected p-value falls below 0.05.

7 Supplemental Results of Interaction Testing

In this section we summarize the main findings we obtained through the computations described above. In the first part, we focus on the smaller family of higher-order interactions and on the second part we compare the outcomes of these interactions with non-standard interactions. In the last part, we focus on specific standard and non-standard interactions which examine how interactions change as the number of species increases.

7.1 Computed standard interaction tests

Nr.	Combination	Daily Fecundity	Development	Bacterial load	Time to death
7	u_{**000}	**1.19**	**-0.67**	**-263560**	5.23
8	u_{*0*00}	**1.15**	**-0.71**	**197180**	3.05
9	u_{*00*0}	0.17	**-0.80**	**-122760**	**6.09**
10	u_{*000*}	0.51	**-0.75**	-60450	**6.92**
11	u_{0**00}	0.55	-0.34	-99780	-1.23
12	u_{0*0*0}	-0.58	0.16	**-346180**	-1.77
13	u_{0*00*}	0.74	0.08	**-307840**	**4.70**
14	u_{00**0}	**-1.40**	**-0.42**	-84420	2.41
15	u_{00*0*}	**-1.44**	0.00	**-225820**	**8.07**
16	u_{000**}	**-1.41**	-0.09	**-319870**	**5.32**
17	u_{***00}	**1.73**	-0.63	187810	2.56
18	u_{**0*0}	-0.65	-0.63	-150060	**6.81**
19	u_{**00*}	**1.65**	**-0.96**	-69910	**8.89**
20	u_{*0**0}	0.14	**-0.92**	200100	4.64
21	u_{*0*0*}	**1.49**	**-0.92**	104680	**7.55**
22	u_{*00**}	0.27	**-0.88**	**-214180**	**9.23**
23	u_{0***0}	-1.16	-0.30	19540	0.39
24	u_{0**0*}	0.40	-0.21	**-338700**	**6.86**
25	u_{0*0**}	-0.51	-0.25	**-371050**	0.42
26	u_{00***}	**-1.61**	-0.59	-64680	3.57
27	u_{****0}	-0.74	**-0.63**	**368660**	6.18
28	u_{***0*}	**2.53**	**-0.96**	88710	**12.62**
29	u_{**0**}	0.42	**-1.04**	-127600	**14.47**
30	u_{*0***}	0.72	**-1.17**	99350	5.38
31	u_{0****}	-1.00	-0.59	79250	-0.40
32	u_{*****}	0.95	**-1.42**	453480	**12.49**

Table 1: **Result for the 26 standard interactions** computed on the raw fecundity per day (daily fec), bacterial load (CFU), time to death (time d) and development rate (dev) data. The first two columns indicate the performed standard tests separated according to the number of bacterial species present in the fly gut (the type of species is indexed by the position of the symbol $*$). Results in bold reached statistical significance ($p < 0.05$) after multiple comparison correction. The geometric description of these interactions is illustrated in Figure 1.

To summarize the results of the standard interactions presented above in Table 1 we averaged the results of all the standard 2-, 3-, 4- and 5-way tests at each level of species diversity (Table 2). Thus, we let a_2 be the sum of all standard 2-way interactions u_{**} divided by the number of 2-way standard interactions (which is 10). Similarly, we calculated a_3, a_4 and a_5.

Term	CFU	dev	fd	td	unif	nor
a_2	-163350	-0.353	-0.053	3.879	-0.197	1.477
a_3	-69645	-0.628	0.174	5.092	-0.112	1.585
a_4	101674	-0.878	0.385	7.650	0.170	2.216
a_5	453480	-1.419	0.947	12.490	0.650	4.080

Table 2: The average interactions terms $a_2, \ldots, a_5$ for the standard interactions and the four phenotypes of CFU, development rate (dev), fecundity per day (fd), and time to death (td) as well as for synthetic data from a uniform distribution on $[0, 1]$ and from a standard normal distribution.

From Table 2 we deduce that in average the interaction tends to increase with the number of terms in the standard formulas. We also note that the sign of the interaction (positive or negative) is already determined by the sign of the average 4-way interactions (or at even lower dimensions). Together with the results of Table 2, we also consider the average interactions of the standard 2-,3-, 4- and 5-way interactions normalized by the number of present bacterial species. That is $n_2 = a_2/2$,$n_3 = a_3/3$, $n_4 = a_4/4$ and $n_5 = a_5/5$, see Table 3 for the corresponding results.

Term	CFU	dev	fd	td	unif	nor
n_2	-81675	-0.177	-0.027	1.940	-0.099	0.739
n_3	-23215	-0.209	0.058	1.697	-0.037	0.528
n_4	25419	-0.220	0.096	1.913	0.043	0.554
n_5	90696	-0.284	0.189	2.498	0.130	0.816

Table 3: The normalized terms $n_2, \ldots, n_5$ for the standard interactions, normalized by the number of bacteria present for the four phenotypes of fecundity per day (fd), CFU, time to death (td) and development rate (dev), as well as for synthetic data from a uniform distribution on $[0, 1]$ and from a standard normal distribution.

It is clear from examining the average interaction values (i.e. the terms $a_2, \ldots, a_5$ in Table 2) that the total contribution increases as the number of species increases. However, when we normalize these average values to the number of species, we see a more constant contribution for each individual species, see Table 3.

Thus, if interactions quantify the degree to which we cannot predict the phenotype of the microbiome when a new species is added, the microbiome becomes less predictable as we add additional species. However, on a per-species basis, the degree of unpredictability stays constant. And if we consider the number of combinations, the results of the interaction tends to increase together with its statistical significance, in this sense the result of the interaction tends to become more predictable. Thus, while our analysis indicates that the microbiome problem increases in complexity as more species are added, there is reason for hope. For instance, if we discover a rule that determines *a priori* which non-standard test will be additive (versus showing an interaction), the predictability of the microbiome will increase as we add species. However, our fundamental conclusion is that the relationships between species rather than the species themselves produce increasingly complex interactions. Therefore, our efforts at building a predictable framework should focus on the interactions between species as much as on the individual species themselves.

7.2 Comparing the relative importance of individual bacterial species versus their interactions in determining physiological traits

When we compare the distributions of the raw data with the results of the standard interactions, we see that linear trends in the raw data do not necessary translate to the same trends in the standard interaction

data (Fig. S13). For example, consider time to death: the raw data indicates that increasing the number of bacterial species results in a decrease in the time to death (see Fig. 2). However, the standard tests indicate that interaction magnitude tends to increase with the number of species involved (see Table 2), and hence with the numbers of terms in the standard interaction formulas. Finally, from the data in the Fig. S13, we deduce that the above observations remain valid by considering the (fewer) significant standard interactions rather than all standard interactions. For completeness, we also computed Spearman's correlation coefficients on all 26 standard interactions, and on the raw CFUs, development rate, daily fecundity, time to death data. See Table 4. The tests in bold in Table 4 which reached significance level ($p < 0.05$). See Table 5 for the results of the normality test (Shapiro-Wilk).

	CFU	**Development**	**Daily fecundity**	**Time to death**
CFU	-	**-0.44** (p=0.0108)	-0.04 (p=0.8142)	**-0.35**(p=0.0465)
Development rate	**-0.61** (p=0.0009)	-	-0.28 (p=0.1246)	**0.39** (p=0.0257)
Daily fecundity	0.29 (p=0.1473)	**-0.56** (p=0.0031)	-	**-0.42** (p=0.0179)
Time to death	0.11 (p=0.5982)	**-0.60** (p=0.0011)	0.33 (p=0.1051)	-

Table 4: **Spearman's correlation coefficients and significance level for all 26 standard interactions and raw data measurements**. Below the diagonal, we indicate Spearman's correlation coefficients and the corresponding p-values for all standard tested interactions (26 samples), similarly above the diagonal for the raw data (32 data points). Bold numbers indicate statistically significant correlations.

7.3 Results for all computed interactions from Figs. 4, 5, and S12

In this section, we describe the results contained in Figs. 4, 5, and S12 in the main text, obtained from computing the 910 non-standard interactions together with 26 standard interactions for the phenotypes of CFUs, development rate, daily fecundity, time to death. We found many significant positive and negative interactions among bacterial species in fruit flies. Moreover, we found that for some phenotypes (CFUs and daily fecundity) the standard interactions fully capture the interaction trends measured by the non-standard interactions (see Fig 4I,L; note overlapping distributions). However, for development rate and time to death we found that many new significant interactions arise when considering non-standard tests (see Fig. 4J,K; note non-overlapping distributions), indicating that the impacts of the bacterial community on the fly depend more on the context of which other bacterial species are present. Finally, comparing the Table 4 with Table 6 we found correlated interactions between phenotypes where neither the raw measurements nor the standard tests were correlated. The complete correlations between the measured phenotypes for the same interactions are shown in Figure S12 (main text). This finding suggests that interactions more than the individual species themselves shape host physiology.

One of the major findings of this work is that interactions between bacteria and their effects on the host are highly dependent on context. By comparing the standard interaction tests to the non-standard interaction tests (*e.g.* Figs. 4, 5 and S12), we quantitatively demonstrated this point for specific combinations of bacteria. Here, we extend that analysis to compare the two probability distributions corresponding to standard and non-standard interactions to ask whether they come from the same continuous distributions. The set of non-standard tests does not include the set of standard tests we computed. However, since standard tested and non-standard tests are computed from the same underlying data, the two sets of tests are statistically dependent. To test the difference between the distributions interactions, we performed a two-sample and two-sided Kolmogorov-Smirnov (KS) test. The results of the KS test for the phenotypes of bacterial CFUs (D = 0.17, p-value = 0.49) and daily fecundity (D = 0.18, p-value = 0.39) indicate that there is little evidence to reject the null-hypothesis of STD tests and non-STD tests coming from the same distributions. On the other hand, the results of the KS test for the phenotypes of development time (D = 0.58, p-value = $8.1 \cdot 10^{-08}$) and time to death (D = 0.46, p-value = $4.0 \cdot 10^{-05}$) suggest that it is unlikely that the STD tests and non-STD tests come from the same distributions. Thus, for these phenotypes, the difference between the standard and non-standard interactions strongly supports the notion that interactions are highly dependent

on context not just for specific cases but also on a global scale.

For completeness, we also ask if any of the STD tests, non-STD tests and significant standard tests come from normal distributions. To test this hypothesis we performed a Shapiro-Wilk test. The results are summarized in Table 5. We see that for the non-standard interactions (significant after multiple testing and before correction) the Shapiro-Wilk tests reach significance. We then conclude that the corresponding distributions fail the normality test.

	W	***p*-value**
CFU	0.98059	$1.204 \cdot 10^{-9}$
CFU STD	0.95586	0.3166
CFU significant	0.92508	$3.375 \cdot 10^{-10}$
Development	0.97131	$2.092 \cdot 10^{-12}$
Development STD	0.97793	0.8272
Development significant	0.8757	0.0001541
Daily fecundity	0.96783	$2.727 \cdot 10^{-13}$
Daily fecundity STD	0.96159	0.4238
Daily fecundity significant	0.90355	$6.433 \cdot 10^{-08}$
Time to death	0.99467	0.002708
Time to death STD	0.97193	0.6737
Time to death significant	0.8995	$1.352 \cdot 10^{-09}$

Table 5: **Shapiro-Wilk-Test**. For each phenotype we summarized the test statistic and the corresponding p-value. The p-values for all non-standard tests (significant after multiple testing correction and before) reached a significance level. We conclude that there is evidence that the various distributions are non-normal. 'STD' appended to a label indicates the interactions where standard, whereas if 'STD' is not appended, it is for the non-standard tests. If 'significant' is appended, it means that the non-standard tests we consider are the ones that reached statistical significance ($p < 0.05$) after multiple testing correction.

	CFU	**Development**	**Daily fecundity**	**Time to death**
CFU	-	**-0.26** ($p < 0.0005$)	**0.17** ($p < 0.0005$)	**-0.21** ($p < 0.0005$)
Development	**-0.88** ($p < 0.0005$)	-	**-0.37** ($p < 0.0005$)	-0.08 ($p = 0.0130$)
Daily fecundity	**0.61** ($p < 0.0005$)	**-0.89** ($p < 0.0005$)	-	**-0.09** ($p = 0.0039$)
Time to death	**-0.68** ($p < 0.0005$)	-0.41 (p= 0.2443)	**-0.78** ($p < 0.0005$)	-

Table 6: **Spearman's correlation coefficients and significance level for all tested interactions**. Below the diagonal, we indicate Spearman's correlation coefficients and the corresponding p-values for statistically significant interactions ($p < 0.05$) after multiple testing correction with 10 to 66 pairwise complete comparisons). Similarly, above the diagonal we compute correlations for all non-standard tested interactions regardless of statistical significance (910 data points).

8 Discussion of Interaction Coordinates

Overall, when we utilize all of the interactions, including the non-standard tests, we see more significant interactions for the different phenotypes. Consistently, we see that the same interaction coordinates have correlated values across the different phenotypes that we measured. A simple explanation is that the rich microbial interactions underlying these phenotypes affect some central aspect of fly physiology that is reflected in multiple life history traits.

With the goal of quantifying higher order interactions we computed various interaction formulas. We also extracted a set of 26 interaction formulas (which we call 'standard interactions') and compared them with the results of 910 (different) 'non-standard' interaction formulas. We found that for certain phenotypes the standard interactions approximate well the distribution of the other more involved non-standard computations. Since the number of all possible interactions is large, and unknown in general, it is important to find a more parsimonious approach based on fewer interactions that still capture the main interaction signals. This is particularly advisable since the number of all possible interactions increases with the number of species and the relative contributions coming from each test are mostly small. Moreover, analyzing smaller sets of particularly expressive and biologically interpretable interactions would not only be computationally more efficient, but also would facilitate the comparisons of higher order genetic interactions arising in different biological contexts (for example infected fruit flies, or fruit flies treated with antibiotics). The recursive approach we propose here to define higher order interaction coordinates, as well as the computations we carried out, easily extends to settings with more species. Thus, our methodology can provide a way to reduce the experimental burden of examining combinatorial interactions in the microbiome by calculating the general shape of the interaction space from fewer experiments.

We also note that our computations are based on discrete data points. However, since the nature of the phenotypes we analyzed is continuous, it would be interesting to extend our studies and consider a fitting continuous setting. Finally, our computations and conclusion consider the propagation of uncertainty in phenotype measurements, and it would be interesting to develop a quantitative statistical framework accounting for possible sensible noise in the data set.

A challenge in the microbiome is to develop a quantitative framework that applies both to the detailed interactions between single species as well as to complex assemblages containing hundreds of species. We believe that our approach is simple enough to be scalable to higher dimensions, and by identifying groups of species that behave as single loci (as detected in specific non-standard tests, which are lower dimensional projections of the n-cube), we can reduce the dimensionality of complex assemblages through this combinatorial framework.

9 Pairwise species interactions (Figure 6)

Each of the 32 fully combinatorial experiments has 24 biological replicates, and for each biological replicate we collected the CFU abundance data by averaging three technical replicates. The raw data are displayed in Figure S5. We segmented this collection of CFU counts according to its bacterial diversity (ranging from 1 to 5), and studied how microbiome properties changed for different diversities. For a given bacterial combination, not all of the introduced bacteria were detected in every replicate. In the following measurements, we exclude replicates in which one or more species was undetected. By excluding these replicates, we intend to capture the deterministic aspect of interactions between bacteria, rather than the stochastic aspect that corresponds to the variability in colonization. However, this exclusion also reduces the available samples for analysis— in the most extreme case only 4 biological replicates remained (Figure S14C,D).

We computed the interaction strength between pairs of bacteria following Paine's method [10], and measured the asymmetry of these interactions. We also used a generalized Lotka-Volterra model to fit bacterial interactions from the CFU data, and found that the inferred interactions qualitatively matched those derived from Paine's method. Lastly, we calculated correlations between pairs of bacteria.

9.1 Bacterial interactions determined by Paine's method (Figure 6C,D, S14A,B)

Paine [10] presented a model-free calculation of interaction strength, which we implemented to probe bacterial interaction strength at low diversity (1 and 2 species) and high diversity (4 and 5 species). Note that this

method for 3 and 4 species diversity is less-straightforward to implement and is omitted here for simplicity. Let $(\mathrm{y}^{+j})_i$ and $(\mathrm{y}^{-j})_i$ be the abundance of species i in the presence and in the absence of the j community. Then, to measure the effect of a single species j on another species i, Paine measured [10]

$$\frac{(\mathrm{y}^{+j})_i - (\mathrm{y}^{-j})_i}{(\mathrm{y}^{-j})_i}. \tag{7}$$

This value is bounded below by -1 (introduction of j eliminates i), negative values indicate i is inhibited by j, and positive values indicate i is increased by j. We consider a rescaling of this value that has a symmetric range, which we call M_{ij}, that is given by

$$M_{ij} = \log_2 \left(1 + \frac{(\mathrm{y}^{+j})_i - (\mathrm{y}^{-j})_i}{(\mathrm{y}^{-j})_i} \right). \tag{8}$$

We compute this value at low ($1 \to 2$) and at high ($4 \to 5$) diversities, where we define the diversity of an experiment as the number of bacterial species that are in the food. For example, to compute M_{12} at low diversities, we consider experiments 10000 and 11000; to compute M_{12} at high diversities we consider experiments 10111 and 11111. Since there are many biological replicates for each experiment, we can bootstrap our samples following the method of Efron and Tibshirani [14] in order to compute the mean and standard error for each interaction value M_{ij}. We use the mean interaction values to populate the interaction matrix M, which we display as a directed graph in the low (Figure 6C) and high (Figure 6D) diversity cases. In the tables below, we also report the standard deviation of the distribution for each interaction (that is, we show the mean(M_{ij}) $\pm$ standard error(M_{ij})). The interaction matrices for high and low diversity interactions are

$$M^{\text{high}} = \begin{pmatrix} 0.00 \pm 0.00 & -0.02 \pm 0.53 & -0.03 \pm 0.58 & -0.56 \pm 0.50 & -0.72 \pm 0.50 \\ -2.48 \pm 0.88 & 0.00 \pm 0.00 & -0.37 \pm 1.08 & -1.59 \pm 0.98 & -0.42 \pm 1.13 \\ -0.93 \pm 0.81 & 0.10 \pm 0.61 & 0.00 \pm 0.00 & -0.44 \pm 0.70 & -1.98 \pm 0.94 \\ -0.68 \pm 0.75 & 0.12 \pm 0.84 & -0.41 \pm 0.78 & 0.00 \pm 0.00 & -0.36 \pm 1.00 \\ -0.14 \pm 0.63 & 0.91 \pm 0.91 & -0.18 \pm 0.70 & -0.38 \pm 0.64 & 0.00 \pm 0.00 \end{pmatrix} \tag{9}$$

and

$$M^{\text{low}} = \begin{pmatrix} 0.00 \pm 0.00 & 0.59 \pm 0.45 & 1.23 \pm 0.41 & 0.69 \pm 0.47 & 0.93 \pm 0.40 \\ -1.14 \pm 0.54 & 0.00 \pm 0.00 & -0.51 \pm 0.51 & 0.06 \pm 0.33 & 0.19 \pm 0.36 \\ 1.09 \pm 0.69 & 1.00 \pm 0.65 & 0.00 \pm 0.00 & -0.28 \pm 0.74 & -0.56 \pm 0.63 \\ -0.37 \pm 0.62 & 0.24 \pm 0.62 & 0.51 \pm 0.84 & 0.00 \pm 0.00 & 0.13 \pm 0.51 \\ 0.14 \pm 0.27 & 0.08 \pm 0.30 & 0.28 \pm 0.39 & 0.34 \pm 0.33 & 0.00 \pm 0.00 \end{pmatrix}. \tag{10}$$

The interactions as defined in Eq. (8) need not be— and generally are not— symmetric. We compute their asymmetry with a metric used by Bascompte et al. [13],

$$AS(i,j) = \frac{|M_{ij} - M_{ji}|}{\max(|M_{ij}|, |M_{ji}|)}. \tag{11}$$

This metric ranges from 0 (perfectly symmetric) to 2 (exact opposites). We consider the mean asymmetry of all 10 pairs. For the low diversity case this mean asymmetry is 1.04 (SD = 0.13), and for the high diversity case this mean asymmetry is 0.77 (SD = 0.08). To estimate the standard deviation, we repeatedly permuted the underlying interaction matrix M and created a distribution of permuted mean asymmetry values and used that standard deviation.

9.2 Bacterial interactions fit by a generalized Lotka-Volterra model (Figure 6c)

We infer the species interactions by assuming that the system obeys the generalized Lotka-Volterra equations,

$$\frac{d}{dt} x_i = x_i \left(\mu_i + \sum_{j=1}^{N} M_{ij} x_j \right) + \sum_{i}^{T} \delta(t - t_i^*) v_i, \tag{12}$$

with growth rate μ, interaction matrix M, and pulsed "feeding" of v_i at times $t_1^*, \ldots, t_T^*$.

Previous experiments have shown that when exposed to a steady supply of bacteria-infused food the fly gut approaches equilibrium within 5 days [3], and in this experiment the flies have been feeding for 10 days (see Materials and Methods). Therefore, we assume that the CFU counts of each experiment are measured at equilibrium, and we assume that the median of each combination's CFU counts is the steady state solution to Eq. (12). We additionally assume that the microbiome returns to equilibrium quickly after feeding, so that we may neglect the $\delta(t - t_i^*)v_i$ term in Eq. (12).

At equilibrium, the time derivative on the left hand side vanishes, and we assume that the steady state is non-trivial (i.e. $x_i \neq 0$). If we call the steady state of each microbe for a given experiment $\tilde{x}_i$, then an experiment of diversity N will correspond to N algebraic equations of the form

$$0 = \mu_i + \sum_{j=1}^{N} M_{ij}\tilde{x}_j. \tag{13}$$

If there are m_i experiments of diversity i, then there are $\sum_{i \in D} m_i i$ equations that must be simultaneously satisfied for diversities D. To match the previous interaction calculations, we consider a low-diversity group $D_{\text{low}} = \{1,\ 2\}$ and a high-diversity group $D_{\text{high}} = \{3,\ 4,\ 5\}$, which separates low-order interactions (2-species) from high-order (3-, 4-, and 5-species). For each group, we can rewrite the linear equations of Eq. (13) in matrix form as $0 = A\vec{y}$, where A is made up of the $\tilde{x}_i$ and is of the form

$$A = \begin{pmatrix} \tilde{x}_1^{10000} & 0 & \cdots & 0 & 0 & \cdots & 1 & 0 & 0 & 0 & 0 \\ 0 & 0 & \cdots & 0 & \tilde{x}_2^{01000} & \cdots & 0 & 1 & 0 & 0 & 0 \\ \vdots & \vdots & \vdots & \vdots & \vdots & \vdots & \vdots & \vdots & \vdots & \vdots & \vdots \\ \tilde{x}_1^{11000} & \tilde{x}_2^{11000} & \cdots & 0 & 0 & \cdots & 1 & 0 & 0 & 0 & 0 \\ 0 & 0 & \cdots & \tilde{x}_1^{11000} & \tilde{x}_2^{11000} & \cdots & 0 & 1 & 0 & 0 & 0 \\ \vdots & \vdots & \vdots & \vdots & \vdots & \vdots & \vdots & \vdots & \vdots & \vdots & \vdots \end{pmatrix} \tag{14}$$

and $\vec{y} = [M_{11}, M_{12}, \ldots, M_{21}, M_{22}, \ldots, M_{55}, \mu_1, \ldots, \mu_5]^T$. We assume $\mu_i = 1$ to obtain a nonzero result for M, which effectively absorbs the growth rates μ_i into the interaction values M_{ij} (so that we are always solving for M_{ij}/μ_i). We solve this system of equations for $\vec{y}$ with linear least-squares. The solution to this least-squares problem is the interaction matrix M, which we plot as a food web in Figure S14.

We tested our inference of the interaction matrix by considering how close the steady states of M were to the experimentally measured medians. At steady state, each combination C corresponds to a set of $|C|$ linear equations, as in Eq. (12), which we write as

$$M_C \vec{x}_C = -\vec{I}_C, \tag{15}$$

where M_C a subset of M pertaining to the bacteria in C, and $\vec{I}_C$ is a vector of ones of length $|C|$. For example, for a combination $C = \{1, 3\}$, we have

$$\begin{aligned} M_{11}x_1 + M_{13}x_3 &= -1 \\ M_{31}x_1 + M_{33}x_3 &= -1. \end{aligned} \tag{16}$$

Therefore, we can solve for the steady state of each combination $\vec{x}_c$ as

$$\vec{x}_C = -M_C^{-1}\vec{I}_C. \tag{17}$$

We compare this predicted steady state $\vec{x}_C$ with the experimentally measured steady state $\vec{x}_C^{\text{exp}}$ over all combinations by considering the error

$$\varepsilon := \frac{|\Delta \text{ SS CFUs }|}{|\text{ SS CFUs }|} = \frac{\sqrt{\sum_{C \in \{0,1\}^5} (\vec{x}_C - \vec{x}_C^{\text{exp}})^2}}{\sqrt{\sum_{C \in \{0,1\}^5} (\vec{x}_C^{\text{exp}})^2}}. \tag{18}$$

The interaction matrix M we fit with the least-squares method has an error ε of 0.322.

We construct a distribution for ε by permuting the entries of M many times, and for each permutation calculating the error ε. From this, we find that the error from the unpermuted interaction matrix M ($\varepsilon = 0.322$) is generally smaller than the permuted matrix errors (median = 5.69, standard deviation = 3.47). Therefore, our least-squares fitting method constructs an interaction matrix that reflects the experimental median CFU counts better than permuted alternatives ($p = 0.01$, comparison with errors of 10000 randomly permuted interaction matrices).

9.3 Pairwise correlations (Figure 6B)

For the set of experiments that have a given diversity N, we compute the pairwise correlation between bacteria i and j in the following way. For the set of experiments of diversity N that contain microbes i and j, the sample CFU counts for i and j for each experiment are aggregated. Then, we calculate the Spearman's rank correlation coefficient of these pairs of data, and arrive at a pairwise correlation value between species i and j that is between -1 (ordinal CFU counts between the species are perfectly anticorrelated) and 1 (perfectly correlated). This process is repeated for each species pairing to build a pairwise correlation matrix for each diversity.

9.4 Determining statistical trends

We first examined whether the interaction values determined with Paine's method became more negative at higher diversities. The quantity $M_{ij}^{\text{high}} - M_{ij}^{\text{low}}$ (where each M_{ij} is the is the mean of the bootstrapped distribution, as described above) is negative for 18 out of 20 entries. We compare this to the null hypothesis that the interaction values are the unchanged, which would predict 10 out of 20 to be negative. Therefore, we found that interactions became more negative at higher diversities (binomial test, p = 2e-4).

Next, we studied how pairwise correlations change at increasing diversity. To achieve this, we compare the same matrix element across different diversities using the non-parametric Kendall rank correlation coefficient. Each matrix element is ranked according to its size over increasing diversities, resulting in an ordinal vector of length 4. Through the Kendall rank correlation coefficient, the ranking for each matrix element is compared to the strictly increasing vector [1, 2, 3, 4], resulting in a τ coefficient that is between -1 and 1. For the correlation matrices there are 10 such τ coefficients with a mean of -0.4 (corresponding to all possible pairings of 5 bacteria). The matrices becoming more negative at higher diversities would correspond to negative τ coefficients. To determine whether the distribution of τ coefficients is significantly more negative than a distribution centered at 0, we apply the Wilcoxon signed-rank test. The resulting one-sided p-value for the correlation matrices is 0.0323, indicating that there is a significant trend in the values of the correlation matrices to decrease. These results are robust to how we threshold CFU counts below the detection limit— if we assume that undetected species have an abundance of 1000 CFUs, corresponding to the limit of detection, the resulting one-sided p-value remains 0.0323.

10 Supplements

10.1 Data transformation

All the interactions we compute are based on and generalize the additive genetic epistasis formula $u_{11} = w_{00} + w_{11} - w_{01} - w_{10}$. This additive formula relates to the multiplicative formula $m_{11} = w_{00}w_{11} - w_{01}w_{10}$ up to a logarithmic transformation. That is, composing the phenotype with a log transformation, we have:

$$\log(w_{00}) + \log(w_{11}) - \log(w_{01}) - \log(w_{10}) = \log(w_{00}w_{11}) - \log(w_{01}w_{10}).$$

To highlight that significant interactions we find do not depend on the additive approach we choose, we computed the same interactions as above also for the logarithmic (in base 2) transformation of the data. With no surprise, the interactions might dependent on the choice of the data transformation. More generally, we conclude by observing that transformations (possibly) depend on the true distribution of the observed (measured) data. Since the true distribution of our measurement remains unknown, we find it more reasonable to present our findings based on the actual measured data.

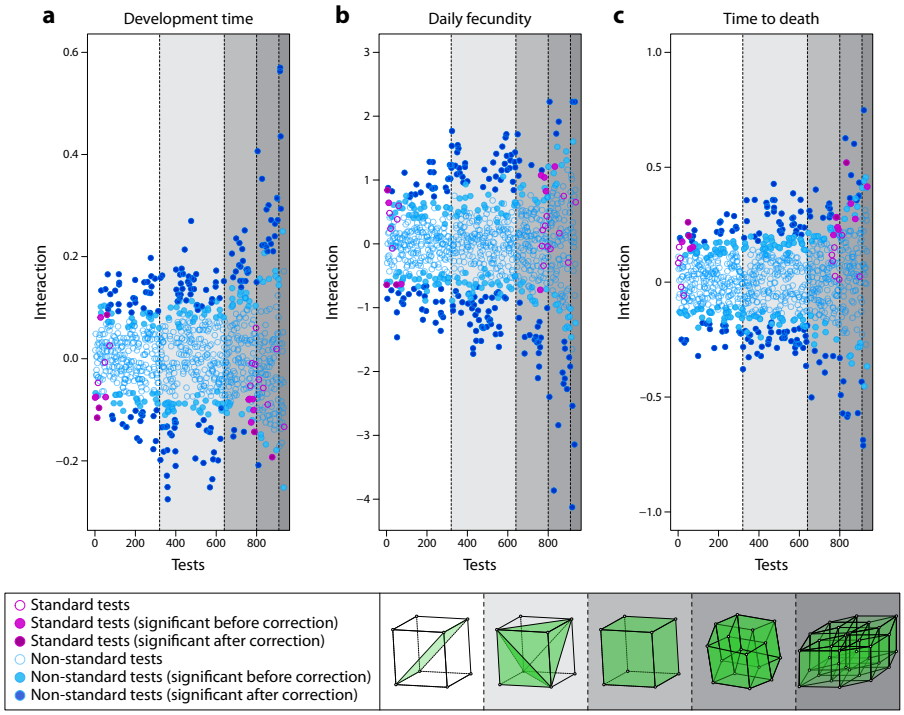

Figure 2: **Scatter plot of all tested interactions on** $\log_2$ **transformed data** (standard in purple and non standard interactions in blue). Interactions for (a) development time, (b) daily fecundity, (c) time to death. Filled circles indicate significant interactions, open circles represent non-significant interactions. Dark blue and dark purple filled circles indicate significance ($p < 0.05$) after multiple testing correction. Filled light blue and filled light purple dots indicate significance ($p < 0.05$) before corrections.

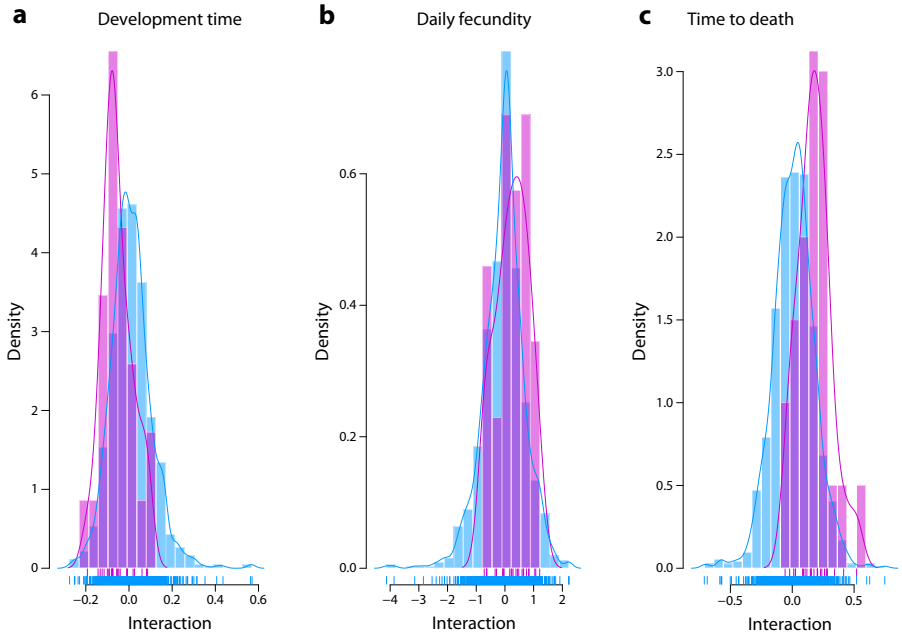

Figure 3: **Density plot of all tested interactions (standard in purple and non standard in blue) for the** $\log_2$ **transformed data.** Interactions for (a) development time, (b) daily fecundity, (c) time to death.

10.2 Spurious epistasis in the microbiome

The invariance of significance under transformation effectively deals with the problem of spurious epistasis, which was the subject of previous authors' work regarding genetic interactions (see [11]). In particular, Sailer and Harms estimated the nonlinear scales of arbitrary genotype-phenotype maps and then linearize these maps in order to remove the effects. Because the interactions we detect are invariant under transformation, the removal of non-linearity (itself a transformation) cannot affect the outcome of our calculations. Furthermore, the spurious epistasis dealt with in [11] is so because it does not represent true genetic interactions. However, none of the interactions that we seek to detect are genetic interactions – they are microbiome interactions, which are the products of whole organism physiologies. We apply the present framework because the simplest model is that these interactions should be additive (and many of them are). Any non-additivity becomes a potentially interesting interaction, but the mechanisms of these interactions are not due to simple inactivation of genes, and the rules by which such interactions occur are not understood. Thus, it is not appropriate to address so-called 'spurious interactions' in the current work.

10.3 Simulated data

In Figures 4 and 5 we represent the results of the standard and non-standard interactions analyzed in this paper for data sampled from the standard normal distribution (on the left) and sampled uniformly at random from $[0, 1]$ (on the right). Figures 4 and 5 can be used to determine difference between two types of random values between 0 and 1 associated to the 32 bacterial combinations and the results obtained in Figure 4 (main text) on the actual experimentally measured data. Here we do not include a study of significant interactions, since these sampled data come without a sampled standard error value, being that the data themselves are randomly generated.

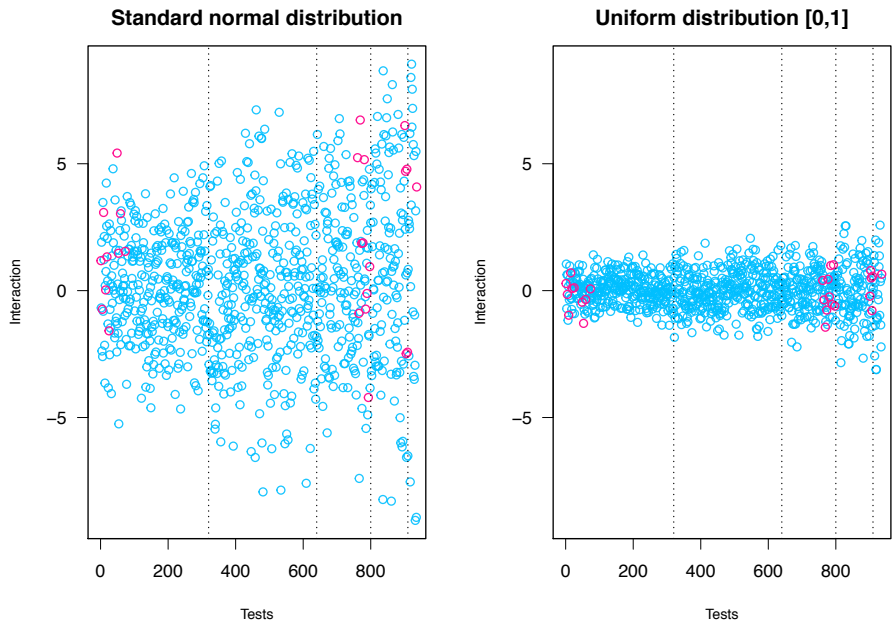

Figure 4: **Scatter plot of all tested interactions on data sampled from the standard normal distribution and from the uniform distribution on** $[0, 1]$ (standard in purple and non standard interactions in blue).

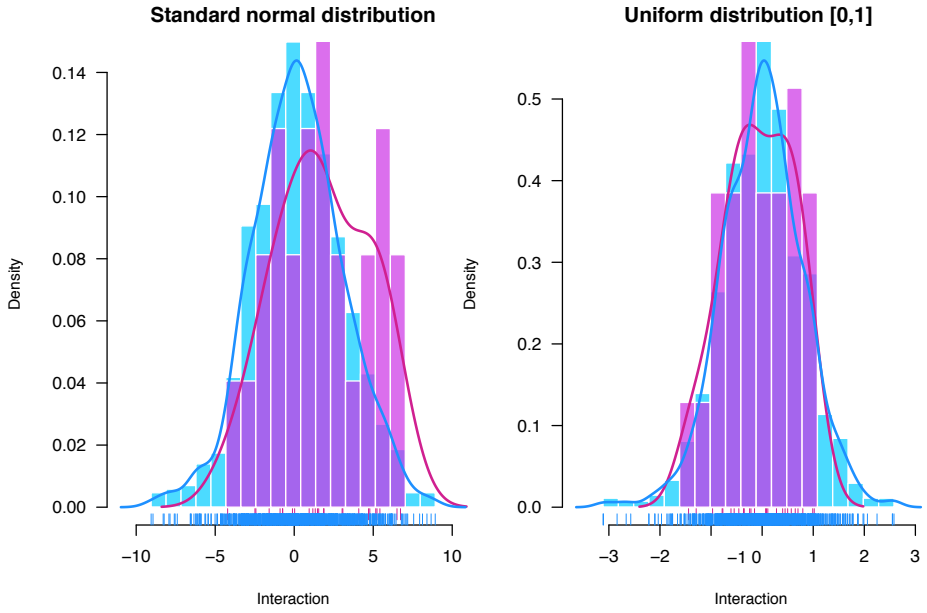

Figure 5: **Density plot of all tested interactions on data sampled from the standard normal distribution and from the uniform distribution on** $[0, 1]$**.**

References

[1] N. Beerenwinkel, L. Pachter, B. Sturmfels, SF. Elena and RE. Lenski, *Analysis of epistatic interactions and fitness landscapes using a new geometric approach*, BMC Evolutionary Biology 20077:60 (2007)

[2] N. Beerenwinkel, L. Pachter, B. Sturmfels, *Epistasis and shapes of fitness landscapes* Statistica Sinica 17, 1317-1342 (2007)

[3] B. Obadia, ZT. Guvener, V. Zhang, JA. Ceja-Navarro, EL. Brodie, WW. Ja, WB. Ludington, *Probabilistic Invasion Underlies Natural Gut Microbiome Stability*, Current Biology, 27, 1999-2014 (2017)

[4] H. S. M. Coxeter. *Regular Polytopes*, London, Methuen,New York, Pitman 1949. 20-321 (1948)

[5] J. A. De Loera, J. Rambau, F. Santos *Triangulations*, Algorithms and Computation in Mathematics, 25, Structures for algorithms and applications, Springer-Verlag, Berlin, xiv+535 (2010)

[6] J. Grilli, G. Barabs, MJ. Michalska-Smith, S. Allesina, *Higher-order interactions stabilize dynamics in competitive network models*, Nature. Aug 10;548(7666):210-213. (2017)

[7] P. Huggins, B. Sturmfels, J. Yu, and DS. Yuster. *The Hyperdeterminant and Triangulations of the 4-Cube.* Mathematics of Computation 77, no. 263 (2008)

[8] N. Korasidis, L. Lamberti, code available at (https://github.com/...)

[9] P. D. Newell, A. E. Douglas, *Interspecies Interactions Determine the Impact of the Gut Microbiota on Nutrient Allocation in Drosophila melanogaster*, Appl. Environ. Microbiol, vol. 80 no. 2 788-796 (2014)

[10] R. T. Paine *Food-web analysis through field measurement of per capita interaction strength*, Nature 355, 73-75 (1992)

[11] R. Sailer, M. Harms, *Detecting High-Order Epistasis in Nonlinear Genotype-Phenotype Maps*, Genetics, (2017)

[12] Weinreich, D. M., Lan, Y., Wylie, C. S., and Heckendorn, R. B. *Should evolutionary geneticists worry about higher-order epistasis?*, Current Opinion in Genetics and Development, 23(6), 700707 (2013)

[13] Bascompte, J., Jordano, P., and Olesen, J. M., *Asymmetric Coevolutionary Networks Facilitate Biodiversity Maintenance*, Science 312.5772 (2006)

[14] Efron, B., Tibshirani, R., *Bootstrap Methods for Standard Errors, Confidence Intervals, and Other Measures of Statistical Accuracy*, Statistical Science, vol. 1 no. 1 54-75 (1986)